Study of the dynamics of spatial point processes in wireless communication networks

Pierre Popineau

PSL
UNIVERSITÉ PARIS

THÈSE DE DOCTORAT
DE L'UNIVERSITÉ PSL

Préparée au Département d'Informatique de l'ENS

Étude de la dynamique de processus ponctuels spatiaux appliqués aux réseaux de communication sans fil

-

Study of the dynamics of spatial point processes in wireless communication networks

Soutenue par
Pierre Popineau
Le 14/06/2023

École doctorale n°386
Mathématiques Paris Centre

Spécialité
Mathématiques

Composition du jury :

Sara Alouf INRIA Sophia Antipolis	*Examinatrice*
François Baccelli INRIA Paris	*Directeur de thèse*
Marceau Coupechoux LTCI - Télécom Paris	*Président du jury*
Sergey Foss Heriot-Watt University	*Examinateur*
Jean-Marie Gorce INSA Lyon	*Rapporteur*
Derya Malak EURECOM	*Examinatrice*
Pascal Moyal IECL - Université de Lorraine	*Rapporteur*
Luis Guilherme Uzeda Garcia Nokia Bell Labs France	*Examinateur*

ENS | PSL Inria Cinics erc European Research Council Established by the European Commission

Résumé

Grâce aux nouveaux paradigmes introduits dans la dernière génération de réseaux sans fil, les attentes concernant le temps de service, la latence et la performance du réseau ont augmenté. Pour modéliser ces réseaux, la théorie des processus ponctuels et la géométrie stochastique se sont avérées utiles car elles fournissent un cadre polyvalent et robuste pour obtenir des résultats lorsque l'on travaille avec ces réseaux sans fil. L'ajout d'une dynamique markovienne pour modéliser les connexions et les temps de service complète le cadre d'analyse de ces réseaux sans fil.

La première contribution du travail présenté dans cette thèse réside dans l'analyse de la différenciation des services : les réseaux 5G NR ont introduit le partitionnement de la bande passante comme outil pour augmenter la performance du réseau. Dans cette configuration de réseau, tous les utilisateurs n'interfèrent pas les uns avec les autres avec la même puissance : les utilisateurs qui émettent avec un spectre de fréquence d'émission plus large auront une plus grande bande passante, mais ils rencontreront également plus d'interférences de la part des autres utilisateurs dans le réseau. En revanche, les utilisateurs dont le spectre est plus étroit subiront moins d'interférences. Nous définissons un cadre markovien pour étudier un tel processus spatial multiclasse de naissance et de mort, et nous décrivons sa région de stabilité. Pour de tels systèmes, les propriétés du régime stationnaire sont analysées, telles que les mesures moment ou l'attraction, ce qui permet de mieux comprendre cette dynamique.

Le deuxième problème que nous examinons est celui de la mobilité, qui est devenue une caractéristique importante des réseaux sans fil en raison de l'utilisation d'antennes hautement directionnelles. En utilisant une architecture simple pour un réseau cellulaire à deux niveaux, nous étudions deux familles de politiques d'association : une première famille qui s'appuie uniquement sur la mobilité de l'utilisateur, et une seconde qui offre un compromis entre la géométrie du réseau et la mobilité de l'utilisateur afin d'augmenter les performances du réseau. Ces politiques sont ensuite comparées à une politique d'association classique de puissance maximale afin d'évaluer leurs performances.

Abstract

Thanks to the new paradigms introduced in the latest generation of wireless networks, expectations concerning service time, latency and network performance have increased. To model such networks, point process theory and stochastic geometry have proven to be useful as they provide a versatile and robust framework to obtain results when working with such wireless networks. Adding to this Markov dynamics to model connections and service times completes this framework to analyze such wireless networks.

The first contribution of the work presented in this thesis lies in the analysis of service differentiation: 5G NR networks have introduced bandwidth partitioning as a tool to increase network performance. Under this network setup, not all users interfere with each other with the same power: users transmitting with a broader transmitting frequency spectrum will have a larger bandwidth, but they will also encounter more interference from the other users in the network. In contrast, users with a narrower spectrum will experience less interference. We define a Markovian framework to study such a multiclass spatial birth-and-death process, and we describe its stability region. For such systems, properties of the stationary regime are analyzed, such as moment measures or statistical clustering, leading to a better understanding of these dynamics.

The second problem we look into is mobility, which has become an important feature in wireless networks due to the use of highly directional antennas. Using a simple architecture for a two-tier cellular network, we study two families of association policies: a first family which only relies on user mobility, and the second offers a trade-off between network geometry and user mobility to increase network performance. These policies are then compared to a classical max-power association policy to assert their performance.

Acknowledgements

The first person I want to thank is my supervisor, François Baccelli, for trusting and accompanying me throughout my PhD. When I started working in NEMO, I had just graduated from Ecole des Mines de Paris, and had very little experience in research, especially in stochastic geometry. He decided to accept me initially as a junior researcher in the team and later as a PhD student to pursue the work I am presenting in this manuscript. François' valuable experience in the field and his extremely precise remarks were invaluable to me. They guided me throughout my PhD and helped me gain a better understanding of the concepts I encountered during my research.

My second word of thanks goes to the people of ERC NEMO. Firstly, my co-PhD students and postdocs: Michel Davydov, Bharath Roy Choudhury, Sayeh Khaniha, Ke Feng, and Guodong Sun. Even though our research subjects are relatively different, we maintained unity through our reading groups, seminars, but most importantly, through random discussions in our shared office whenever one of us was stuck on a problem (which happened to be me, most of the time). Secondly, I would like to thank Bartek Blaszczyszyn for accepting my application as a junior researcher at the beginning of my journey, and for guiding the operations at the head of the Dyogene team, Ali Khezeli for animating the scientific life of our group by organizing our seminar series and Julien Guieu, who has been of great help at the interface with INRIA. I also wanted to thank Sara Alouf, Marceau Coupechoux, Sergey Foss, Jean-Marie Gorce, Derya Malak, Pascal Moyal and Luis Uzeda Garcia for accepting to be a part of the jury for this PhD.

During these years, I divided my time between working at INRIA Paris and LINCS (*Laboratory on Information, Networking, and Communication Sciences*, hosted by Telecom Paris). LINCS holds a special place in these acknowledgments as it is a unique place of scientific exchange, where I had the chance to meet researchers from various fields and have exciting conversations. I especially want to thank Anna Frisone for her presence and valuable help with administrative and non-administrative matters. I also thank all LINCS researchers whom I met, worked with, talked to, played Concept with, or had coffee with: Fabien Mathieu, François Durand, Ludovic Noirie, Ana Bušić, Francesca Bassi, Leonardo Linguaglossa, Marc-Olivier Buob, Rémi

Varloot, Maxime Mouchet, Céline Comte, and many more.

Little did I know, when I registered as a PhD student in February 2020, what the future held for us. Starting a PhD during a pandemic was a peculiar experience, as it is a pivotal moment where I needed guidance the most. But I held on tight, and after the end of the lockdown, I was extremely lucky to have access to an office at LINCS, located then inside Paris, to have a dedicated workplace to escape my small apartment. These times were special, as having a whole laboratory for mostly three persons—Anna, Fabien, and I—was strange, but we made the most out of it.

Next, I would like to thank my co-authors. Sanket Kalamkar was of great help when it came to helping me write my first article and gave me very valuable advice during our discussions. Seva Shneer, whom I had the chance to visit in Edinburgh, had very constructive discussions with me over the past year and a half and provided input on earlier versions of some of the proofs presented here, for which I am grateful.

Finally, I want to express my last word of thanks to my parents, Joëlle and Fabrice, my brother, Maxime, and all of my friends: Irène, Valentine, Guillaume B., Léa, Guillaume dL., Romy, Héloïse, and the members of the West Coast Swing and Rock 4 Temps communities in Paris, and more generally, anyone that kept listening when I randomly started talking about mathematics at some point in a discussion. Your support during these years of PhD was invaluable to me, and I am grateful to have had you by my side, especially during the last year of this PhD.

Many thanks to anyone who embarks on the adventure of discovering this work, and I wish you a pleasant reading!

Introduction

Wireless networks have seen an important growth over the past decades, driven by the increasing demand for mobile communication services and the development of wireless technologies. This growth was accompanied by a number of constraints resulting from the intrinsic properties of wireless networks, where network performance depends on the spatial configuration of transmitting users at a given moment. The latest generation of wireless networks have brought another layer of constraints, notably with the introduction of multi-tier networks and service differentiation. These considerations have brought a multitude of questions about network load, communication latency and transmission performance, and the need for robust frameworks to model such networks.

Communication networks have been studied extensively in queuing theory, as information about user latency and service times has become increasingly interesting. Among the properties of interest, stochastic stability ensures to avoid congestion or overload in the network, and provides useful bounds in population of the network. Under the Markov property, the stability condition is also important to ensure the convergence of latency to a stationary distribution which one wants to characterize analytically. Jackson networks ([55]) and their multi-class extension, BCMP networks ([24]), fall within the classes of studied networks, but stability results about networks with service differentiation as intended in this work remains an open question.

Another tool that has risen in popularity to study and model communication networks is stochastic geometry ([12], [48]), as it provides a flexible and reliable framework to encapsulate the features of wireless communications. This has become especially true in the most recent wireless networks, as the standards set in terms of reliability and latency have become very high, for which stochastic geometry has proven to be useful ([53]). A vast literature exists on stochastic geometry ([86]) and its applications to wireless networks ([18]), as the framework it offers allows to obtain bounds and performance guarantees in wireless networks ([42]).

This manuscript will tackle two different aspects of wireless networks combining these two approaches. In the two first parts, we consider a dy-

namical system network modeled on Markov jump process, where immobile users arrive and leave upon the completion of a transmission, for which we establish conditions for its stochastic stability and provide results about its steady-state dynamics through Palm calculus and stochastic geometry. In the last part of this thesis, we will look to a fixed network with mobile users and look to obtain results about network performance when taking into account user velocity. The work presented here is seen as a first step towards designing a comprehensive mathematical framework to encapsulate all the features of 5G NR networks and their future releases.

Stochastic stability in communication networks

Spatial interactions and spatial interacting queuing systems have been studied for a long time, as they prove to be useful to model a large variety of physical phenomena, ranging from physics to epidemiology, biology or communication theory. Queuing systems have also been studied extensively, as many results have been obtained about their behavior, especially under the Markov assumption, which provides a framework where several additional properties can be reached (existence of a stationary distribution, converging times, etc.). Adding spatial interactions to queuing systems defines the theory of *spatial queuing networks* ([82]), which form a class of queuing systems where the locations of queues are not fixed locations in space, and where the arrival and departure times depend on the geometry of the system at a given time. Such systems have been introduced by Preston ([75]) as jump processes over the set of counting measures on a given region of space.

A particularity of wireless networks comes from the nature of spatial interactions between users. In a device to device wireless network, users arrive at random locations in time and space and their service rate at any time is a function of the interference created by other users transmitting at the same time in the network. In [80], the authors introduced a framework to study such wireless spatial birth-and-death networks, derived the stability region, i.e, the set of arrival rates for which the network is stochastically stable, which happens to be an interval, and studied the stationary regime of this class of dynamics. On the other hand, when working with cellular networks, the study of stability happens to be more complex, as metastable regimes may emerge ([4]). Both problems have been studied in a setup where all users use the same communication channels, which ensures that all users interact with each other.

Various instances of spatial queuing networks have been studied and results have been obtained using queuing theory tools to assert the recurrence and stability conditions for such systems in a Markov setup ([3], [16], [17], [29]). Among the numerous fields in which spatial queuing systems have been studied, communication systems provide an interesting framework, as many communication protocols prove to respect the Markov property (ALOHA,

DMAA under natural assumptions - [85]).

Service differentiation in wireless networks

The latest generations of wireless networks, such as 4G LTE and 5G NR ([9]), have introduced service differentiation as a means to increase bandwidth and network performance ([39]), and to decrease user latency and increase communication reliability ([62]). This service differentiation uses bandwidth partitioning algorithms ([67]) in order to assign to users communication channels matching their needs and respecting certain fairness criteria.

In the multiclass wireless networks considered here, users can transmit on several frequency bands. Those using a large number of bands transmit with a strong signal, but generate a lot of interference for other users, hence slowing down their transmission. On the other hand, users transmitting on a small number of bands have a weaker signal, but generate less interference and block less the other transmissions. It it also to note that some users do not interfere with each other, as the sets of frequency bands allocated to them do not overlap, while others may interfere with all present users, e.g. when they use the whole available spectrum of bands to transmit.

A first goal of this thesis is to develop frameworks designed at modelling dynamic multiclass wireless networks, and studying some of their properties: stability, stationary regime and establishing results about network performance based on the parameters. To capture the space-time interactions between users, we use a birth-and-death process of wireless dipoles (see [12], [47]). In this model, dipoles arrive according to a Poisson rain of constant intensity, representing the arrival rate of users in the network, and leave with a rate inversely proportional to a shot-noise of the configuration. These dynamics are standard when studying wireless networks and represent a linearized version of the Shannon-Hartley formula in the interference limited case, corresponding to low SINR, modelling the capacity of a transmission channel ([83]). This relatively simple framework captures some of the key features of bandwidth partitioning in a 5G network and has been an open question for several years.

As mentioned, the novelty of this works lies in the study of this network of interacting point processes. Spatial birth-and-death processes in the single-class setup have been studied in [80], but they cannot be immediately generalized to a multiclass network. The main difficulty lies in the presence of multiple available communication channels, which we have to take into account in the proofs. In this work, we will restrict our study to a network in a square torus. Studying spatial queuing networks in a finite region of space allows for an easier study, as most classical methods fail or are harder to generalize when considering the whole Euclidean plane (see [16], [81] for instance). This thesis is a first step towards studying more complex networks: the hypothesis considered in this work are restrictive compared to real life systems, but the network setup we decided to study gathers some key features of wireless communication networks and bandwidth sharing and

partitioning policies used in telecommunication protocols, while allowing us to establish a methodology for their study.

Association policies in heterogenous networks

Another question of interest when considering dynamics of wireless networks is the study of heterogenous and multi-tier networks. Since the introduction of microcells, picocells until the emergence of femtocells in 4G LTE ([57]), association policies have become a key feature of wireless networks. Such multitier network architectures have emerged as a means to improve signal power and reduce interference ([39]), as they allow the network load to be spread over multiple parallel instances of a network ([40]). Multiple types of association policies have been studied ([65]), but max-power association remains a good performer ([79]).

Among the important features an association policy has to take into account, user mobility has become a prominent factor with the democratization of beam-based communications, which rely on narrow beams to concentrate transmission power. In this network paradigm, when a user moves out of the beam it uses to communicate with its serving base station, it has to reselect a new beam, which halts the transmission with the network. These *beam reselections* are added to the cell handover, performed when a user moves out of the coverage of a base station to create an *overhead* in the transmission, significantly decreasing the network performance over a transmission. Thus, designing relevant association policies when studying such networks have to take user mobility into account.

In this line of thoughts, association policies need to be rather simple as more complex association policies may prove to be computationally heavy and may need a controller to associate users to different tiers, which becomes less interesting with the increase of the number of connected users to a network. As a result, decentralized, user-centric association scheme have become prominent in massive MIMO networks ([25]), which have to consider a large amount of connections simultaneously. We will propose a simple 2-tier wireless networks with macro and micro base stations, capturing some essentials features of 5G NR networks (directional beamforming, mobility and beam misalignment), using a similar analysis as developed in [53].

Organization of the manuscript

This manuscript consists in three parts. The first part of this work is dedicated to establishing a framework to study the stability of a multiclass spatial queuing system with wireless interactions. There, we extend a framework introduced in [80] to adapt it to the multiclass setup. In a first step, we introduce a symmetry assumption to simplify the study of the system and allow us to obtain a closed form fo the critical arrival rate in the system. This study relies on the use of the definition of adequate interference queue-

ing networks (see [81]) to obtain bounds for the stability region. Due to the nature of these dynamics, fluid limits ([78]) provide a useful framework to obtain conditions for stability ([37]). In a second step, we relax this symmetry assumption and manage to obtain a general stability condition for spatial queuing systems for which fluid limits follow a certain evolution, giving a reciprocal to a result presented in [84]. Finally, we present numerical simulations for our result and discuss some natural extensions of the model.

The second part focuses around the study of the stationary regime of the dynamics presented in Part I. We start by presenting two heuristics to estimate the spatial user densities in the stationary regime with the use of stochastic geometry tools (see [12]) as well as Palm calculus (see [14]) in order to obtain heuristics for user densities in the stationary regime. A first heuristic relies on a mean-field approximation for the interacting point processes. These approximations are known to provide a powerful framework to obtain both qualitative and quantitative results in many cases. From [80] we know that a monotype wireless network displays clustering, i.e. attraction between users in the stationary regime, which leads us to investigate this property in the multiclass regime, as the spatial interaction between users are different. Finally, we prove the existence of exponential moments for the system. This last property allows us to bound the tails of the steady-state distribution of the dynamics, which have an important practical implications for wireless communications.

The third part revolves around the study of association policies for a two-tier heterogeneous wireless network, based on a study presented in [53]. Because mobility has become a prominent feature to take into account when designing wireless networks ([10], [23]), we introduce a category of association policies based on user velocity to maximize the spectral efficiency in the network. This class of association policies is interesting as they manage to outperform the classical max-power association policies in some network setups. Because these policies only rely on the user velocity and not on network geometry, we introduce *velocity-biased max power* policies to take into account these two components and we propose a computational framework to study them under a set of networks parameters.

Included papers

- P. Popineau and F. Baccelli, *On multiclass spatial birth-and-death process with wireless type interactions*, https://arxiv.org/abs/2205.15799, submitted for publication to IEEE Transactions on Information Theory.

- P. Popineau, S. S. Kalamkar and F. Baccelli, *On velocity-bassed association policies for multi-tier 5G wireless networks*, 2021 IEEE Global Communications Conference (GLOBECOM), Madrid, Spain, 2021, pp. 1-6, https://ieeexplore.ieee.org/document/9685210.

- P. Popineau, V. Shneer, *An instability condition for queuing systems*

with state-dependent departure rates, https://arxiv.org/abs/2304.08853, submitted for publication to Queueing Systems.

Acknowledgements

The work presented here is supported by the ERC NEMO grant, under the European Union's Horizon 2020 research and innovation programme, grant agreement number 788851 to INRIA.

Contents

List of Figures

Chapter A

Mathematical Foundations

In this chapter, we will detail the mathematical framework as well as some basics properties, results and theorems about the mathematical objects that will be used in this thesis.

A.1 Notation

Firstly, let us define some notations. Vectors will be denoted as bold-faced letters and their coordinates in regular script (for instance, $\mathbf{x} = (x_i)_{0 \leq i \leq d-1} \in \mathbb{R}^d$), and $\leq$ will denote the coordinate-wise partial ordering when used for vectors. Let S be a second-countable locally compact Hausdorff space. In the manuscript, S will either be equal to the positive real line $\mathbb{R}_+$, the Euclidean plane $\mathbb{R}^2$ or a compact subset of it. Let $\mathcal{S}$ be the canonical Borel σ-algebra associated with S. Let $(\Omega, \mathcal{F}, \mathbb{P})$ be a probability space, and we define $\mathcal{M}(S)$ the set of counting measures on S.

For $N \in \mathbb{N}$, we denote by $D([0,\infty), \mathbb{R}^N)$ the set of càdlàg (right-continuous with left limits) functions from $\mathbb{R}_+$ to $\mathbb{R}^N$. We consider stochastic processes as measurable maps from $(\Omega, \mathcal{F})$ to $(D([0,\infty), \mathbb{R}^N), \mathcal{S})$. Let d^0_∞ be the infinite norm in $\mathbb{R}^d$, $|x|$ be the L^1 norm and $\|x\|$ denote the L^2 norm of x.

For a sequence $(x_n)_{n \geq 0}$ and x in $D([0,\infty), \mathbb{R}^N)$, we write $x_n \to x$ if, for all $T > 0$:

$$\lim_{n \to \infty} \sup_{0 \leq t \leq T} \|x_n(t) - x(t)\| = 0. \tag{A.1}$$

In the rest of this thesis, if no mode of convergence is specified, this definition of convergence is used.

We denote by $\mathcal{E}(\mathbb{R}^d)$ the set of probabilities on $\mathbb{R}^d$ (with $d \geq 1$), and we define the partial ordering of probability measures $\leq_i$. We define:

$$I = \{f \in \mathcal{E}(\mathbb{R}^d), f \text{ is coordinate-wise non-decreasing}\}.$$

For each $F, G \in I$, we write $F \leq_i G$ if and only if

$$\int_{\mathbb{R}^d} f(x)F(\mathrm{d}x) \leq \int_{\mathbb{R}^d} f(x)G(\mathrm{d}x),$$

for all $f \in I$. $\leq_i$ is a partial order on the set of random vectors of $\mathbb{R}^d$. The next table resumes all the notations used in this chapter.

Let Ψ and Ψ' be two point processes on $\mathcal{D}$. We write $\Psi \leq \Psi'$ if we have $\Psi(\mathcal{D}) \leq_i \Psi'(\mathcal{D})$. In the rest of this thesis, we will use this partial order when comparing stochastic processes. Finally, we say that a random variable X with values in $\mathbb{R}^d$ *dominates* Y if the cumulative distribution functions of X and Y, denoted as F_X and F_Y, are such that $F_Y \leq_i F_X$. A consequence of stochastic domination is, for all $\mathbf{x} \in \mathbb{R}^d$ and for all probabilities $\mathbb{P}$ defined on $\mathbb{R}^d$, we have $\mathbb{P}[X > \mathbf{x}] \geq \mathbb{P}[Y > \mathbf{x}]$.

Finally, for two random variables X and Y, we write $X \overset{d}{\sim} Y$ if X and Y have the same probability distribution.

A.2 Point process theory

The main mathematical object we manipulate in this manuscript are point process. The most common way to visualize a point process is to consider a random collection of points of a set, whether is it the real line, the Euclidean plane or any mathematical space. Point processes have been introduced as a means to model and study a vast variety of physical processes, like the position of stars in the sky (which gave the idea to John Mitchell in 1767 of what would become the Poisson point process). Nowadays, point processes are used to study a variety of physical phenomena, ranging from biology ([41], [90]) and epidemiology ([66]) to wireless communication networks ([80]). This section aims at presenting point processes and some basics properties and results of point processes that will be used throughout this manuscript.

The first object we define is the point process:

Definition A.1. *A* point process *on S is a map $\Phi : \Omega \times \mathcal{S} \mapsto \mathbb{N}$ such that:*

- *For all $\omega \in \Omega$, $\Phi(\omega, \cdot)$ is a locally finite counting measure on S, i.e. for all $x \in S$, there exists an open neighborhood N_x of x such that $\Phi(\omega, N_x) < +\infty$.*
- *For every $B \in \mathcal{S}$, $\Phi(\cdot, B)$ is a random variable on $\mathbb{N}$.*

A point process Φ is a random variable over $\mathcal{M}(\mathcal{S})$ over the set of locally finite counting measures on S in a sense that for all ω, $\Phi(\omega, \cdot)$ is a counting measure on $\mathbb{N}$, selected randomly. In this thesis, all point processes will

Notation	Description
S	A second-countable, separable Hausdorff space (assimilated to $\mathbb{R}_+$, $\mathbb{R}^2$ or any compact subset of $\mathbb{R}^2$)
$\mathcal{S}$	Canonical Borel σ-algebra associated with S
$(\Omega, \mathcal{F}, \mathbb{P})$	A probability space
$D(A, B)$	Set of càdlàg function from A to B
d_∞^0	Infinite norm in $\mathbb{R}^d$
$\lvert\cdot\rvert$	L^1 norm
$\lVert\cdot\rVert$	L^2 norm
$\mathcal{M}(S)$	Set of counting measures on $(S, \mathcal{S})$
Φ	Point process
δ	Dirac measure
ν	Lebesgue measure on S
Λ	Intensity measure of Φ
$\mathcal{C}$	Campbell measure of a marked point process
$\mathbb{P}_\Phi^0$	Palm probability measure with respect to the point process Φ
$\mathbb{E}_\Phi^0$	Palm expectation with respect to the point process Φ
$\star$	Convolution of probability distributions
$K(\cdot, \cdot)$	Kernel of a Markov jump process
$\lambda(x)$	Jump intensity function of a jump process
$\Pi(\cdot, \cdot)$	The transition matrix of a jump process
$\bar{x}$	Fluid limit associated with the Markov chain X
ℓ	Path loss function
$\mathcal{N}_0$	Thermal noise density in the network

Table A.1: Table of notations of Chapter A

be considered as random locally finite counting measures, and for simplicity, we will write $\Phi(\cdot)$ to denote either the random variable Φ or one of its realizations.

A common way to visualize point processes is as a random set of points in S: let $X_1, \cdot, X_n$, where n may be infinite and the X_i may not necessarily be distinct, be the points in S for which $\Phi(\{X_i\}) > 0$. Then, to represent the point process, one can write $\Phi = \{X_1, \dots X_n\}$ to emphasize this interpretation. Because point processes are also random measures on S, we will also use two other representations, which involve measure theory. The first one is:

$$\Phi = \sum_{i=1}^{n} \delta_{X_i},$$

where n is an integer-valued random variable denoting the number of points of the realization of Φ and δ is the Dirac measure. The second representation for point process we will use is the counting notation. Let T be a compact subset of S. Then, we define:

$$\Phi(T) = \int_{x \in T} \Phi(\mathrm{d}u).$$

This way, $\Phi(T)$ represents the number of points of Φ in T. This counting notation will be particularly useful when studying stationary point processes in Part II. We will also use the classical set operations on point processes: $x \in \Phi$ means that x belongs to a realization of the point process Φ, and we will use the notations $\Psi \subset \Phi$, $\Phi \cup \Psi$, $\Phi \cap \Psi$ and $\Phi \backslash \Psi$ in their usual sense to respectively denote inclusion, union, intersection and difference between the random sets Ψ and Φ. Finally, the translation operator $x + \Phi$, where $x \in S$ and the dilation operator $\lambda\Phi$ with $\lambda \in \mathbb{R}$ keep their usual meaning.

If, for all $x \in S$, we have $\Phi(\{x\}) \leq 1$, then the point process is said to be *simple*. A point process is said to be *stationary* if for all $y \in S$, the process $\tilde{\Phi} = \Phi + y$, defined as the set $\{y + X_i, X_i \in \Phi\}$ has the same distribution as Φ. A point process is said to be *isotropic* if it is invariant by rotation, i.e. if $R(\Phi)$ has the same distribution as Φ, where R is a rotation of S. The study of stationary point processes is a vast field of research in itself, as it has a lot of interesting properties (see for instance Chapter 4 from [86] or Chapter 1 from [14]).

Two important quantities for point processes are their *intensity measure* and their *distribution*. The intensity measure of a point process is a measure on $\mathcal{S}$ defined, for all $B \in \mathcal{S}$, by:

$$\Lambda(B) = \mathbb{E}\left[\Phi(B)\right].$$

In other words, the intensity measure of a point process is the mean number of points of the point process is a given Borel set B. If the point process is stationary, this intensity measure is translation-invariant. An important result in measure theory is that every isometry invariant Radon measure is absolutely continuous with regard to the Lebesgue measure, which can be applied here. As such, if the point process is stationary, there exists $\lambda \in \mathbb{R}$ such that for all Borel set B:

$$\Lambda(B) = \lambda\nu(B),$$

where ν is the Lebesgue measure on $\mathcal{S}$. λ is called the *intensity* of the point process, and it can be interpreted as the average number per unit of space of the process, or its spatial intensity.

The distribution of the Point process is defined as $(\mathbb{P}[Y \in \Phi])$ for all the configuration sets Y. This distribution uniquely determines the point process.

The Poisson point process

Among existing point processes, a common instance is the Poisson point process (PPP). The main idea behind the Poisson point process is to model random events sparsely separated spatially or temporally.

To define a Poisson point process, let us take a locally finite intensity measure Λ on $\mathcal{S}$, and we define the Point process Φ such that:

– For all $B \in \mathcal{S}$, $\Phi(B)$ is distributed according a Poisson law, i.e., for all $n \in \mathbb{N}$:

$$\mathbb{P}\left[\Phi(B) = n\right] = \frac{\Lambda(B)^n}{n!} e^{-n},$$

– The number of points in n disjoint Borel subsets of S are independent random variables, i.e., for all $B_1, \dots, B_n \in \mathcal{S}$ such that $i \neq j \Rightarrow B_i \cap B_j = \emptyset$, we have:

$$\mathbb{P}\left[\Phi(B_1) = m_1, \dots, B_n = m_n\right] = \prod_{i=1}^{n} \mathbb{P}\left[\Phi(B_i) = m_i\right].$$

The second property of Poisson point processes is also referred to as *independent scattering* or *increment independence*, as it captures the lack of interaction between of points in the Poisson process. A consequence of this property is that the points of a Poisson point process are uniformly distributed on S.

If there exists $\lambda > 0$ such that $\Lambda = \lambda\nu$, where ν is the Lebesgue measure on $\mathcal{S}$, then we say that the Poisson point process is *homogenous*. An interesting property of homogenous Poisson point processes is that, when used to model arrival times of events the independent scattering tells us that the time between events is exponentially distributed with mean $1/\lambda$.

A second interesting property of the Poisson point process is that it is both stationary and isotropic. This allows for the definition of a *typical* point for the point process, which we usually assume to be located at the origin, useful to obtain results about the process.

A first interesting result about point processes is Campbell's Theorem (named after the work of Campbell, see [33])

Theorem A.1. *Let $f : S \mapsto \mathbb{R}$ be a non-negative measurable function. Then:*

$$\mathbb{E}\left[\sum_{x \in \Phi} f(x)\right] = \int_{y \in S} f(y)\Lambda(\mathrm{d}y).$$

This theorem is an application of Fubini's Theorem to the random sum, after rewriting it as a double integral. Campbell's theorem is a particularly useful too when working with shot-noises over point processes, because it allows for a practical way to express the value of a shot-noise of the point process. It is to note that if Φ is a homogenous PPP with intensity λ, we get the following alternative form:

$$\mathbb{E}\left[\sum_{x \in \Phi} f(x)\right] = \lambda \int_{y \in S} f(y)\mathrm{d}y.$$

Marked point processes

When using point processes, it is common to attach to each point a characteristic (or mark). Let $\mathbb{M}$ be the space of marks and $\mathcal{M}$ its Borel σ-algebra.

We define a *marked point process* $\Psi = \{[x_m, y_m]\}$, where the points $\{x_m\}$ form a point process with intensity measure Λ, called the ground process, and the y_m is the process of marks. We can define an intensity measure for the marked point process for all $B \in \mathcal{S}$ and $M \in \mathcal{M}$ as:

$$\Upsilon(B \times M) = \mathbb{E}\left[\Psi(B \times L)\right].$$

For all $M \in \mathcal{M}$, the measure $\Upsilon(\cdot \times M)$ is absolutely continuous with regard to the intensity of the ground process. There exists a probability distribution $\mathbb{P}_m$, depending on $x \in S$, on $\mathcal{M}$ such that:

$$\Upsilon(\mathrm{d}(x, m)) = \mathbb{P}_m(x, \mathrm{d}m)\Lambda(\mathrm{d}x).$$

If the marked point process is stationary, then, $\mathbb{P}_m(x, \cdot) = \mathbb{P}_m(\cdot)$ for all $x \in S$, and we have:

$$\Upsilon(B \times M) = \lambda \mathbb{P}_m(M)\nu(B). \tag{A.2}$$

Let Ψ be a stationary marked point process with marks in $(\mathbb{M}, \mathcal{M})$. We can define the following random counting measure on $(S \times \mathbb{M}, \mathcal{S} \otimes \mathcal{M})$:

$$\mathcal{C}(B \times M) = \int \phi(B)\mathbb{1}_{\{M\}}(B)\mathbb{P}(\mathrm{d}\phi). \tag{A.3}$$

In other words, this measure counts the average number of points in B with marks in M. This measure is called the *Campbell* measure of the point process Ψ.

Palm calculus

When studying point processes, an important question is that of the existence of some events, or the value of certain quantities conditioned on a point being present at a given location. For instance, the probability that a point has no neighbor located closer than r is equal to $\mathbb{P}\left[\Phi(B(x, r)) = 1 || x \in \Phi\right]$. This conditional probability is ambiguous, because the conditioned event has a probability 0. In order to define such conditional events, we introduce the Palm probability distribution. In this section, we will propose two definitions of the Palm probability distribution: a first one relying on the Campbell measure defined above, and a second one based an interpretation from Matthes.

Let us take Ψ a stationary marked point process. From (A.2), we know that the intensity measure of Ψ is a product form involving the Lebesgue measure, the intensity of the ground process of Ψ and a probability distribution $\mathbb{P}_m$. Taking the definition of the Campbell measure from (A.3), we get:

$$\mathcal{C}(B \times M) = \int \phi(B)\mathbb{1}_{\{M\}}(B)\mathbb{P}(\mathrm{d}\phi) = \lambda \int_B \mathbb{P}_m(M)\nu(\mathrm{d}x).$$

The probability distribution $\mathbb{P}_m$ is called the Palm probability distribution, and it can be seen as the Radon-Nikodym derivative of the Campbell

measure with regard to the intensity measure of the ground process of Ψ. Although this definition is implicit, it underlines its dependency with the Campbell measure of a stationary marked point process. The following definition will give an explicit definition and another interpretation for the Palm probability distribution:

Definition A.2. *Let Φ be a stationary point process with a finite, nonzero intensity λ. The Palm probability distribution (at 0) is the probability distribution defined on $(\mathbb{N}, \mathcal{N})$ as:*

$$\mathbb{P}^0_\Phi[Y] = \frac{1}{\lambda\nu(B)} \int \sum_{x\in\Phi(B)} \mathbb{1}\{\Phi - x \in Y\}\mathbb{P}(\mathrm{d}\Phi), \tag{A.4}$$

where B is an arbitrary Borel set with positive measure. It is to note that this definition does not depend on the choice of set B.

The Palm probability distribution introduces a measure which acts as a condition probability given that a point of Φ is located at 0. To understand why, we can use Matthes' interpretation. Let us associate to each point in Φ a mark, equal to 0 or 1 whether the shifted point process $\Phi - x$ belongs to Y. To come back to the previous example, with $Y = \{\Phi, \Phi(B(0,r) = 0)\}$, a point x will have mark 1 if and only if its nearest neighbor is located at a distance greater than r. The process of marks is stationary, and we can extract the subprocess of points with marks 1, which has intensity $\lambda_{\{1\}}$. The mark distribution M is given by:

$$M(\{1\}) = \frac{\lambda_{\{1\}}}{\lambda}.$$

Let us take a Borel set B. The average number of points in B that have mark 1 has mean $\lambda_{\{1\}}\nu(B)$, implying that:

$$\mathbb{P}^0_\Phi[Y] = M(\{1\}),$$

and that the choice of B does not play a role in (A.4).

A second definition of the Palm probability distribution can be reached from the Campbell measure (see Section 4.3.4 from [86]). This measure can be proven to be absolutely continuous with respect to the intensity measure of the point process Φ, which allows us to derive the Palm probability distribution.

Using the Palm probability measure, we can define the Palm expectation. This expectation can be interpreted as the average of a variable at the points of the process Φ. This expectation can be expressed in terms of Φ as:

$$\mathbb{E}^0_\Phi[Y] = \frac{1}{\lambda\nu(B)}\mathbb{E}\left[\sum_{x\in B} Y + x\right],$$

where $Y + x = \{y + x, y \in Y\}$. To illustrate the Palm expectation, let us consider a point process N on the positive real line $\mathbb{R}^+$ with probability $\mathbb{P}$, and let us take a stochastic process (defined in the next chapter) Z. If the

point process is ergodic, we can use ergodic theorems (see [27] or Theorem 1.6.4 from [14]) and (A.4), then we can write the Palm expectation and the classical expectation as follows:

$$\mathbb{E}_N^0[Z(0)] = \lim_{t\to\infty} \frac{1}{N((0,t])} \int_0^t Z(s)N(\mathrm{d}s) \qquad \mathbb{E}[Z(0)] = \lim_{t\to\infty} \frac{1}{t} \int_0^t Z(s)\mathrm{d}s.$$

The difference between Palm expectation and regular expectation is fundamental in our work, especially when we will study the properties of the stationary regime of the system considered in Part II. The Palm expectation works as a *user average*, as it only considers the values of Y at locations in the Point process Φ, as the classical expectation can be interpreted as a *system average*.

An important result linking the Palm probability measure and Poisson point processes is Slivnyak's Theorem (sometimes referred to as Slivnyak-Mecke's theorem):

Theorem A.2 (Slivnyak)**.** *Let Φ be a point process with intensity measure Λ and distribution $\mathbb{P}$. Then, for all $x \in S$, we have:*

$$\mathbb{P}_x = \mathbb{P} \star \delta_x,$$

where $\star$ is the convolution of distributions and δ_x is the distribution of the point process consisting of the non-random point x.

In other words, the Palm distribution of Φ with respect to x is the distribution of Φ, with an added point at x, as the convolution of distributions corresponds to the superposition of point processes. This theorem allows to link the Palm probability measure, and subsequently the Palm expectation, with the original distribution of Φ.

A second important result is the inversion formula of Slivnyak and Ryll-Nardzewski:

Theorem A.3. *Let Y be a non-negative random variable. We have:*

$$\mathbb{E}[Y] = \lambda \mathbb{E}_\Phi^0 \left[\int_{x\in S} (Y + x)\, \mathrm{d}x \right]. \tag{A.5}$$

This result links the Palm probability measure, the intensity of the point process Φ and the expectation. We can use (A.5) as well as (A.4) to obtain a second equation to express a random sum over a point process. We have, for all $B \subset S$ and for all non-negative function $f : S \to \mathbb{R}$:

$$\mathbb{E}\left[\sum_{x\in\Phi(B)} g(x) \right] = \mathbb{E}[\Phi(B)] \mathbb{E}_\Phi^0 \left[g(0) \right]. \tag{A.6}$$

This formula is a mean-value formula and uses the user average interpretation for the Palm probability. To put it in words, to obtain the average

value of the sum of Φ, we multiply the expected value for one user, the typical user, an multiply it by the number of users in the process.

Another result about Palm calculus that we will use in this thesis links the Palm probability distribution of a superposition of point processes and the intensities of these processes:

Lemma A.4. *Let Φ_1 and Φ_2 be two stationary point processes on $\mathcal{D}$ with respective intensities μ_1 and μ_2, and denote $\Phi = \Phi_1 + \Phi_2$ the superposition of the two processes. Then, we have:*

$$\mathbb{E}^0_\Phi[F(0,\Phi_0)] = \frac{\mu_1}{\mu_1+\mu_2}\mathbb{E}^0_{\Phi_1}[F(0_1,\Phi_0)] + \frac{\mu_2}{\mu_1+\mu_2}\mathbb{E}^0_{\Phi_2}[F(0_2,\Phi_0)], \quad \text{(A.7)}$$

where 0, 0_1 and 0_2 respectively denote the typical users of Φ, Φ_1 and Φ_2, and F is a shot-noise of the point processes.

Proof. Let F be a shot-noise over Φ. Then, we have, from the definition of the Palm probability distribution:

$$\mathbb{E}\left[\sum_{x\in\Phi} F(x,\Phi)\right] = \mathbb{E}^0_\Phi[F(0,\Phi)]\mathbb{E}[\Phi(\mathcal{D})] = \mathbb{E}^0_\Phi[F(0,\Phi)](\mathbb{E}[\Phi_1(\mathcal{D})] + \mathbb{E}[\Phi_2(\mathcal{D})]).$$

We also know that:

$$\begin{aligned}\mathbb{E}\left[\sum_{x\in\Phi} F(x,\Phi)\right] &= \mathbb{E}\left[\sum_{x\in\Phi_1} F(x,\Phi)\right] + \mathbb{E}\left[\sum_{x\in\Phi_2} F(x,\Phi)\right] \\ &= \mathbb{E}^0_{\Phi_1}[F(0_1,\Phi)]\mathbb{E}[\Phi_1(\mathcal{D})] + \mathbb{E}^0_{\Phi_2}[F(0_2,\Phi)]\mathbb{E}[\Phi_2(\mathcal{D})].\end{aligned}$$

We combine these two equations to conclude the proof. □

The last important formula we will mention about Palm calculus in this section is the Papangelou formula, which gives a Radon-Nikodym derivative of the Palm probability measure.

Theorem A.5. *Let Φ be a point process and $\mathcal{F}_t$ be a history of Φ adapted to the flow $\{\theta_t\}$. Assume furthermore that the $\mathcal{F}_t$-predictable structure is adapted to $\{\theta_t\}$. Then, Φ admits an intensity $\lambda(t)$ if and only if $P^0 \ll P$. In this case, we can chose $\lambda(t)$ of the form $\lambda(t) = (\mu \circ \theta_t)\lambda$, where μ is the Radon-Nikodym derivative of P^0 on $\mathcal{F}_0^-$ with respect to $\mathbb{P}$:*

$$\mu = \left.\frac{\mathrm{d}\mathbb{P}^0_\Phi}{\mathrm{d}\mathbb{P}}\right|_{\mathcal{F}_0^-}.$$

This result allows to reduce the value of an unknown Palm probability measure using possibly known values of the stochastic intensity of other processes. Papangelou's formula, when combined with the inversion formula from (A.5) allows to obtain meaningful results about point processes, as displayed in Part II.

A.3 Poisson-Voronoi Tessellations

The last notion regarding point process theory we will cover in this chapter is the Poisson-Voronoi tessellation (for more results about random plane tessellations, see [13]). A *tessellation* is a partition of the plane, i.e. a set $\Theta = \{T_i\}_{i \in I}$ such that:

- $\bigcup_{i \in I} T_i = \mathbb{R}^2$,
- for all $i \neq j$, $T_i \cap T_j = \emptyset$.

Let $\mathbb{T}$ be the set of all possible tessellations of $\mathbb{R}^2$. When considering set of points $S = \bigcup_{i=1}^{n} \{x_i\}$ with $x_1, ... x_n \in S$, one can derive the *Voronoi tessellation* associated with S, $\mathcal{V}(S) = \{c_1, ..., c_m\}$ where, for all $1 \leq i \leq m$:

$$c_i = \{y \in S, \|y - x_i\| < \|y - x_j\|, j \neq i\}.$$

In other words, the Voronoi *cell* i is the set of points of S that are closer to x_i than to any other point x_j, with $j \neq i$. It is to note that the cells c_i may be infinite. Voronoi tessellations (also called Voronoi diagrams or Dirichlet tessellations) have a lot of applications, but the one we will focus on comes from information theory and wireless communications. Let us consider a collection of antennas in a wireless network. If we assume that users in the network always associate with the closest antenna to their location, the result association policy creates a Voronoi tessellation of the plane.

Let Φ be a homogenous PPP with intensity $\lambda > 0$. As a random collection of points of S, we can associate it with a Voronoi tessellation $\mathcal{V}(\Phi)$. This Voronoi diagram is called a *Poisson-Voronoi (PV) tessellation* of S.

When studying PV tessellations of the plane, two cells are of interest:

- The *typical* cell, whose existence comes from the stationarity of the PPP used to generate the diagram, which can be seen as a cell sampled randomly in the tessellation, denoted as V,
- The *0-cell*, which is the cell containing the origin, denoted as V_0.

Multiple results exist about the typical cell of a PV tessellation (see Chapter 9 of [86]). For instance, we know that the average volume of the typical cell is equal to:

$$\mathbb{E}[|V|] = \frac{1}{\lambda}. \tag{A.8}$$

An important lemma linking the volumes of V and V_0 in PV tessellations is:

Lemma A.6. *In a PV tessellation, the 0-cell is on average larger than the typical cell:*

$$\mathbb{E}[|V|] \leq \mathbb{E}[|V_0|].$$

Proof. Let us define α_0 as the point process of vertices of the tessellation, α_1, the point process of the edge midpoints and denote as λ_0 and λ_1 their respective intensities, and let $\beta = \alpha_0 \oplus \alpha_2 \oplus \Phi$, which has intensity λ_β. The Palm probability of β is defined as:

$$\lambda_\beta \mathbb{P}^0_\beta[Y] = \int_{\theta \in \mathbb{T}} \sum_{\beta([0,1])} \mathbb{1}_Y\{\theta - x\}\, \mathbb{P}(\mathrm{d}\theta). \tag{A.9}$$

Let f be a measurable function on $\mathbb{T}$ and $T = \{\theta \in \mathbb{T}, 0 \in \Phi\}$ be the set of tessellations for which the origin is the center of a cell. Let us define:

$$\mathbb{E}_2[f(\Theta)] = \frac{\lambda_\beta}{\lambda} \int_{T_2} f(\theta)\mathbb{P}(\mathrm{d}\theta).$$

We have:

$$\lambda \mathbb{E}_2\left[\int_{V_0} f(\Theta - x)\mathrm{d}x\right] = \lambda_\beta \int_{\mathbb{T}} \int_{\mathbb{R}^2} \mathbb{1}_{T_2}(\theta)\mathbb{1}_{V_0(\theta)}(-x) f(\theta + x)\mathbb{P}^0_\beta(\mathrm{d}\theta).$$

We use the mass transportation principle. We have, for any measurable function v:

$$\lambda_\beta \int_T \int_{\mathbb{R}^2} v(x,\theta)\mathrm{d}x\mathbb{P}^0_\beta(\mathrm{d}\theta) = \int_{\mathbb{T}} \sum_\beta v(x, \theta - x)\mathbb{P}(\mathrm{d}\theta).$$

With $v(x,\theta) = \mathbb{1}_{T_2}(\theta)\mathbb{1}_{V_0(\theta)}(-x)f(\theta + x)$ we get:

$$\lambda \mathbb{E}_2\left[\int_{V_0} f(\Theta - x)\mathrm{d}x\right] = \int_{\mathbb{T}} \sum_{x \in \beta} \mathbb{1}_{T_2}(\theta - x)\mathbb{1}_{V_0(\theta - x)}(-x) f(\theta)\mathbb{P}(\mathrm{d}\theta).$$

We know that $\mathbb{1}_{T_2}(\theta - x)\mathbb{1}_{V_0(\theta - x)}(-x) = 1$ if and only if $-x$ belongs in the 0-cell of $\theta - x$. In each θ, there is only one such x, giving:

$$\lambda \mathbb{E}_2\left[\int_{V_0} f(\Theta - x)\mathrm{d}x\right] = \int_{\mathbb{T}} f(\theta)\mathbb{P}(\mathrm{d}\theta) = \mathbb{E}[f(\Theta)]. \tag{A.10}$$

Using this result with $f = 1$ yields:

$$\lambda E_2\left[\int_{V_0} \mathrm{d}x\right] = \lambda \mathbb{E}[|V|] = 1,$$

which is the volume of the typical cell of a PV tessellation. Using (A.10) with $f = 1/|V_0|$ gives:

$$\mathbb{E}\left[\frac{1}{|V_0|}\right] = \lambda = \frac{1}{\mathbb{E}[|V|]}.$$

Using Jensen's inequality gives:

$$\mathbb{E}\left[|V|\right] \leq \mathbb{E}[|V_0|],$$

which is the intended result and concludes the proof. □

Another interesting result about the link between the 0-cell and the typical cell in a PV tessellation comes from [69]:

Lemma A.7 (Mecke, 1998)**.** *For any measurable, non-negative function g, we have:*

$$\mathbb{E}[g(|V_0|)] = \frac{1}{\mathbb{E}[|V|]}\mathbb{E}[|V|g(|V|)].$$

Lemma A.7 gives an interesting link when comparing quantities linked with the volume of the 0-cell and the typical cell, which is usually easier to compute - for instance in the case of homogenous PPP.

Although the PV tessellation is one of the simplest instances of random tessellations of the plane, there are very few analytical results about the size distribution of PV cells, but several heuristics and approximation for this distribution. Among the different existing heuristics, [43] provides a simple, one-parameter yet performant heuristic to approximate the size distribution of PV cells:

$$p(y) = Ay^{5/2}\exp\left(-\frac{7}{2}y\right), \tag{A.11}$$

where $A = \frac{(\frac{7}{2})^{\frac{7}{2}}}{\Gamma(\frac{7}{2})}$ is a normalization constant. Using this heuristic allows us to derive an approximation for the size of the 0-cell. We have:

$$\mathbb{E}[|V_0|] \simeq \int_0^{+\infty} xp(x)\mathrm{d}x = \frac{9}{7}\frac{1}{\lambda} \simeq 1.28\mathbb{E}[|V|].$$

This numerical approximation holds when simulating the average size of the typical cell against the size of the 0-cell of a PV tessellation. Figure A.1 displays the size of the zero-cell (in dashed line) against the size of the typical cell (in plain line) for several values of λ.

In wireless communications, an interesting problem is to study the number of users connected to the same antenna (for reasons exposed in the next chapter). To do so, if we assume that antennas and mobile users are distributed according to two PPP of respective intensities λ and ν, a naive heuristic to obtain the average number of users in the zero-cell of the network is given by:

$$\mathbb{E}\left[\frac{1}{Z}\right] \approx \frac{1}{1+1.28\frac{\lambda}{\nu}}. \tag{A.12}$$

Though, as we will see late in this section, this approximation performs poorly to estimate the inverse load in a network. This leads us to defining the following heuristic, using (A.11):

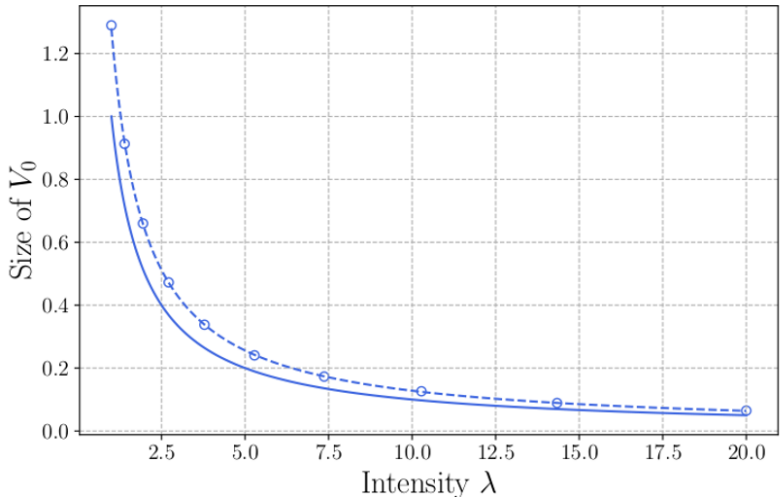

Figure A.1: Size of the 0-cell (dashed line) against the size of a typical cell (plain line) for a homogenous PV tessellation

Lemma A.8. *Let Φ and Ψ be two PPPs of respective intensities λ and ν. Let V_0 be the 0-cell of the PV tessellation associated with the process Φ and let $Z = 1 + |\Psi \cap V_0|$. Finally, let $L : x \mapsto x\left(1 - \left(\frac{1}{1+\frac{2}{7x}}\right)^{7/2}\right)$. The moment of order -1 of Z can be approximated by:*

$$\mathbb{E}\left[\frac{1}{Z}\right] \approx L\left(\frac{\lambda}{\nu}\right).$$

Proof. The number of users in Ψ in the zero-cell of the Poisson-Voronoi tessellation associated with Φ is distributed with a Poisson law of parameter $\nu|V_0|$, where V_0 is the 0-cell of the tessellation. We have:

$$\begin{aligned}
\mathbb{E}\left[\frac{1}{1+|\Psi(V_0)|}\right] =& \mathbb{E}\left[\sum_{N=0}^{\infty} \frac{1}{1+N} \mathbb{P}\left[|\Psi(V_0)| = N\right]\right] \\
=& \mathbb{E}\left[\sum_{N=0}^{\infty} \frac{1}{1+N} \frac{(\nu|V_0|)^N}{N!} e^{-\nu|V_0|}\right] \\
=& \mathbb{E}\left[\frac{1}{\nu|V_0|}\left(1 - e^{-\nu|V_0|}\right)\right].
\end{aligned}$$

We can use Lemma A.7, with $g(V) = \frac{1}{V}\left(1 - e^{-\nu V}\right)$ and $\mathbb{E}[|V|] = 1/\lambda$.

$$\mathbb{E}\left[\frac{1}{1+|\Psi(V_0)|}\right] = \frac{\lambda}{\nu}\left(1 - \mathbb{E}\left[e^{-\frac{\nu}{\lambda}(\lambda|V|)}\right]\right). \tag{A.13}$$

Equation A.13 is the Laplace transform of the random variable $\lambda|V|$ at $s = \frac{\nu}{\lambda}$. Using (A.11) to evaluate the Laplace transform, we get the following approximation:

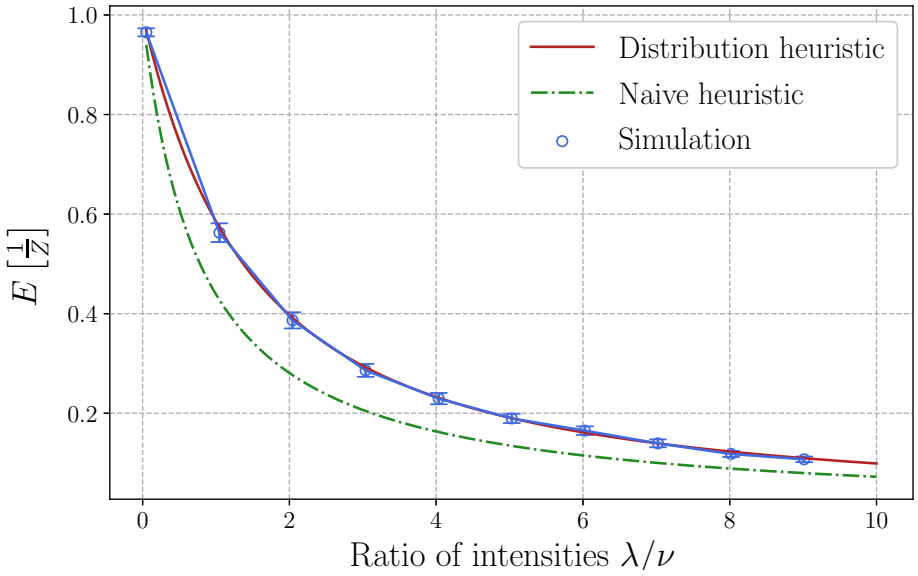

Figure A.2: Performance of the heuristic of Lemma A.8 (plain line) against the simulation (circles) and the naive heuristic (dashed-dotted line) for different values of λ/ν.

$$\mathbb{E}\left[e^{-\nu|V|}\right] = \left(1 + \frac{2}{7}\frac{\nu}{\lambda}\right)^{-7/2}.$$

Substituting this result in (A.13) leads to the result. □

It is to note that this result only relies on the ratio of intensities $\frac{\lambda}{\nu}$, and not on the value of the intensities themselves.We can use numerical simulation to assert the performance of this heuristic, by simulating the inverse load in a homogenous PPP of intensity λ and a homogenous PPP of intensity ν. Figure A.2 shows the comparison between the simulation results (in circles) with the heuristic from Lemma A.8 (in dashed line) and the naive heuristic from (A.12) (in dashed-dotted line)

The reason for this numerical setup will be explained in Part III of this manuscript, as having a performant approximation for the average inverse load in the typical cell of the PV tessellation will allow us to define heuristics to maximize some network metrics.

A.4 Markov Jump Processes

In this section, we will present some basic results about Markov processes. We will consider stochastic processes as measurable maps from $(\Omega, \mathcal{F})$ to $(S, \mathcal{S})$. The main category of stochastic processes we consider in this work are Markov Jump Processes, which is an extension of Markov chain in continuous time. Intuitively, a Markov jump process is a piece-wise constant stochastic process with exponentially distributed interevent times.

Firstly, we define a *Markov kernel* (or probability kernel) as any map $P : S \times \mathcal{S} \to [0, 1]$ such that:

1. The map $x \mapsto P(x, A)$ is measurable for all $A \in \mathcal{S}$.

2. For every $x \in S$, the map $A \mapsto P(x, A)$ is a probability measure on $(S, \mathcal{S})$.

If, instead of having mass 1 on S, we have $P(x, S) \leq 1$ for all $x \in S$, we say that P is a *sub-Markov kernel*. We then say that the family of Markov kernels $(P_t)_{t\geq 0}$ is a transition function on S if:

1. For all $x \in S$, $A \in \mathcal{S}$ and $s, t \geq 0$, (P_t) satisfies the Chapman-Kolmogorov equations:
$$\int_{y\in S} P_s(y, A)P_t(x, \mathrm{d}y) = P_{s+t}(x, A).$$

2. $P_0(x, A) = \delta_x(A)$ for all $x \in E$ and $A \in \mathcal{S}$.

Now, let $(X_t)_{t\geq 0}$ be a stochastic process with state space S and $\mathcal{F}_t = \sigma\{X_s, s \leq t\}$ be its canonical filtration. We say that $(X_t)_{t\geq 0}$ satisfies the simple Markov property with respect to $\mathcal{F}$ if for all $t, h \geq 0$, we have:

$$\mathbb{P}[X_{t+h} \in A|X_s, s \leq t] = \mathbb{P}[X_{t+h} \in A|X_t]\mathbb{P} - \text{a.s.} \tag{A.14}$$

We then say that (X_t) has transition function (P_t) if and only if:

$$\mathbb{P}[X_{t+h} \in A|X_t] = P_h(X_t \in A). \tag{A.15}$$

Equations (A.14) and (A.15) can be seen as the extension of the well-known Markov property for discrete-time processes to continuous time.

Now, we can move on to defining jump processes. Let Π be a Markov Kernel on $(S, \mathcal{S})$, and let $\lambda : S \to [0, \infty)$ be a non-negative, measurable function. We define the *jump kernel* as:

$$K(x, \mathrm{d}y) = \lambda(x)\Pi(x, \mathrm{d}y).$$

We can then move to defining the *jump-hold construction* of the Markov jump process: let us take a law μ, random variables $(Z_n)_{n\geq 0}$ with values in S and $(t_k)_{k\geq 1}$ positive random variables (possibly infinite) such that:

– $(Z_n)_{n\geq 0}$ is a Markov chain with transition kernel Π and initial law $Z_0 \sim \mu$. (Z_n) is called the *embedded jump chain* or embedded Markov chain.

– The variables $(t_k)_{k\geq 1}$ conditional on (Z_n) are independent exponential variables are exponential random variables with respective parameters $\lambda(Z_{k-1})$. The $(t_k)_{k\geq 1}$ are called the *holding times* of the process.

This jump-hold construction displays the two main properties of a Markov jump process: the existence of an embedded Markov chain, representing the jumps in the process, and a collection of exponentially distributed family of holding times depending at each step only on the previous jump. This exponential distribution of holding times and the fact that jumps are following a Markovian evolution justify the name *Markov* jump process, as each jump and the time to wait until the next jump are entirely determined by the present state of the system.

Another determination of Markov jump process comes from its transition function (P_t). Let us take $(x_n)_{n\geq 0}$ be elements of S and take $0 < t_1 < \cdots < t_k < t$ be real numbers. Taking a jump process with jump kernel $K(x, \mathrm{d}y) = \lambda(x)\Pi(x, \mathrm{d}y)$, a path from x_0 to x_k in time t in k jumps at times $(t_i)_{1\leq i\leq k}$ and locations $x_1, \dots, x_{k-1}$ can be associated with weight:

$$\lambda(x_0)\Pi(x_0, \mathrm{d}x_1)e^{-\lambda(x_1)(t_2-t_1)}\Pi(x_1, \mathrm{d}x_2) \dots e^{-\lambda(x_{k-1})(t_k-t_{k-1})}.$$

Let us define the following sequence, for $n \geq 0$, $t > 0$, $x_0 \in S$ and $A \in \mathcal{S}$:

$$\begin{aligned} P_t^n(x_0, A) =& e^{-\lambda(x_0)t}\delta_{x_0}(A) + \sum_{k=1}^{n} \int_{0<t_1<\cdots<t_k\leq t} \mathrm{d}t_1 \dots \mathrm{d}t_k \\ & \int_{S^k} \Pi(x_0, \mathrm{d}x_1) \dots \Pi(x_{k-1}, \mathrm{d}x_k)\mathbb{1}_{x_k\in A} \\ & \times \lambda(x_0)e^{-\lambda(x_0)(t_1)}\lambda(x_1)e^{-\lambda(x_1)(t_2-t_1)} \dots \lambda(x_{k-1}) \\ & e^{-\lambda(x_{k-1})(t_k-t_{k-1})} + e^{-\lambda(x_0)t}\mathbb{1}_{x_0\in A}. \end{aligned}$$

We can prove that this family of functions is increasing, and that the point-wise limit $P_t^\star(x, A) = \lim_{n\to\infty} P_t^n(x, A)$ exists for all $x \in S$ and $A \in \mathcal{S}$. We can also prove that $P_t^\star$ is a sub-Markov kernel.

The main result about the family $P_t^\star$ is the following:

Theorem A.9. *The $P_t^\star$ is the solution to the* Kolmogorov backward equation*:*

$$\frac{\partial}{\partial t}P_t^\star(x, A) = \int_S K(x, \mathrm{d}y)(P_t^\star(y, A) - P_t^\star(x, A)). \tag{A.16}$$

Every other sub-Markov kernel solution to (A.16) *is greater than $P_t^\star$. Finally, if $(P_t^\star)$ is a family of Markov kernels, i.e. if $P_t^\star(x, S) = 1$ for all $x \in S$, then it is the unique solution to* (A.16)*.*

This Theorem gives us a second characterization of Markov jump processes, through its transition functions. If the transition function of the process is a Markov kernel, then the only solution of (A.16) fully characterizes the jump process, and it uniquely characterizes the transition kernel of the jump process.

Spatial birth-and-death process

Among the Markov jump processes, birth-and-death processes have been used often to model physical phenomena, especially in biology.

We say that a Markov jump process is a birth-and-death process if the only possible transitions from a state with n elements are towards a state with either $n-1$ or $n+1$ elements. For instance, the continuous-time M/M/1 queue with an arrival parameter λ and a departure parameter ν is a simple example of a birth-and-death process.

Though there exists a large variety of birth-and-death processes, the category we will focus in this work is the spatial birth-and-death (SBD) process. This class of birth-and-death process form a Markov jump process on point process of a region (or the entirety) of $\mathbb{R}^d$, and where arrivals and departures depend on the spatial configuration of the system.

These processes have been introduced for the first time by Preston in [75]. In a spatial birth-and-death process, the law of the jump kernel K depends on the spatial configuration of the system at a given time.

To define such a process, assume that at a given time t, points are located at $X_1, \dots, X_n$ in S. Then, we need two functions b and d such that:

- b is a finite measure on $(S, \mathcal{S})$ such that the probability that a point arrives in $A \in \mathcal{S}$ between times t and $t+s$ is equal to $b(X_1, \dots, X_n; A)s$.
- $d : S \to \mathbb{R}^+$ is a measurable function such that the probability that a point x leaves the system between times t and $t+s$ is equal to $d(\{X_i, X_i \neq X\}; X)s$.

These two functions, called respectively the *birth* and the *death* functions of the process, define a Markov jump process, with state space $\mathcal{M}(S)$, the state of counting measures on S. We can consider that at each time, the elements of the Markov jump process form a point process on S.

A.5 Stability theory

The final section we will tackle in this chapter comes from the study of the stability of Markov chains. The results and definitions presented here will be used throughout Part I of this manuscript.

The study of the behavior of Markov chains is an interesting question, as it allows to obtain a lot of asymptotical results about the processes we study. In this section, $\mathbf{X}$ denotes a Markov chain with state space $\mathbb{N}$ (these results can be extended to any Markov chain with countable state space).

The first notion we define is the *irreducibility* of a Markov chain:

Definition A.3. *The Markov chain X is ϕ-irreducible if and only if there exists a measure ϕ on $\mathcal{B}$ such that whenever $\phi(A) > 0$ for $A \in \mathcal{B}$, we have $\Pi(x, A) > 0$ for all $x \in S$. A Markov jump process is irreducible if and only if its embedded Markov chain is ϕ-irreducible for some measure ϕ.*

In other words, a chain is ϕ-irreducible whenever we can find an irreducibility measure ϕ such that any event with positive measure ϕ can be reached from any given state. A consequence is that a ϕ-irreducible Markov

chain has only one *communication class*, i.e., that any state can be reached from any given given starting point with non-zero probability.

We can now move to defining notions about stability of the Markov chain. The *time of first return* to state $i \in \mathbb{N}$ is the first moment at which the chain hits state i given it started in this state:

$$T_i = \inf\{k \geq 1, X_k = i | X_0 = i\}.$$

A state i is said to be *transient* if $\mathbb{P}[T_i = \infty] > 0$ and *recurrent* otherwise. Moreover, we say that a state is *positive recurrent* if the state i is recurrent and we have:

$$\lim_{n\to\infty} \frac{1}{n} \sum_{0\leq k\leq n-1} \mathbb{1}_{\{X_k=i\}} = \pi_i > 0. \tag{A.17}$$

In other words, a state is recurrent if is return time is almost surely finite, and transient otherwise, i.e., if we have a non-zero probability to never return to it. Finally, a state is positive recurrent if we return to it a significant portion of the time. An equivalent definition to A.17 for positive recurrence is that $\mathbb{E}[T_i | X_0 = i] < \infty$, i.e., that the average return time to state i is always finite. If this mean return time to state i is infinite but it is recurrent, we say that it is *null recurrent.*

We say that the Markov chain is *recurrent* if all its states are recurrent, and *transient* if all its states are transient. Finally, we say that a chain is *positive recurrent* if all its states are positive recurrent.

Positive recurrence for Markov chain is an important property as it gives an easy characterization for the stationary distribution of the Markov chain: let us define π_i as in (A.17). Then, $(\pi_i)_{i\in\mathbb{N}}$ forms a probability distribution on $\mathbb{N}$, which is the stationary distribution for the chain $\mathbf{X}$. It also allows for the use of large deviation inequalities, and gives bounds for the speed of convergence to the stationary distribution of the chain.

Definition A.4. *We say that a Markov chain is* stable *if it is positive recurrent. Otherwise, it is* unstable.

From the definitions of positive recurrence, transience and null recurrence, this definition of stability ensures that $\mathbb{P}$-almost surely, the value of $X(t)$ is finite.

A first interesting result linking ϕ-irreducibility and state classification of a Markov chain comes from Theorem 8.2.5 from [70]:

Theorem A.10 (Meyn, Tweedie)**.** *Every ϕ-irreducible Markov chain is either transient or recurrent.*

This result about the classification of Markov chain will help us in obtaining a description of recurrence and transience of Markov chains. The main result about stability for Markov chains comes from Foster (see [44]):

Theorem A.11 (Foster, 1953)**.** *Let* $\mathbf{Y}$ *be a Markov process with countable state space* E*. Let* $C \subset E$ *be a compact subset of the state space,* $\alpha, \beta > 0$ *be two constants and* $V : \mathbb{N}^N \to \mathbb{R}^+$ *be a positive definite function. Then, if:*

$$\Delta V(x) = \mathbb{E}\left[V(\mathbf{Y}(T_1)) - V(\mathbf{Y}(0))|\, \mathbf{Y}(0) = x\right] \leq \beta \mathbb{1}_{x \in C} - \alpha \mathbb{1}_{x \notin C},$$

where t_1 *is the time of the first event in the system, then,* $\mathbf{Y}$ *is positive recurrent.*

In other words, if we find a positive definite function V, i.e., such that $V(x) > 0$ for all x, and $V(x) = 0$ if and only if $x = 0$ and a compact subset of the state space such that this subset acts as an attractor for the dynamics, then we obtain the positive recurrence for the Markov chain. Sometimes, this theorem is referred to as the Foster-Lyapunov theorem, as it is reminiscent of arguments used in stability theory to find attractors for dynamical systems, and the condition stated resembles the negative Lie derivative requirement to obtain stable points or intervals for systems of ODEs.

This class of arguments, called *drift* arguments, as we need to bound the average increase in the chain over one (or several) jumps. Unfortunately, the main limitation for the use of this Theorem is the need to find an appropriate Lyapunov for the Markov chain we study. Outside of certain go-to forms for certain classes of dynamics, there are not particular method to find an appropriate Lyapunov function for Markov jump processes. Thus, we will rely on another method to obtain stability for Markov processes: fluid limits.

Fluid limits

Fluid limits have been introduced by Rybko and Stolyar in [78] to study the stability for queues of networks using a different method than the classical arguments stated above. The main idea behind fluid scaling is the following: let $\mathbb{X}$ be a Markov chain, and we define the *fluid-scaled* sequence of processes $\mathbf{X}^n$ as:

$$\begin{cases} \mathbf{X}^n(0) & = n \\ \mathbf{X}^n(t) & = \frac{1}{n}\mathbf{X}(nt). \end{cases}$$

The goal is to study the limit as n goes to infinity of the fluid-scaled sequence $\mathbf{X}^n$. If such a function exists, we denote its value at time t as $\bar{x}(t)$. If the function $\bar{x}$ is continuous, we call it a *fluid limit* for the stochastic process $\mathbf{X}$. Usually, when studying this limit, we obtain function equations defining the function $\bar{x}$, which we call a *fluid model* for the dynamics.

We can generalize fluid scaling to any positive increasing sequence $(a_n)_{n\geq 0}$ with $\lim_{n\to\infty} a_n = \infty$. The sequence of fluid-scaled processes wth $(a_n)_{n\geq 0}$ is defined as:

$$\begin{cases} \mathbf{X}^n(0) & = a_n \\ \mathbf{X}^n(t) & = \frac{1}{a_n}\mathbf{X}(a_n t). \end{cases}$$

It is to note that multiple fluid limits can exists for a given process, as it may depend on the sequence used for scaling. For the same scaling sequence, fluid limits may not be unique. For instance, [77] show an example of a queuing system where fluid limits are random.

Definition A.5. *We say that a fluid limit is* stable *if and only if there exists* $\delta > 0$ *such that* $\bar{x}(\cdot + \delta) = 0$.

The main interest for fluid limits is its ties with positive recurrence in Markov chains. The main result linking the two comes from Theorem 4.4 from [37]:

Theorem A.12 (Dai, 1995)**.** *If the fluid limit* $\bar{x}$ *is stable, the Markov chain* $\mathbf{X}$ *is positive recurrent.*

An example to display how fluid limits work is the M/M/1 queue with an arrival rate $\lambda > 0$ and a departure rate $\mu > 0$ and an initial condition $\mathbf{X}(0)$. The stochastic recurrence for the queue length process $\mathbf{X}(t)$ is:

$$\mathbf{X}(t) = \mathbf{X}(0) + \mathcal{A}(\lambda t) - \mathcal{D}(\mu t),$$

where $\mathcal{A}$ and $\mathcal{D}$ are PPP with intensity 1 (see [31]). Let us take the fluid scaled process with $a_n = n$. We have:

$$\mathbf{X}^n(t) = \frac{1}{n}\mathbf{X}(0) + \frac{1}{n}\mathcal{A}(\lambda n t) - \frac{1}{n}\mathcal{D}(\mu n t).$$

Using the strong law of large numbers, we get the equation ruling the evolution of the fluid limit $\bar{x}$, called the *fluid model*:

$$\bar{x}(t) = 1 + (\lambda - \mu)t. \tag{A.18}$$

We can immediately see that the condition for the fluid limit to reach 0 after a certain point is $\lambda < \mu$, which is the well-known stability condition for the $M/M/1$ queue.

Among the results giving stability for fluid models, an interesting one that we will use later in this work comes from [84]:

Lemma A.13 (Shneer, Stolyar, 2020)**.** *Let* $\mathbf{X} = (X_i)_{0 \le i \le N-1}$ *be a Markov chain with the following fluid model:*

$$\begin{cases} \bar{x}_i'(t) & = \lambda_i - \psi_i(\bar{x}(t)) \\ \bar{x}(0) & = \mathbf{x}_0, \end{cases}$$

where $\mathbf{x}_0 \in \mathbb{R}^N$ (ψ_i) *are function such that:*

1. ψ_i *is non-increasing in* x_j*, for all* $j \neq i$*,*
2. *for all* i*,* ψ_i *is 0-homogenous, i.e.,* $\psi_i(st) = \psi_i(t)$ *for all* $s, t > 0$*,*
3. $\sum_i x_i(t) > 0$ *implies that* $x_i(\tau) > 0$ *for* τ *sufficiently close to* t*.*

Let $\mathcal{C} = \{\mathbf{z} \in \mathbb{R}_+^N, z_i \leq \psi_i(\mathbf{p})$ *for some* $\mathbf{p} \in \mathbb{R}_+^N\}$. *Assume there exists* $\nu \in \mathcal{C}$ *such that for all* i, $\lambda_i \leq \nu_i$. *Then, for all* $0 < \delta < K < \infty$, *there exists* $T > 0$ *such that for any trajectory with* $\|\bar{x}(0)\| = K$, *we have:*

$$\|\bar{x}(T)\| < \delta.$$

To obtain stability for the chain $\mathbf{X}$, we use this results with $K = 1$ and $\delta = 1 - \varepsilon$, for some $\varepsilon > 0$. This result linking positive recurrence and fluid limits will be used in Part I to reach a stability condition for the system.

Lemma A.13 allows to give bounds for the stability region, but in certain cases, these bounds are not tight, and it allows only for a partial description of the stability region. Unfortunately, the reciprocal for this result is not true: Bramson, in [30], showed that there exists transient queuing networks for which the fluid limit match the condition of Theorem A.12.

To obtain a reciprocal, we need to loosen the condition, and define the notion of *weak instability*, from [38]. We say that a fluid model is weakly unstable if for any fluid limit $\bar{x}$ such that $\bar{x}(0) = 0$, there exists $\delta > 0$ such that $\bar{x}(\delta) > 0$. The reciprocal for Theorem A.12 becomes:

Theorem A.14. *If the fluid model is weakly unstable, then we have:*

$$\mathbb{P}\left[\lim_{t\to\infty} \mathbf{X}(t) = +\infty\right] = 1.$$

This result implies that the Markov chain $\mathbf{X}$ is transient, which gives a description of regions where the chain $\mathbf{X}$ is positive recurrent or transient. Coming back to the M/M/1 queue, with an empty initial condition, (A.18) becomes:

$$\bar{x}(t) = (\lambda - \mu)t.$$

Immediately, we can see that if $\lambda > \mu$, the fluid limit $\bar{x}(t)$ is strictly increasing and the fluid model is weakly unstable, which gives us instability for the M/M/1 queue. This also shows a limitation of fluid limits, where it is not uncommon to obtain a stability and an instability region that do not cover all cases: here, we cannot answer the case $\lambda = \mu$ (which is null recurrent).

This concludes this chapter about the mathematical foundations of the work presented in this manuscript. The next chapter will cover the basics of wireless communications we modelled in this work.

Chapter B

Wireless Networks

This chapter focuses on wireless networks as well as some elements of information theory that will be used in this thesis. Results shown here as well as more details can be found in Volume I and II of [12], in [36] and in [8].

In our work, we will consider two types of network architectures: cellular networks and device-to-device networks. These two network architectures have a radically different conception of communications: in cellular network, the network is vertical, i.e, there is one particular user, the base station, to which all users of the network connect, either to transmit or receive data. On the opposite, device-to-device networks are horizontal in the sense that each transmitter has its own dedicated receiver, and all receiver-transmitter pairs in the networks are treated equally in the network. This chapter will cover the basics of the models we use for wireless communications.

B.1 Channel capacity and Shannon rate

When working with communication channels, a most important quantity to consider is the rate at which information is transmitted in the channel. Let us consider a simple communication system.

Figure B.1 shows a basic communication system, where W is the message to transmit, X is the channel input, Y is the channel output and $\widehat{W}$ is the transmitted message, which is an estimate of the original message W, and f (resp. g) are the encoding (resp. decoding) functions. $p(y|x)$ represents the noisy channel as a conditional probability distribution, i.e. the probability

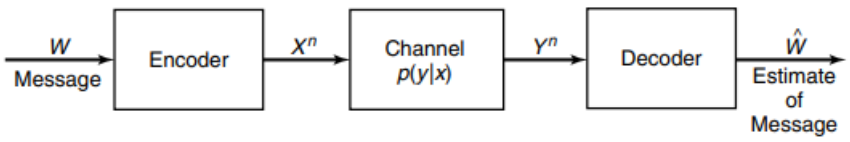

Figure B.1: Basic communication system

that the output is Y given the input is message X. This condition probability is a property of the communication channel. In this setup, the distribution of input messages p_X fully determines the joint distribution $p_{(X,Y)}(x) = p(y|x)p_X(x)$

We also define the *mutual information* of the two random variables X and Y as:

$$I(X;Y) = D_{\mathrm{KL}}(p_{(X,Y)}||p_X \otimes p_Y),$$

where D_{KL} is the Kullback-Leibler divergence (see [59]). Then, the channel capacity is defined as:

$$C = \sup_{p_X} I(X;Y).$$

In other words, the channel capacity is the maximum amount of information that can be transmitted over the communication channel with arbitrary precision. The Shannon-Hartley theorem (see [83]) gives a useful expression for channel capacity in a particular case:

Theorem B.1. *The channel capacity C in a communication channel subject to additive white Gaussian noise is equal to:*

$$C = B \log_2 \left(1 + \frac{S}{N}\right), \tag{B.1}$$

where B is the bandwidth of the channel, S is the average signal power received over the bandwidth and N is the average power of the noise and interference.

In the presence of interference, and if we consider interference as noise, the quantity $\frac{S}{N}$ has to be replaced by $\frac{S}{N+I}$, where N is the noise power and I is the interference power.This ratio is called the *Signal-to-Noise and Interference Ratio* (SINR). In the rest of this work, the channel capacity from (B.1) will be noted as $\mathcal{R}$ and referred to as the *Shannon rate*. In a more general case, when working with non-deterministic networks, the result from Theorem B.1 becomes:

$$\mathcal{R} = B\mathbb{E}\left[\log(1 + \mathrm{SINR})\right]. \tag{B.2}$$

Cover and outage probabilities

When considering SINR and channel capacity, an interesting property to study is coverage. Let us set $T > 0$ a SINR threshold. We say that a point x is in *coverage* if and only if $\mathrm{SINR}(x) > \beta$. If a point is not in coverage, then we say it is in outage.

The study of SINR cells and spatial coverage is a subject of study in itself (see Chapter 5 of [12]). In our work, we will consider the coverage probability, defined as:

Definition B.1. *Let $\beta > 0$. The* coverage probability *at point x is defined as:*

$$p_c(x, \beta) = \mathbb{P}[\text{SINR}(x) > \beta].$$

In this definition of the coverage probability, the SINR is a random variable depending on the distribution of the base station process. Using the definition of the channel capacity, we can rewrite (B.1) using the coverage probability:

Lemma B.2. *Given the coverage probability, the channel capacity can be rewritten as:*

$$\mathcal{R}(x) = \int_0^\infty \frac{p_c(x, \beta)}{\beta + 1} \mathrm{d}\beta.$$

This result is obtained by using an integration by parts on (B.2). Lemma B.2 gives a useful link tying the coverage probability and the Shannon rate, which we will exploit later in this manuscript.

B.2 Wireless networks and stochastic geometry

Stochastic geometry has emerged to become a powerful tool to model wireless networks (see [6], [48]), as it provides a flexible framework to define and compute network metrics and encapsulate the main features of wireless networks.

In this work, we will assume that base stations (BSs) will be spatially distributed according a homogeneous Poisson point process Φ with intensity $\lambda > 0$. Mobile users (MUs) are distributed according an independent homogeneous PPP Φ_u with intensity λ_u. Finally, we will assume that MUs move in a straight line with velocities i.i.d. with distribution f. The stationary and isotropy of the MU process is allows us to define the *typical MU* located at the origin.

When it comes to access policies, we assume that the networks will always be in open access, i.e., that all users can connect without restrictions and that there are no communication abandonments. We also assume that a MU will always connect to its closest antenna. This association policy defines a Voronoi diagram based on the BS process. Because they are distributed according a homogeneous PPP, it forms a PV tessellation and we can use results presented in A.3.

When modeling wireless communications, we have to take into account the attenuation of the signal among the link between the receiver and the transmitter. To take into account signal decay over the distance and electromagnetic and atmospheric phenomena, we use an omnidirectional path-loss (OPL) function to model attenuation over the link. For wireless network, we will use an OPL3 function (see Section 23.1.2 from [12]) of the form

$\ell(x) = Kx^{-\alpha}$, with $K > 0$ being a constant depending on the frequency used for the communications and $\alpha > 2$ denotes the attenuation of the signal. It is to note that this function has a singularity when x becomes close to 0.

When studying systems at a smaller scale, like D2D networks, to avoid singularities, we use the OPL2 function of the form $\ell(x) = \frac{K}{1+x^{\alpha}}$ for D2D networks, which is defined when $x = 0$. As for the path-loss exponent, for numerical applications, we will use $\alpha = 4$, which gives a satisfactory approximation of the signal attenuation in a environment with a lot of reflection and obstacles, like a city.

A phenomenon we need to take into account is fading, which models the effects of propagation of the signal in the environment. In our models, we will only consider the case of Rayleigh fading, which gives a good approximation of signal fading in urban areas (see [34]). Under Rayleigh fading, the signal over the communication channel is multiplied by a fading coefficient h_x distributed exponentially with mean $\frac{1}{\mu}$, where μ denotes the fading power in the system. When not specified, we will take a fading $\mu = 1$ in our calculations.

The interference in the network is a shot-noise of the base station process. Let us assume that the base stations in the system form a point process Φ. We can define the interference seen from transmissions at location x as:

$$I(x, \Phi) = \sum_{y \in \Phi \setminus \{x\}} K h_y \ell(\|x - y\|).$$

Assuming that the transmitter associated with the receiver located at x is at a distance r_x and that the network has a noise power density $\mathcal{N}_0$, we have:

$$\mathrm{SINR}(x) = \frac{K h_x \ell(r_x)}{\mathcal{N}_0 + I(x, \Phi)}.$$

As mentioned earlier, this rather simple SINR model encapsulates most of the key phenomena needed to model wireless and radio transmissions, and it proves to be interesting as a lot of closed-form result can be obtained from it, as shown in Part III of this manuscript.

B.3 Beam-based communications

In the latest generation of wireless communications, antennas use directional beamforming to communicate with MUs (see [49]) as this technology has emerged as a mean to increase the spectral efficiency of millimeter-wave networks ([11]). The main idea behind this technology is for antennas to use narrow and directive beams tracking users in order to increase the bandwidth in the network. The bean in which the user is located is called its *reference beam*. To ensure that the user is always located in its reference beam, the network sends a synchronization signal at a fixed frequency τ, called a *synchronization signal burst* (SSB).

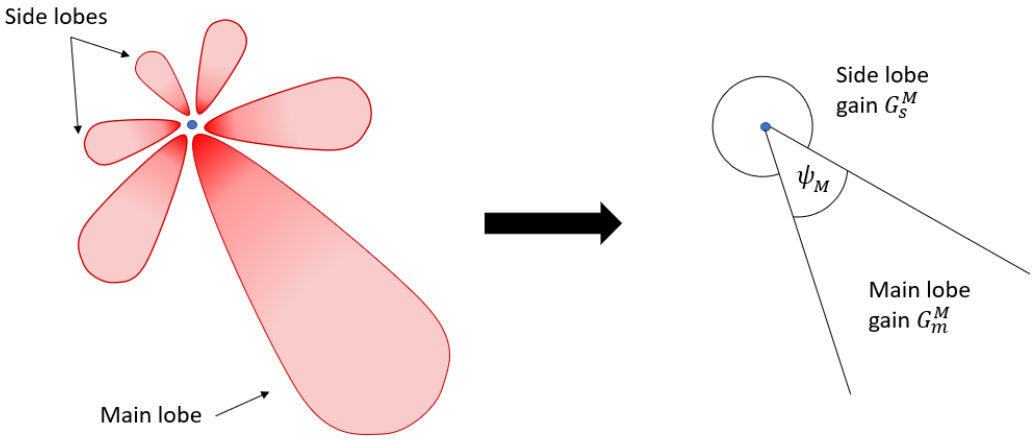

Figure B.2: Sector approximation of the antenna gains

Directional beam forming and sector approximation

In this setup, each antenna has a fixed number n of beams, usually, we have $N = 2^k$ for some $k > 0$. Under directional beamforming, the MU is tracked by the BS so that communication operate through the reference beam. We model beam-based communications using a sector approximation of the antenna. The beam tracking the user thus has an antenna gain equal to the gain of the main lobe of the antenna. To model the residual power emitted around the antenna, we add side lobes to the antenna, which users outside of the beamwidth of the main lobe see. Each beam has the same angular width $\psi = \frac{2\pi}{n}$. The main lobe is restricted to the beamwidth. The antenna gain in the macro tier is assumed to be:

$$G^M(\theta) = \begin{cases} G_m^M & \text{if } |\theta| \leq \psi_M/2 \\ G_s^M & \text{else,} \end{cases}$$

where G_m^M is the main lobe gain and G_s^M is the side lobe gain. The probability that an MU lies within the main lobe of an interfering BS is $p_m = \frac{\psi}{2\pi} = \frac{1}{n}$. The BS antenna gain g_x, seen at the origin of the system, of an interfering BS located at x in the macro tier is given by:

$$g_{M,x} = \begin{cases} G_m^M & \text{w.p.} \quad p_{M,m} \\ G_s^M & \text{w.p.} \quad 1 - p_{M,m}. \end{cases} \tag{B.3}$$

This approximation is a first order approximation of the distribution of antenna gains in space. More complex models exist to obtain more precise calculations, but they fall out of the scope of our work.

Overhead and beam reselections

When an MU crosses the boundary of the cell of its serving BS, it needs to select a new antenna to connect and it performs a *handover* to the next BS. Similarly, when an MU moves outside of its reference beam, it needs to select the next beam of its serving BS, performing a *beam reselection.*

Using stochastic geometry tools, for an MU moving in a straight line at velocity v, we can compute the time intensity ν_c of BS handovers in a wireless network using Theorem 2 of [54]:

$$\nu_c = \frac{4\sqrt{\lambda}}{\pi} v \qquad \nu_b = \frac{n\sqrt{\lambda}}{\pi} v$$

Let T_c and T_b be the time of a BS handover and a beam reselection, respectively. We define the total overhead per unit of time T_o^M as the fraction of time in which MUs are not transmitting to the network due to cell handovers and beam reselections:

$$T_o^M = \nu_c T_c + \nu_e T_b. \tag{B.4}$$

An interesting thing to note in the definition of the overhead is the existence of a velocity v such that $T_o = 1$. In this case, the moving MU spends all of its time reshuffling for new beams or new BS to connect to, and will not be able to transmit to the network. This velocity, denoted as $v_{\max}$, is equal to:

$$v_{\max} = \frac{\pi}{\sqrt{\lambda}(4T_c + nT_b)}. \tag{B.5}$$

With the previous definitions and results, we can define the *effective* Shannon rate (ESR) $\mathcal{R}_{\text{eff}}$ as:

$$\mathcal{R}_{\text{eff}}(v) = \mathcal{R}\left(1 - T_o(v)\right)^+, \tag{B.6}$$

where $x^+ \triangleq \max(0, x)$. This definition of the ESR comes from an ergodic interpretation: when the MU is reselecting a new beam, or performing a handover at the boundary between two cells in the network, it cannot transmit. Figure B.3 displays the overhead of a moving MU in a single-tier network.

Mobility-induced beam misalignment

Due to intra-cell mobility, an MU has to reselect a beam when it moves from the coverage of one beam to another. Such a beam reselection in a 5G network occurs during a synchronization signal block (SSB) burst with period τ. If the MU moves out of the main lobe of its original connection beam (also called the reference beam) between two consecutive SSB bursts without selecting a new beam, a beam misalignment occurs, namely, the MU receives from the serving BS via a side lobe. We assume, as in [54], that the probability p_{bm}^M that there is a beam misalignment event for an MU moving at velocity v is equal to:

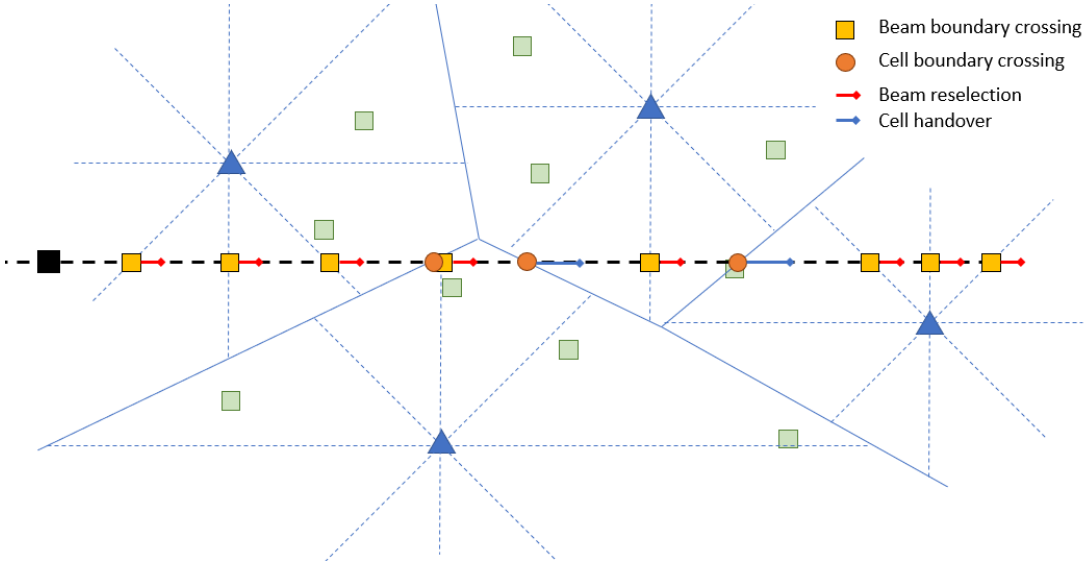

Figure B.3: Illustration of the total overhead for a moving MU. Each red (resp. blue) line represents the amount of time needed for a beam reselection (resp. a cell handover).

$$p_{\mathrm{bm}}^{M}(v) = 1 - \exp\left(-v\nu_{M,b}\tau\right), \tag{B.7}$$

where $\nu_{M,b}$ is the time intensity of beam reselections. Hence, taking this beam misalignment into account, the antenna gain $g_{M,0}$ at the serving BS of the typical MU is given by:

$$g_{M,0} = \begin{cases} G_m^M & \text{w.p.} \quad 1 - p_{\mathrm{bm}}^{M}(v) \\ G_s^M & \text{w.p.} \quad p_{\mathrm{bm}}^{M}(v). \end{cases} \tag{B.8}$$

We also have to take beam misalignment into account when computing the overhead of users in the system: if the time intensity of beam reselections is higher than the frequency of SSBs, beam reselections happen during each SSB. If the time intensity of beam reselections is lower, the user may stay in the same reference beam between two consecutive SSB bursts, and thus, there are no beam reselection. Thus the effective time intensity ν_e of beam reselections in macro tier is:

$$\nu_e = \min\left(\frac{1}{\tau}, \nu_b\right).$$

B.4 Bandwidth partitioning

The densification of wireless communication networks and the arrival of new generation communication protocols set new standards in terms of network performance, among which reliability and latency take a prominent place. To match these standards, the latest generation of telecommunication networks have introduced service differentiation as a mean to provide more flexibility and broader capacities for wireless networks. An important improvement

introduced in 5G networks is the adaptive use of multiple frequency bands available for communications ([1], [2], [88]). The idea is to increase the network capacity through a more flexible frequency band allocation, adapted to the needs of users. In such a setup, the number of bands allocated to a transmission depends on its nature: users transmitting less information (phone calls or text messages) will be allocated less frequency bands than users transmitting large amounts of data (video streaming for instance).

Service differentiation has been extensively studied in queueing networks. For instance, BCMP type queueing networks ([24]) extend the Jackson framework to the multi-class setting. When it comes to bandwidth sharing, an important problem comes from the allocation of resources to users in the network. A most common allocation is to attribute radio resources proportionnally to the needs of users as to maintain fairness in the system (see [56], [67]).

In 4G LTE and 5G wireless networks, this bandwidth partitioning is implemented in a time divisive way: when transmitting, messages are encoded during radio frames, that are each divided in a certain number fo subframes. Then, each subframe in divided in a resource grid, where frequencies are discretized, of *resource blocks*. These resource blocks consist in a certain number N_{sc}^{RB} (12 for 5G NR networks for instance) of *physical resource blocks* (PRBs) that can support in parallel $N_{symb}^{slot} \cdot 2^{\mu}$ transmissions. When a MU transmits on the network, it receives a number of resource blocs, usually contiguous to ease the allocation, of PRBs, on which it will transmit. Figure B.4 gives an illustration of the

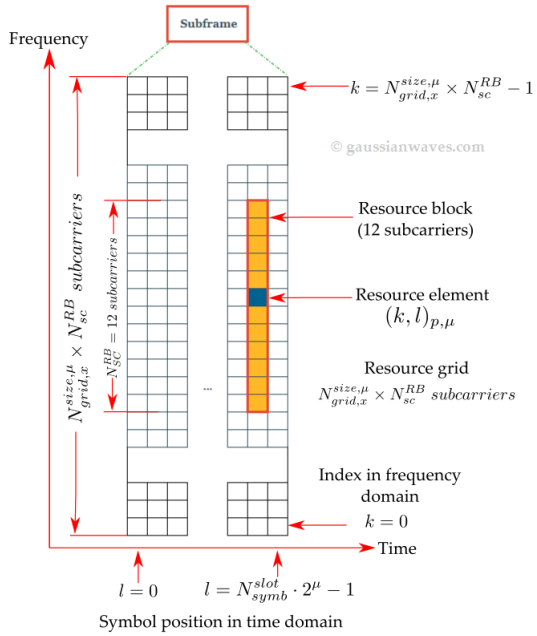

Figure B.4: Physical layer of 5G NR networks (source: [87])

When considering bandwidth partitioning in our study, we will assume that the frequency space is divided in K channels, and that each MU receives a set of bands according a probability distribution that represents user needs.

In a first time, we will assume that all PRB configuration are possible (although this is not the case in real-world applications), and we may relax this assumption later in the manuscript.

Part I

Multiclass spatial queuing networks

Chapter 1

Mathematical framework: multiclass SBD processes

1.1 Network setup: bandwidth partitioning

Let us consider an infrastructureless wireless network, where arrivals of transmitters follow a Poisson rain of intensity $\lambda > 0$ on a compact subset $\mathcal{D}$ of $\mathbb{R}^2$. We assume that the region $\mathcal{D}$ is a square torus. This choice is motivated by the difficulty to obtain results on queuing systems over the whole Euclidean plane (see [81]).

To each arriving transmitter we associate a receiver located at a fixed distance $r \geq 0$ in a random direction, with r small compared to the side of the square. This framework defines a Poisson dipole network, as introduced in [12]. We describe the configuration of users present in the network at a given time as receiver-transmitter pairs, denoted by $\Phi_t = \{(x_1, y_1), ... (x_{N_t}, y_{N_t})\}$, where N_t is the number of pairs present in the network at time t, $(x_i)_{1 \leq i \leq N_t}$ denotes the location of receivers and $(y_i)_{1 \leq i \leq N_t}$ that of transmitters. Let Φ_t^T be the point process describing the location of transmitters in the network and Φ_t^R be that of the locations of receivers at a given time t. We will refer to receiver-transmitter pairs or dipoles as *users*. The process Φ_t is thus collection of random segments of fixed length for which one of the ends is a part of a Poisson point process. In this part, we will start by studying the case $r = 0$, in which the receivers and the transmitters processes are the same as the user process. In this case, we will denote as Φ_t this unique process. Later in Part I, we will generalize the result to the case $r > 0$.

K orthogonal transmission channels of equal width are available to users arriving in the network. Channels $i \neq j$ do not interfere with one another. Let $\mathcal{P}(K)$ denote the set of non-empty subsets of $[1, 2, ..., K]$ (in the dynamics

involved in this thesis, a transmitter using $\emptyset$ as a communication channel cannot transmit any signal to its receiver and will not interfere with other users in the network). An arriving user selects a set of channels $C \in \mathcal{P}(K)$ on which to transmit according a given distribution $\{p_C\}_{C\in\mathcal{P}(K)}$. This selection is made independently of the state of the network. In the rest of this chapter, we will call C the *class* of a user.

A receiver-transmitter pair $(x, y) \in \mathcal{D}$ of class C arrives with a file of random size $L_{x,y}$ attached. File sizes for users in the same class C are i.i.d. random variables distributed with an exponential law of mean L_C. Once the file has been transmitted to the receiver, the pair or dipole (x, y) leaves the network. Finally, let $\mathcal{N}_0$ denote the thermal noise density in the network.

Wireless interactions and service times

Let ℓ be a non-negative, bounded and non-increasing path-loss function with $\langle \ell_{\mathcal{D}} \rangle < \infty$. Without loss of generality, we assume that $\ell(0) = 1$.

The interference experienced by a receiver located at $x \in \mathcal{D}$ of class C_x, whose transmitter is located at $y \in \Phi_t^T$, is equal to:

$$I(x, \Phi_t) = \sum_{z\in\Phi_t^T\setminus\{y\}} |C_x \cap C_z| \ell(\|x - z\|), \tag{1.1}$$

where C_z is the class of the transmitter located at z. Note that a receiver does not interfere with its own transmitter. We assume a low-SINR approximation, which allows us to linearize the the Shannon-Hartley formula (see Theorem B.1 and Equation (B.2)). Here, $|C_x|\ell(r)$ is the signal power received by the receiver located at $x \in \mathcal{D}$ from its transmitter, and $\mathcal{N}_0 + I(x, \Phi_t)$ is the noise and interference power seen by this receiver. Under these considerations, the rate-of-transmission function for the receiver located at x is:

$$R(x, \Phi_t) = \frac{|C_x|\ell(r)}{\mathcal{N}_0 + I(x, \Phi_t)}, \tag{1.2}$$

The instantaneous departure rate of a receiver-transmitter pair of class C with receiver located at $x \in \mathcal{D}$, at time t, is equal to:

$$d(x, t) = \frac{1}{L_C} R(x, \Phi_t). \tag{1.3}$$

Using this setup, we can formulate this problem as follows:

Definition 1.1. *The stochastic process Φ_t is a Markov jump process on the set of counting measures on $\mathcal{D}$, $\mathcal{M}(\mathcal{D})$, which we call a* BWP model. *At all times $t > 0$, Φ_t is a point process on $\mathcal{D}$.*

We define $\Delta : (\Phi_0, \lambda, \mathbf{L}, R) \mapsto \Phi_t$ as the realization of the dynamics, where Φ_0 is the initial condition of the network, λ is the arrival rate, $\mathbf{L}$ is the vector of average file sizes and R is the rate-of-transmission function.

To understand why Φ_t is a Markov jump process, we can reformulate the dynamics presented earlier using a stochastic recurrence relation for each of the subprocesses $\Phi_{C,t}$. Let $(T_{C,n})_{n\leq 0}$ be the times at which events (either an arrival or a departure) happen in $\Phi_{C,t}$. The relation between $\Phi_{C,T_{C,n}}$ and $\Phi_{C,T_{C,n+1}}$ is given by:

$$\begin{cases} \Phi_{C,T_{C,n+1}} & = \Phi_{C,T_{C,n}} + \mathcal{B}_{C,n} - \mathcal{D}_{C,n}, \\ T_{C,n+1} & = T_{C,n} + \tau_{C,n}, \end{cases} \tag{1.4}$$

where $\mathcal{B}_{C,n}$ and $\mathcal{D}_{C,n}$ are $\mathcal{M}(\mathcal{D})$-valued random variables that are defined as follows: let b_C be a real-valued random variable distributed according to an exponential distribution with rate λp_C and $\mathbf{d}_{C,n}$ be a $\mathbb{R}^{\Phi_{C,n}(\mathcal{D})}$-valued random variable where each coordinate is distributed according an independent exponential distribution with rate $\frac{1}{L_C}R(x_i, \Phi_{T_{C,n}})$, for each $x_i \in \Phi_{C,T_{C,n}}$. Then, the values of $\mathcal{B}_{C,n}$ and $\mathcal{D}_{C,n}$ are given as follows :

- $\mathcal{B}_{C,n}$ is equal to the null measure if $b_C \geq \min \mathbf{d}_{C,n}$, or equal to δ_x, where x is sampled uniformly in $\mathcal{D}$ otherwise;

- $\mathcal{D}_{C,n}$ is equal to the null measure if $b_C \leq \min \mathbf{d}_{C,n}$ or if $\Phi_{C,n}(\mathcal{D})$ in the null measure, or equal to δ_x, for some $x \in \Phi_{C,n}$.

Finally, the time between events is equal to $\tau_{C,n} = \min\{b_C, \min \mathbf{d}_{C,n}\}$. With this stochastic recurrence, we can see that Φ_t is a jump process, and the Markov property comes from the exponential distribution of the file sizes for each user and of the time between arrivals.

We define $\langle \cdot_{\mathcal{D}} \rangle$ as follows:

$$\langle f_{\mathcal{D}} \rangle = \begin{cases} \int_{\mathcal{D}} f(\|x\|)\mathrm{d}x, & \forall f : \mathbb{R} \to \mathbb{R} \\ \int_{\mathcal{D}} f(x,0)\mathrm{d}x, & \forall f : \mathbb{R}^2 \times \mathbb{R}^2 \to \mathbb{R}, \end{cases} \tag{1.5}$$

whenever the integrals are defined. We use here the same notation for two different notions; this choice is motivated by results presented in this part. Table 1.1 summarizes the notation we use in this part.

1.2 Monotonicity and irreducibility

A first result about BWP models we can prove is the following.

Theorem 1.1. *Φ_t is a ϕ-irreducible Markov jump process on $\mathcal{M}(\mathcal{D})$.*

It is to note that the similarity in notation between ϕ-irreducibility and the point process Φ_t is coincidental, the two notions are independent.

Proof. Let ϕ be the set function defined as:

Notation	Description
Φ_t^R, Φ_t^T	Receiver (resp. transmitter) locations at time t
$\Phi_{C,t}$	Point process of users of class C at time t
$\mathcal{P}(K)$	Set of subsets of $[1, ... K]$ with the exception of $\emptyset$
ℓ	Path-loss function
r	Receiver-transmitter distance
λ	Intensity of the arrival process
$(p_C)_{C\in\mathcal{P}(K)}$	Arrival distribution of users of each type
L_C	Average file size for users of class C
R	Rate-of-transmission function
$\mathcal{N}_0$	Thermal noise density in the network
$\langle \ell_{\mathcal{D}} \rangle$	$\int_{\mathbf{x}\in\mathcal{D}} \ell(\|\mathbf{x}\|)\mathrm{d}\mathbf{x}$
$\Phi_{0,C}$	Stationary point process of users of type C
μ_C	Spatial intensity of point process $\Phi_{0,C}$
$\mathbb{E}^0_{\Phi_{0,C}}$	Palm expectation with respect to $\Phi_{0,C}$

Table 1.1: Table of notations

– $\phi(\{0_{\mathcal{M}(S)}\}) = 1$, where $0_{\mathcal{M}(S)}$ is the measure associated with the null counting measure,

– For $k \in \mathbb{N}$ and $B_1, B_2, ..., B_N$ disjoint Borel subsets of S, we define the event $A_n = \{\Phi \in \mathcal{M}(S) : \Phi(S) = n, \Phi = (y_1, y_2, ..., y_n) \in B_1 \times \cdots \times B_n, \Phi(B_1) > 0, ... \Phi(B_n) > 0\}$. We then set:

$$\phi(A_n) = \frac{1}{2^n} H(B_1)H(B_2) ... H(B_n), \tag{1.6}$$

where H is a Haar measure on the square torus $\mathcal{D}$.

Here, ϕ is a set function on the *semiring* of sets $(A_n)_{n\in\mathbb{N},(B_i)\in\mathcal{F}^n}$. Using Theorem 11.3 from [26], we can extend ϕ in a unique way to a measure on the σ-field generated by the set of events $\{A_n : n \in \mathbb{N}, (B_i) \in \mathcal{F}^n\}$, which is equal to $\mathcal{F}$. For ease of notation, we will denote this measure by ϕ as well. This way, ϕ is a measure defined on the set of counting measures $\mathcal{M}(S)$.

To obtain ϕ-irreducibility, we will proceed in two steps: in the first step, we prove that, from each state X with N points, we can reach the empty state with positive probability, and in the second step, we prove that, from the empty state, we can reach any state A with $\phi(A) > 0$ with positive probability in a finite number of steps, which allows us to conclude.

Let us assume that at a given time t, the SBD process is in state $\mathbf{x} = \{x_1, ..., x_n\} \in S^N$ with N being the number of points in the SBD. The probability that we have the departure of the N points in the next N steps is equal to:

$$\mathbb{P}[N \text{ departures in a row} \,|\Phi_t] = \prod_{i=1}^{N} \frac{d_{C_i}}{d_{C_i} + b_{C_i}},$$

where $b_{C_i} = \lambda p_{C_i} |\mathcal{D}|$ and $d_{C_i} = \frac{1}{L_{C_i}} R(x_i, \Phi_{t_i})$, with Φ_{t_i} being the network configuration after the departure of the user (x_i, y_i). This probability is non-null, i.e., we can reach the null measure with nonzero probability from any other state.

Similarly, assume we start from the empty state, let n be an integer, $B_1, \dots, B_n$ be n disjoint Borel subsets of S, and let us define A_n as previously. By definition, $\phi(A_n) > 0$. The probability to reach A_n from the empty state $\emptyset$ can be expressed as:

$$\mathbb{P}^n(\emptyset, A_n) = \int_{y_1 \in B_1} \dots \int_{y_n \in B_n} \int_{t_1=0}^{\infty} \int_{t_2=t_1}^{\infty} \dots \int_{t_n=t_{n-1}}^{\infty} H(\mathrm{d}y_1) \dots H(\mathrm{d}y_n)$$
$$e^{-\lambda p_{C_1} t_1} e^{-\lambda p_{C_2}(t_2 - t_1)} \dots e^{-\lambda p_{C_n}(t_n - t_{n-1})} \lambda p_{C_1} \mathrm{d}t_1 \dots \lambda p_{C_n} \mathrm{d}t_n \prod_i \frac{b_{C_i}}{b_{C_i} + d_{C_i}},$$

where C_i denotes the class of the i-th user. This probability is positive, which means that we can reach A_n from the empty measure with positive probability in n steps, which gives us ϕ-irreducibility for the process Φ_t. □

The second property we need for our study is stochastic monotonicity, which we use to obtain bounds for the dynamics of the network through the definition of queuing systems that dominate or are dominated by the original dynamics. We need the following theorem:

Theorem 1.2. *Let $\Phi = \Delta(\Phi_0, \lambda, d)$ and $\Phi' = \Delta(\Phi'_0, \lambda', d')$. The following conditions are sufficient for Φ' to dominate Φ (with all the other parameters taken equal) :*

i) $\lambda \leq \lambda'$;

ii) $\mathbf{L} \leq \mathbf{L}'$;

iii) for all point processes $\Psi \leq_i \Psi'$ on $\mathcal{D}$ and $x \in \mathcal{D}$, $R'(x, \Psi') \leq R(x, \Psi)$;

iv) $\Phi_0 \subseteq \Phi'_0$.

It is to note that condition *iii)* is met when we have two path-loss functions ℓ and ℓ' such that for all $r \geq 0$, $\ell(r) \leq \ell'(r)$.

Proof. To obtain domination, we use a coupling argument between two instances of the dynamics to obtain the domination relation, similar as the ones used in Appendix B of [81].

Let us take $0 < \lambda < \lambda'$ with the same fixed initial condition Φ_0, a vector $\mathbf{L}$ and a rate-of-transmission function R, and let $\Phi_t = \Delta(\Phi_0, \lambda, d)$ and $\Phi'_t = \Delta(\Phi_0, \lambda', d)$. The quantities related to Φ' will be denoted with a prime. We want to prove that for all times $0 \leq t$, $\Phi_t \subseteq \Phi'_t$.

We couple both the arrival and the departure processes in the network as follows: the arrival process of Φ is a Poisson rain $\mathcal{A}$ with parameter λ, and the arrival process for Φ' is $\mathcal{A} \cup \mathcal{A}'$, with $\mathcal{A}'$ being a Poisson rain with

intensity $\lambda' - \lambda > 0$ independent from $\mathcal{A}$, so that common arrivals in Φ_t and Φ'_t happen at the same locations and times. Using this coupling, we will show that, at all times t, $\Phi_t \subseteq \Phi'_t$.

At time $t = 0$, we have trivially $\Phi_0 \subseteq \Phi_0$. At time $t > 0$, we know that both $\Phi_t(\mathcal{D})$ and $\Phi'_t(\mathcal{D})$ are almost surely finite. Let us write $\Phi_t = \sum_{C\in\mathcal{P}(K)} \sum_{i=1}^{\Phi_{C,t}(\mathcal{D})} \delta_{x_{C,i}}$ and $\Phi'_t = \sum_C \sum_{i=1}^{\Phi'_{C,t}(\mathcal{D})} \delta_{x'_{C,i}}$.

Assume that up to time t, $\Phi_t \subseteq \Phi'_t$ and assume that tne next event happens at a time $\hat{t} \geq t$. It can be one of the following nature:

- The arrival of a user of class C in Φ_t;
- The arrival of a user of class C in Φ'_t;
- The departure of a user of class C in Φ_t;
- The departure of a user of class C in Φ'_t.

Because arrivals are coupled, an arrival in either Φ_t or Φ'_t maintains the inclusion. The same holds if an element of Φ_t leaves. The last case to look at is the departure of an element x of Φ'_t.

Let $\hat{t}^-$ be such that $\hat{t}^- = \hat{t}$ but the departure of x has not happened yet. From our assumptions, we know that $\Phi_{D,\hat{t}^-} \subseteq \Phi'_{D,\hat{t}^-}$ for all classes $D \in \mathcal{P}(K)$. Assume the next departure is for a user at x of class $C \in \mathcal{P}(K)$:

$$\begin{aligned} R(x, \Phi_{\hat{t}^-}) &= \frac{|C|\ell(r)}{\mathcal{N}_0 + \sum_{U\in\mathcal{P}(K)} \sum_{y\in\Phi_{U,\hat{t}^-}} |C\cap U|\ell(\|x-y\|)} \\ &\geq \frac{|C|\ell(r)}{\mathcal{N}_0 + \sum_{U\in\mathcal{P}(K)} |C\cap U| \left(\sum_{y\in\Phi_{U,\hat{t}^-}} \ell(\|x-y\|) + \sum_{y\in\Phi'_{U,\hat{t}^-}\setminus\Phi_{U,\hat{t}^-}} \ell(\|x-y\|)\right)} \\ &= R(x, \Phi'_{\hat{t}^-}). \end{aligned}$$

In other words, the departure rates in $\Phi_{\hat{t}^-}$ are larger than in $\Phi'_{\hat{t}^-}$.

We take the *Poisson imbedding* of the departure processes (see [31]): let $\mathcal{D}_{C,t}$ and $\mathcal{D}'_{C,t}$ be the point processes of users of class C that left each system up to time t. These processes have respective stochastic intensities $\frac{1}{L_C} R(x, \Phi_t)$ and $\frac{1}{L_C} R(x, \Phi'_t)$. Using Lemma 3 from [31], we can imbed them on the same Poisson point process $\mathcal{N}$ of intensity 1 on $\mathbb{R}^2$.

Using this Poisson imbedding, any point x leaving $\Phi'_{C,\hat{t}^-}$ has already left $\Phi_{C,\hat{t}^-}$, which proves that the inclusion is maintained if the next event to come is a departure in Φ'_t and this concludes the proof of Condition i).

To obtain the other conditions, we use the same argument and we compare the rate-of-transmission functions in each case to get the required inclusion. □

Theorem 1.2 is central to our study, because it will allow us to bound from above and below the dynamics of the network we are studying in order to obtain bounds for the limits of the stability region of the network.

1.3 Critical arrival rate

In the definition of the dynamics we presented here, the value of the arrival parameter λ plays an important role on the behavior of the dynamics of the system. Intuitively, if λ becomes too large, then no receiver-transmitter pair can transmit and the population of the system explodes, preventing arriving users from transmitting. Conversely, if λ becomes very low, transmissions can terminate and we can conjecture that the population of the system can stay bounded. The study of this particular kind of network is also dependent on inter-class interactions, as not all users interfere with each other.

The first result linking the value of λ and the stability of the system is the following:

Theorem 1.3. *Under the foregoing assumptions, there exist two values* $0 \leq \lambda_c^- \leq \lambda_c^+$ *such that:*

- $\forall \lambda < \lambda_c^-$, Φ_t *is stable;*
- $\forall \lambda > \lambda_c^+$, Φ_t *is unstable.*

Proof. This theorem is a consequence of Theorem 1.2: if the system is stable for a given λ_0, then it is stable for each $\lambda < \lambda_0$ and if the system is unstable for a given λ_1, then it is unstable for all $\lambda > \lambda_1$. The existence of cutoff (or critical) arrival rates is well-established in monotonic queueing networks, and was adapted to spatial birth-and-death processes (see Theorems 1 and 2 of [80] for instance). Let λ_c^- and λ_c^+ be defined as:

$$\lambda_c^- = \sup_{\lambda>0}\{\lambda \text{ such that } \Phi_t \text{ is stable}\},$$
$$\lambda_c^+ = \inf_{\lambda>0}\{\lambda \text{ such that } \Phi_t \text{ is unstable}\}.$$

Φ_t is an irreducible Markov chain on $\mathcal{M}(\mathcal{D})$. We know that the Markov chain is either recurrent or transient (see Theorem A.10). Using stochastic monotonicity in the network from Theorem 1.2, we know that the chain Φ_t is positive recurrent for all $\lambda \leq \lambda_c^-$ and transient for all $\lambda \geq \lambda_c^+$, which gives $\lambda_c^- \leq \lambda_c^+$. Since the system is trivially stable for $\lambda = 0$ (in which case Φ_t is constantly equal to the null measure), λ_c^- and λ_c^+ are well defined and $\lambda_c^- \geq 0$, which concludes the proof.

□

Once the two values of λ_c^+ and λ_c^- are defined, a natural question arising is their respective values. In a favorable case, these two values are equal, which would give a clear description of the stability region of the network. We can prove this intermediate result, giving a simple lower bound for λ_c^- and an upper bound for λ_c^+:

Lemma 1.4. λ_c^- *and* λ_c^+ *satisfy:*

$$\frac{\ell(r)}{K\bar{L}\langle \ell_{\mathcal{D}} \rangle} \leq \lambda_c^- \leq \lambda_c^+ \leq \frac{K\ell(r)}{\underline{L}\langle \ell_{\mathcal{D}} \rangle}, \tag{1.7}$$

where $\bar{L} = \max_C L_C$, $\underline{L} = \min_C L_C$ *and* $\langle \ell_{\mathcal{D}} \rangle = \int_{x \in \mathcal{D}} \ell(\|x\|) \mathrm{d}x$.

Proof. The rate-of-transmission is bounded from below by that where all interfering users transmit on all channels (i.e., are of class $[1, \dots, K]$) and the transmitting user uses only one channel, i.e., for all x, t:

$$R(x, \Phi_t) \geq R_u(x, \Phi_t) \triangleq \frac{\ell(r)}{\mathcal{N}_0 + \sum_{y \in \Phi_t \setminus \{x\}} K\ell(\|x - y\|)}.$$

Moreover, by definition, $\mathbf{L} < \bar{L}$ component-wise.

Conversely, the rate-of-transmission is bounded from above by that where interfering users use a single channel and the transmitting users use all K channels, i.e., for all x, t:

$$R(x, \Phi_t) \leq R_d(x, \Phi_t) \triangleq \frac{K\ell(r)}{\mathcal{N}_0 + \sum_{y \in \Phi_t \setminus \{x\}} \ell(\|x - y\|)},$$

and $\underline{L} \leq \mathbf{L}$ component-wise. For any given initial condition Φ_0 and arrival rate λ, let $\Phi_{u,t} = \Delta(\Phi_0, \lambda, \underline{L}, R_u)$ and $\Phi_{d,t} = \Delta(\Phi_0, \lambda, \bar{L}, R_d)$. Φ_u and Φ_d two monotype dipolar Poisson networks, as defined in [80]. Using the main result of [80], we know that the cut-off arrival rate is equal to $\frac{\ell(r)}{K\bar{L}\langle \ell_{\mathcal{D}} \rangle}$ for $\Phi_{d,t}$ and to $\frac{K\ell(r)}{\underline{L}\langle \ell_{\mathcal{D}} \rangle}$ for $\Phi_{u,t}$.

We apply Theorem 1.2, which states that $\Phi_{u,t}$ dominates Φ_t and $\Phi_{d,t}$ is dominated by Φ_t to obtain the intended inequality. Since $\frac{\ell(r)}{K\bar{L}\langle \ell_{\mathcal{D}} \rangle} > 0$ and $\frac{K\ell(r)}{\underline{L}\langle \ell_{\mathcal{D}} \rangle} < \infty$, we can conclude that $0 < \lambda_c^-$ and $\lambda_c^+ < \infty$. □

When taking $K = 1$ in (1.7), we obtain:

$$\lambda_c^- = \lambda_c^+ = \frac{\ell(r)}{\langle \ell_{\mathcal{D}} \rangle L},$$

which is the value of the critical arrival rate obtained in [80]. In the light of this remark, we can hope to obtain that $\lambda_c^- = \lambda_c^+$ in the multiclass system as well, and in this case, which we will also call critical arrival rate.

Chapter 2

Stability of symmetric systems

In this chapter, we will study the BWP model in a particular case, which introduces several simplifications in the combinatorics of the system: *symmetric* systems.

Definition 2.1. *A BWP model is* symmetric*, if all users transmitting on the same number of bands have the same stochastic properties, i.e., whenever* $|C| = |D|$*, we have* $p_C = p_D$ *and* $L_C = L_D$*.*

An instance of a symmetric model is that of a system where user needs are split in K categories, depending on their needs (e.g. phone calls, text messages, web browsing or video streaming). Each arriving user has a probability p_j of having a need of category j. Upon arrival, users with needs of category j are given a set of j bands to transmit, sampled uniformly at random among the $\binom{K}{j}$ possibilities. Thus, the probability that a user transmits on a given set C of j bands is equal to $p_C = \frac{p_j}{\binom{K}{j}}$. The quantity of information this arriving user has to transmit to the network is thus sampled from an exponential distributions with parameter L_j with $1 \leq j \leq K$. Setting $L_C = L_j$ and $p_C = \frac{p_j}{\binom{K}{j}}$ gives an example of a symmetric system. The symmetry in the system will be important to simplify the combinatorics we will encounter in Section 2.1, when proving Theorem 2.2.

In this chapter, we study the stability of symmetric BWP models as defined in the previous parts. Using Theorem 1.2, we bound from above and from below the dynamics in the network in order to obtain meaningful bounds in the symmetric case to describe the stability region of the system in terms of the value of λ.

2.1 Discretization of the dynamics

To study our dynamics, we introduce the following discretization: for $\varepsilon > 0$, we tessellate $\mathcal{D}$ in N_ε square cells of side length ε, such that the origin is at the center of its cell. We denote by A_i the cell centered at $a_i \in \mathcal{D}$. Finally, we introduce the stochastic process $\mathbf{X}_\varepsilon(t) = (X_{i,C}(t))_{0 \leq i \leq N_\varepsilon - 1, C \in \mathcal{P}(K)}$, where for all i, C, $X_{i,C}(t) = \Phi_{t,C}(A_i)$ is the number of receiver-transmitter pairs of type C in cell i.

We now use this discretization of the dynamics to define two *interference queueing networks* (as defined in [81]) $\bar{\mathbf{X}}_\varepsilon$ and $\underline{\mathbf{X}}_\varepsilon$ with state space $\mathbb{N}^{N_\varepsilon \times 2^K - 1}$ such that:

- $\bar{\mathbf{X}}_\varepsilon$ dominates $\mathbf{X}_\varepsilon$
- $\underline{\mathbf{X}}_\varepsilon$ is dominated by $\mathbf{X}_\varepsilon$.

Let $\bar{X}_{i,C}(t)$ and $\underline{X}_{i,C}(t)$ denote the respective number of users of type C in cell i in each of the two processes. For a given configuration of each process, we define the dynamics as follows:

- The birth process of $\bar{\mathbf{X}}_\varepsilon$ is a Poisson rain of intensity $\lambda|\mathcal{D}|$ and the death rate for users in cell i of class C at time t is $\frac{\bar{X}_{i,C}(t)}{L_C} \bar{R}_{i,C}(t)$
- The birth process of $\underline{\mathbf{X}}_\varepsilon$ is a Poisson rain of intensity $\lambda|\mathcal{D}|$ and the death rate for users in cell i and class C at time t is $\frac{\underline{X}_{i,C}(t)}{L_C} \underline{R}_{i,C}(t)$.

To define the functions $\bar{R}_{i,C}$ and $\underline{R}_{i,C}$, we start by defining two path-loss functions ℓ^ε and ℓ_ε as follows:

$$\begin{cases} \ell^\varepsilon(x,y) = \ell^\varepsilon(a_i, a_j) & \forall x \in A_i, y \in A_j, \text{with} \\ \ell^\varepsilon(a_i, a_j) = \max\left\{\ell(\|b_i - b_j\|), b_j \in \mathcal{V}_j, b_i \in \mathcal{V}_i\right\}, \end{cases} \tag{2.1}$$

and

$$\begin{cases} \ell_\varepsilon(x,y) = \ell_\varepsilon(a_i, a_j) & \forall x \in A_i, y \in A_j, \text{with} \\ \ell_\varepsilon(a_i, a_j) = \min\left\{\ell(\|b_i - b_j\|), b_j \in \mathcal{V}_j, b_i \in \mathcal{V}_i\right\}, \end{cases} \tag{2.2}$$

where, for $0 \leq i \leq N_\varepsilon - 1$, we define $\mathcal{V}_i = \{b_i, \|b_i - a_i\| \in \{0, \varepsilon\}\}$. This way, we know that for all $x, y \in \mathcal{D}$, we have:

$$\ell_\varepsilon(x,y) \leq \ell(\|x - y\|) \leq \ell^\varepsilon(x,y). \tag{2.3}$$

Using the dominated convergence theorem, we get:

$$\lim_{\varepsilon\to 0^+}\langle \ell^{\varepsilon}_{\mathcal{D}}\rangle = \lim_{\varepsilon\to 0^+}\langle \ell_{\varepsilon,\mathcal{D}}\rangle = \langle \ell_{\mathcal{D}}\rangle, \tag{2.4}$$

where $\langle\cdot_{\mathcal{D}}\rangle$ is defined in (1.5). Because of the square torus topology of $\mathcal{D}$, we have:

$$\forall i,\quad \sum_{k=0}^{N_\varepsilon-1}\ell^{\varepsilon}(a_i,a_k) = \sum_{k=0}^{N_\varepsilon-1}\ell^{\varepsilon}(0,a_k) = \frac{1}{\varepsilon^2}\langle \ell^{\varepsilon}_{\mathcal{D}}\rangle. \tag{2.5}$$

The same result holds for ℓ_ε.

The interferences $\bar{I}_{i,C}$ and $\underline{I}_{i,C}$ experienced by users in cell i of class C and with path-loss functions ℓ^ε and ℓ_ε are respectively equal to:

$$\begin{aligned}
\bar{I}_{i,C}(t) &= \sum_{k=0}^{N_\varepsilon-1}\sum_{U\in\mathcal{P}(K)}|C\cap U|\ell^{\varepsilon}(a_k,a_i)\left(\bar{X}_{k,U}(t)-\mathbf{1}_{\{U=C,i=k\}}\right)\\
\underline{I}_{i,C}(t) &= \sum_{k=0}^{N_\varepsilon-1}\sum_{U\in\mathcal{P}(K)}|C\cap U|\ell^{\varepsilon}(a_k,a_i)\left(\underline{X}_{k,U}(t)-\mathbf{1}_{\{U=C,i=k\}}\right).
\end{aligned}$$

Finally, the rate-of-transmission functions of users in cell i of class C are defined by:

$$\bar{R}_{i,C}(t) = \frac{|C|}{\mathcal{N}_0+\bar{I}_{i,C}(t)},\qquad \underline{R}_{i,C}(t) = \frac{|C|}{\mathcal{N}_0+\underline{I}_{i,C}(t)}.$$

Theorem 2.1. *$\bar{\mathbf{X}}_\varepsilon$ and $\underline{\mathbf{X}}_\varepsilon$ are two irreducible Markov jump processes with state space $\mathbb{N}^{N_\varepsilon\times 2^K-1}$. Moreover, $\bar{\mathbf{X}}_\varepsilon$ stochastically dominates $\mathbf{X}_\varepsilon$, and $\underline{\mathbf{X}}_\varepsilon$ is stochastically dominated by $\mathbf{X}_\varepsilon$.*

Proof. From 2.3, we can obtain that for all $C\in\mathcal{P}(K)$, $0\le i\le N_\varepsilon-1$, $x\in A_{i,C}$ and a given network configuration Φ_t, we have:

$$\bar{R}_{i,C}(t)\le R(x,\Phi_t)\le \underline{R}_{i,C}(t). \tag{2.6}$$

To obtain the domination relation, we can now apply Theorem 1.2. Irreducibility is obtained by developing the same argument as for Theorem 1.1, which concludes the proof. □

Using Theorem 2.1, we can now reduce the study of the SBD process Φ_t to the study of the stability of the two processes $\underline{\mathbf{X}}_\varepsilon$ and $\bar{\mathbf{X}}_\varepsilon$. In the next section, we introduce a framework to obtain a condition on the arrival rate such that the former is unstable, and the latter is stable.

2.2 Fluid model and fluid limits

From the definitions of the dynamics in our system, we can establish an equation for the dynamics of $\bar{\mathbf{X}}_\varepsilon$, which will allow us to obtain a condition on λ_c^- for the stability of the system.

Let $(\mathcal{A}_{i,C})$ and $(N_{i,C})$ be two families of independent Poisson processes with intensity 1. By definition of the dynamics of the discretized systems, arrivals of users in cell i of class C happen with rate $\lambda p_C \varepsilon^2$. If the system is in state $x = (x_{i,C}) \in \mathbb{N}^{N_\varepsilon \times 2^K - 1}$ at time t, users in cell i and class C have a departure rate equal to $\frac{1}{L_C} x_{i,C}(t) \bar{R}_{i,C}(t)$. We thus obtain the following equation ruling the evolution of the population in the chain $\bar{\mathbf{X}}_\varepsilon$:

$$\bar{X}_{i,C}(t) = \bar{X}_{i,C}(0) + \mathcal{A}_{i,C}(\lambda p_C \varepsilon^2 t) - N_{i,C}\left(\frac{1}{L_C}\int_0^t \bar{X}_{i,C}(u)\bar{R}_{i,C}(u)\mathrm{d}u\right). \tag{2.7}$$

The goal of this section is to find a condition on λ so that the Markov chain $\bar{\mathbf{X}}_\varepsilon(t)$ is positive recurrent.

2.3 Main result

In this section, we study the stability of the system through stochastic domination and the use of a discretization of the dynamics of the SBD process. We state the following theorem:

Theorem 2.2. *In the symmetric setup,* $\lambda_c^- = \lambda_c^+ \triangleq \lambda_c$*, where* λ_c *is the* critical *arrival rate, equal to:*

$$\lambda_c = \frac{K\ell(r)}{\langle \ell_{\mathcal{D}} \rangle \mathfrak{L}}, \tag{2.8}$$

where $\mathfrak{L} \triangleq \sum_C p_C |C| L_C$.

We start by proving Theorem 2.2 in the case $r = 0$ (we remind that we assumed, without loss of generality, that $\ell(0) = 1$). We then extend the result in the case $r > 0$ to obtain the intended stability condition.

Stability of the dominating chain

We start by studying the stability of the chain $\bar{\mathbf{X}}_\varepsilon$. The stability condition for the chain is obtained though the study of its fluid limits. We can state the following result:

Theorem 2.3. *The fluid limits for the chain* $\bar{\mathbf{X}}_\varepsilon$ *exist and are solutions to the following system of equations:*

$$\bar{x}'_{i,C}(t) = \lambda p_C \varepsilon^2 - \frac{1}{L_C} \frac{|C|\bar{x}_{i,C}(t)}{\sum_{k=0}^{N_\varepsilon - 1} \sum_{U \in \mathcal{P}(K)} |C \cap U| \ell^\varepsilon(a_k, a_i) \bar{x}_{k,U}} \quad \text{if } \bar{\mathbf{x}}(t) \neq 0$$
$$\bar{\mathbf{x}}_0 = \bar{\mathbf{X}}_\varepsilon(0).$$

In this theorem, the convergence is taken in the sense of (A.1). The proof of this result, based on a construction presented in [76], is presented in Section 3.1. It is to note that these dynamics are not well-defined in the case $\bar{\mathbf{x}}(t) = 0$, but we do not need such a definition: the results about stability and fluid limits we use involve fluid limits with a strictly positive initial condition.

Once the evolution of the fluid limit is established, we can obtain the following Theorem:

Theorem 2.4. *Let $\varepsilon > 0$ and $\bar{\lambda}_\varepsilon = \frac{K}{\mathfrak{L}\langle \ell^\varepsilon_{\mathcal{D}} \rangle}$. If $\lambda < \bar{\lambda}_\varepsilon$, then the chain $\bar{\mathbf{X}}_\varepsilon$ is stable.*

Proof. To obtain stability for the chain $\bar{\mathbf{X}}_\varepsilon$, we will rely fluid limits and Lemma A.13. We start by obtaining the existence of fluid limits for this chain. The proof of this result is presented in Section 3.2 of the next chapter. □

We know from Theorem 2.1 that the process $\bar{\mathbf{X}}_\varepsilon$ dominates the original dynamic. From Theorem 1.2, we obtain that, for all $\varepsilon > 0$, $\lambda_c \geq \frac{K}{\mathfrak{L}\langle \ell^\varepsilon_{\mathcal{D}} \rangle}$. Taking the limit as ε goes to 0 gives us:

$$\lambda_c^- \geq \frac{K}{\mathfrak{L}\langle \ell_{\mathcal{D}} \rangle}.$$

Instability of the dominated chain

We know from Theorem A.14 that the conditions to obtain instability for Markov chains are weaker than the ones to obtain stability. Unfortunately, to use this result, we have to study fluid limits starting from 0, and the dynamics of our fluid limit model are not defined when $\bar{\mathbf{x}} = 0$.

To obtain instability for the system, we use stochastic domination and an adequate Markov chain to bound $\mathbf{X}_\varepsilon$ from below. We have the following theorem:

Theorem 2.5. *Let $\underline{\lambda}_\varepsilon = \frac{K}{\langle \ell_{\varepsilon,\mathcal{D}} \rangle \mathfrak{L}}$. In the symmetric case, if $\lambda > \underline{\lambda}_\varepsilon$, then $\underline{\mathbf{X}}_\varepsilon$ is unstable.*

The proof of this theorem is presented in Section 3.3. We know that the network is unstable if $\lambda > \frac{K}{\langle \ell_{\varepsilon,\mathcal{D}} \rangle \mathfrak{L}}$ for each $\varepsilon > 0$. Taking the limit as ε goes to 0, we conclude:

$$\lambda_c^+ \leq \frac{K}{\langle \ell_{\mathcal{D}} \rangle \mathfrak{L}}. \tag{2.9}$$

When combining the results of Theorem 2.4 and Theorem 2.5, we obtain that:

$$\lambda_c^- = \lambda_c^+ = \frac{K}{\langle \ell_{\mathcal{D}} \rangle \mathfrak{L}}, \tag{2.10}$$

which concludes the proof of Theorem 2.2 in the case $r = 0$.

Generalization to $r > 0$

In the previous section, all the calculations were made with the assumption that $r = 0$, i.e., in the case where the receiver and the transmitter are located in the same cell in the discretized system. To generalize the result of Theorem 2.2 to an arbitrary link length $r > 0$, we have to consider the location of the transmitters and of the receivers in the system, because a transmitter will not necessarily located in the same cell as its receiver.

Let us define $\bar{\mathbf{Z}}_\varepsilon(t) = (Z_{i,C}(t))$ the $N_\varepsilon \times 2^K - 1$ vector of transmitter locations in the dominating system and $\bar{\mathbf{M}}_\varepsilon(t)$ be such that $\bar{M}_{i,C}(t)$ is a $N_\varepsilon \times 2^K - 1$ vector whose coordinate (j, D) denotes how many transmitters in cell j of class D have a receiver in cell i of class C at time t in the network.

We define the process:

$$\bar{\mathbf{S}}(t) = (\bar{\mathbf{X}}_\varepsilon(t), \bar{\mathbf{Z}}_\varepsilon(t), \bar{\mathbf{M}}_\varepsilon(t)),$$

which is a Markov chain with countable state space. The dynamics of $\bar{\mathbf{S}}(t)$ are as follows: to each receiver of class C arriving in cell i, we pick uniformly a point $x \in A_i$. We then draw a circle with radius r centered at x and we pick a point y uniformly at random on the circle to decide in which cell the transmitter is located.

To obtain the interference in the network, we have to take into account the positions of the receivers. The interference experienced by a transmitter of class C located in cell i with its receiver located in cell k_C in this new system becomes:

$$\bar{I}_{i,C}(t) = \sum_{k,U} |C \cap U| \ell^\varepsilon(a_k, a_i) \bar{Z}_{k,U}(t) - \mathbb{1}_{\{U=C, k=k_C\}}$$

The rate-of-transmission function changes to:

$$\bar{R}_{i,C}(t) = \frac{|C| \ell(r) \bar{X}_{k,U}(t)}{\mathcal{N}_0 + \bar{I}_{i,C}(t)}$$

Using the definitions of the process $\bar{\mathbf{S}}(t)$ and the same steps as for Theorem 2.3, we can obtain the existence of fluid limits for the process $\bar{\mathbf{S}}_\varepsilon(t)$, denoted as $\bar{s}(t)$:

$$\begin{aligned} \frac{\mathrm{d}}{\mathrm{d}t} \bar{x}_{i,C}(t) &= \lambda p_C \varepsilon^2 - \frac{1}{L_C} \frac{|C| \ell(r) \bar{x}_{i,C}(t)}{\sum_{k,U} \ell^\varepsilon(a_k, a_i) |C \cap U| \bar{z}_{k,U}(t)} \\ &\triangleq \lambda p_C \varepsilon^2 - \psi_{i,C}(\bar{s}(t)). \end{aligned}$$

We can now use similar arguments as for Theorem 2.4 to obtain the stability of the Markov process $\bar{\mathbf{S}}(t)$ under the condition:

$$\lambda_c^+ \leq \frac{K\ell(r)}{\mathfrak{L}\langle \ell_{\mathcal{D}}^{\varepsilon} \rangle}. \tag{2.11}$$

To obtain the reciprocal, we define similarly a chain $\underline{\mathbf{S}}(t)$, with the same interference and rate-of-transmission - using the adequate quantities - as for $\bar{\mathbf{S}}(t)$. From this, we can use a similar argument as the ones used to obtain Theorem 2.5 to bound the chain $\underline{\mathbf{S}}(t)$ by an appropriate M/M/1 queue and obtain its instability whenever:

$$\frac{K\ell(r)}{\mathfrak{L}\langle \ell_{\mathcal{D}}^{\varepsilon} \rangle} \leq \lambda_c^-. \tag{2.12}$$

Letting ε go to 0 gives us the intended result and proves Theorem 2.2.

Simulations

To obtain a numerical validation of Theorem 2.2, we can simulate the dynamics of the symmetric network. To do so, we consider a simple network setup with 2 channels, meaning there are $2^2 - 1 = 3$ classes denoted as $\{1\}$, $\{2\}$ and $\{1, 2\}$. We take as average file sizes are $L_{\{1\}} = L_{\{2\}} = 1$ and $L_{\{1,2\}} = 2$ and the probability distribution is $p_{\{1\}} = p_{\{2\}} = 0.4$ and and $p_{\{1,2\}} = 0.2$. The path-loss function is $\ell(x) = (1 + x)^{-4}$, and the domain $\mathcal{D}$ is the square torus centered at the origin with side length 10.

To simulate the dynamics of the system, we use the jump-hold construction of the Markov jump process: at each iteration, we compute the time to the next birth by drawing a time t_b from an exponential distribution with mean $\lambda|\mathcal{D}|$ and a random vector $\mathbf{t}_D$ where each coordinate corresponds to a user located at x_i of class C_i and is drawn from an exponential distribution with mean $\frac{1}{L_{C_i}} R(x_i, \Phi_t)$.

We then compare the values of t_b and the minimum of $\mathbf{t}_D$: if the former is lower, a user arrives at a location x taken uniformly at random in $\mathcal{D}$; if the latter is lower, the corresponding user leaves the system. We then update the value of the interference in the system and move forward in time to the next event. If $(T_0 = 0, T_1, \ldots, T_n)$ are the event times in the network and X is the embedded Markov chain, we obtain that $\Phi_{T_n} = X_n$, which gives us the representation of process Φ_t.

Figure 2.1 shows the behavior of the system for two values of λ: one that shows stability, and the other, instability.

As expected by the result of Theorem 2.2, when λ is lower than the value λ_c, the population in the network stays bounded, as if λ is larger than λ_c, the population diverges to infinity. A reliable criterion to study the stability of the system is Little's law (see [64]), that links the average staying time W of a user in the system, the arrival rate λ and the number of users L in the system in the stationary regime:

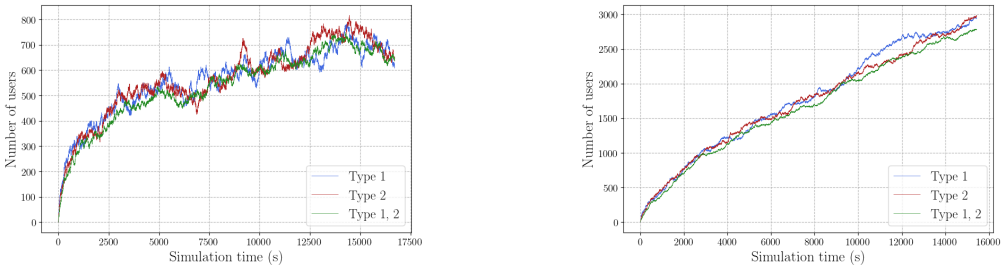

Figure 2.1: Number of active users in the network over time with $K = 2$ bands for two values of λ. On the left, $\lambda = 0.95\lambda_c$ and we can see that the number of users in the network stays bounded. On the right, $\lambda = 1.05\lambda_c$. In this case, population grows linearly over time in the network, showing the instability of the system.

$$L = \lambda W. \tag{2.13}$$

Using the parameters for our system, (2.13) becomes:

$$\mathbb{E}\left[\Phi_{t,C}(\mathcal{D})\right] = \lambda p_C W_C, \tag{2.14}$$

where W_C is the staying time of a user of class C and $\mathbb{E}\left[\Phi_{t,C}(\mathcal{D})\right]$ is the average number of users of class C in the stationary regime. When simulating the dynamics of the network, we can compute the average time spent by users in the network in each class. If the value converges to a fixed, finite value, then the network is stable and the number of users follow (2.14). If the time lived in the network grows linearly and diverges to infinity, then the network is not stable.

Figure 2.2 shows the average staying time of users in the network for two different values of λ. The phase transition in the network happens as expected: for $\lambda = 0.9\lambda_c$, the system appears to be stable and for $\lambda = 1.1\lambda_c$, the average staying time grows linearly, meaning that no stationary regime exists for in the network, and that our dynamics are unstable.

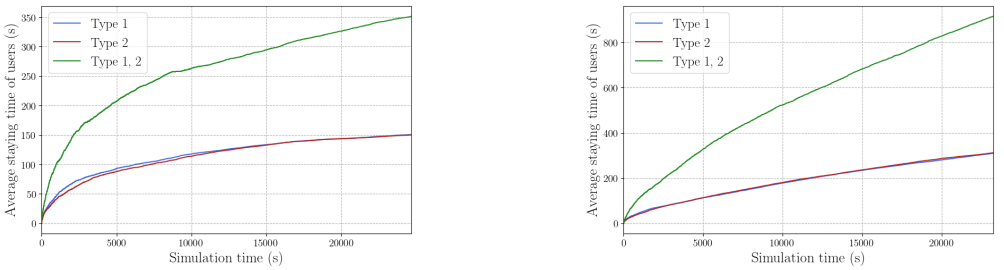

Figure 2.2: Average staying time of users in the network with $K = 2$ channels for two different values of λ: $\lambda = 0.9\lambda_c$ (left) and $\lambda = 1.1\lambda_c$ (right).

The implementation used for simulation runs the system in linear type with respect to the number of steps desired, so we can further verify this conjecture for other configuration, though, the number of possible configuration

grows exponentially with K. To be able to consider a system with a large number of bands, we can consider not allowing all possible configurations in the network, which contradicts our initial assumption that $p_C > 0$ for all $C \in \mathcal{P}(K)$. In Chapter 5, we will discuss how blocking certain configurations of bands may change the stability condition for the system.

Figure 2.3 shows the sojourn time in a system with $K = 4$ bands (the legend has been omitted for readability). In the stable case (on the left), we can observe that users with the same number of bands have sojourn times converging to the same values. This property of the system will be investigated in Part II of this thesis.

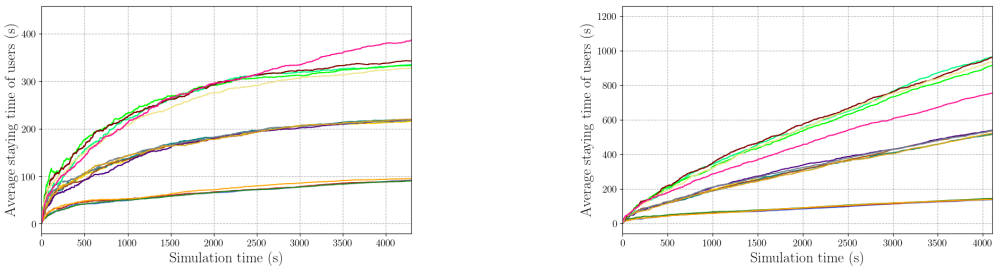

Figure 2.3: Staying time in the system for $K = 4$ bands, with $\lambda = 0.95\lambda_c$ on the left and $\lambda = 1.05\lambda_c$ on the right.

In this chapter, we have seen how fluid limits and combinatorics allows us to obtain a simple closed-form for the critical arrival rate for the system with the symmetry assumption. As mentioned in the introduction, this symmetry assumption is featured in a variety of resource allocation policies. In the next chapter, we will study the system without the symmetry assumption.

Chapter 3

Proofs of Theorems of Chapter 2

This chapter focuses around proving the Theorems about stability of the dominating chain $\bar{\mathbf{X}}_\varepsilon$ and the instability of the chain $\underline{\mathbf{X}}_\varepsilon$ presented in Chapter 2.

We start by establishing the fluid model for the dynamics by proving Theorem 2.3. Then, we move on to proving the stability of the chain $\bar{\mathbf{X}}_\varepsilon$, establishing Theorem 2.4. The last part of this chapter proposes a proof for the instability of $\underline{\mathbf{X}}_\varepsilon$, giving Theorem 2.5.

3.1 Proof of Theorem 2.3

Let us take a sequence of initial conditions $\bar{\mathbf{X}}^n_\varepsilon(0) = (\bar{x}^n_{i,C})$ for our system, with $\lim_{n\to\infty} \bar{x}^n_{i,C} = \infty$. The goal in this section is to study the limit of the sequence of fluid-scaled processes $\left(\frac{1}{n}\bar{\mathbf{X}}_\varepsilon(nt)\right)$ and to obtain a system of ODEs for which the limit of this sequence is a solution.

Using (2.7), we get, for all i, C:

$$\frac{1}{n}\bar{X}_{i,C}(nt) = \frac{1}{n}\bar{x}^n_{i,C} + \frac{1}{n}\mathcal{A}_{i,C}(\lambda p_C \varepsilon^2 nt) - \frac{1}{n}N_{i,C}\left(\frac{1}{L_C}\int_0^{nt} \bar{X}_{i,C}(u)R_{i,C}(\bar{\mathbf{X}}_\varepsilon(u))\mathrm{d}u\right). \quad (3.1)$$

We use the variable change $u = ns$ in the integral to get:

$$\int_0^{nt} \bar{X}_{i,C}(u) R_{i,C}(\bar{\mathbf{X}}_\varepsilon(u))\mathrm{d}u$$
$$= \int_0^t \bar{X}_{i,C}(ns) R_{i,C}(\bar{\mathbf{X}}_\varepsilon(ns)) n \mathrm{d}s$$
$$= \int_0^t \frac{|C|\bar{X}_{i,C}(ns)}{\mathcal{N}_0 + \sum_{k,U} \ell^\varepsilon(a_k, a_i)|C \cap U| \left(\bar{X}_{k,U}(ns) - \mathbf{1}_{\{U=C, i=k\}}\right)} n \mathrm{d}s$$
$$= n \int_0^t \frac{|C|\frac{1}{n}\bar{X}_{i,C}(ns)}{\frac{\mathcal{N}_0}{n} + \sum_{k,U} \ell^\varepsilon(a_k, a_i)|C \cap U| \left(\frac{1}{n}\bar{X}_{k,U}(ns) - \frac{1}{n}\mathbf{1}_{\{U=C, i=k\}}\right)} \mathrm{d}s.$$

We define:

$$R^n_{i,C}(x) = \frac{|C|}{\frac{\mathcal{N}_0}{n} + \sum_{k,U} \ell^\varepsilon(a_k, a_i)|C \cap U| \left(x_{k,U} - \frac{1}{n}\mathbf{1}_{\{U=C, i=k\}}\right)}.$$

Using this, (3.1) becomes:

$$\frac{1}{n}\bar{X}_{i,C}(nt) = \frac{1}{n}\bar{x}^n_{i,C} + \frac{1}{n}\mathcal{A}_{i,C}(\lambda p_C \varepsilon^2 nt)$$
$$- \frac{1}{n} N_{i,C}\left(\frac{n}{L_C}\int_0^t \frac{1}{n}\bar{X}_{i,C}(ns) R^n_{i,C}\left(\frac{1}{n}\bar{\mathbf{X}}_\varepsilon(ns)\right)\mathrm{d}s\right),$$

Let $M^n_{i,C}(z) = \frac{1}{n}N_{i,C}(nz) - z$ for $z \in \mathbb{R}$, and let us define:

$$\bar{Y}^n_{i,C}(t) = \frac{1}{n}\bar{x}^n_{i,C} + \frac{1}{n}\mathcal{A}_{i,C}(\lambda p_C \varepsilon^2 nt)$$
$$- M^n_{i,C}\left(\frac{1}{L_C}\int_0^t \frac{1}{n}\bar{X}_{i,C}(ns) R^n_{i,C}\left(\frac{1}{n}\bar{\mathbf{X}}_\varepsilon(ns)\right)\mathrm{d}s\right). \quad (3.2)$$

We can note that $M^n_{i,C}$ is a martingale and $\bar{Y}^n_{i,C}$ is its compensator, for which we obtain a limit in order to obtain the fluid limit. By using (3.1), we have:

$$\frac{1}{n}\bar{X}_{i,C}(nt) = \bar{Y}^n_{i,C}(t) - \frac{1}{L_C}\int_0^t \frac{1}{n}\bar{X}_{i,C}(ns) R^n_{i,C}\left(\frac{1}{n}\bar{\mathbf{X}}_\varepsilon(ns)\right)\mathrm{d}s. \quad (3.3)$$

Let us denote $\bar{\mathbf{x}}_0 = \lim_{n\to\infty} \frac{1}{n}\bar{x}^n_{i,C}$ when it exists. We say that $\bar{\mathbf{x}}_0$ is finite if and only if all its coordinates are finite.

Lemma 3.1. *If $\bar{\mathbf{x}}_0$ exists and is finite, then:*

$$\forall t \geq 0, \forall i, C, \quad \lim_{n\to\infty} \bar{Y}^n_{i,C}(t) = \bar{X}_{i,C}(0) + \lambda p_C \varepsilon^2 t. \quad (3.4)$$

Proof. Using the strong law of large numbers yields, $\mathbb{P}$-almost surely:

$$\lim_{n\to\infty} \frac{1}{n}\mathcal{A}_{i,C}(\lambda p_C \varepsilon^2 nt) = \lambda p_C \varepsilon^2 t.$$

Moreover, we have:

$$\begin{aligned}
&\frac{1}{L_C}\int_0^t \frac{1}{n}\bar{X}_{i,C}(ns) R^n_{i,C}\left(\frac{1}{n}\bar{\mathbf{X}}_\varepsilon(ns)\right)\mathrm{d}s \\
&\qquad = \frac{1}{L_C}\int_0^t \frac{1}{n}\bar{X}_{i,C}(ns)\frac{|C|}{\frac{N_0}{n}+\sum_{k,U}|C\cap U|\ell^\varepsilon(a_k,a_i)\frac{1}{n}\bar{X}_{k,U}(ns)}\mathrm{d}s \\
&\qquad \leq \frac{1}{L_C}\int_0^t \frac{1}{n}\bar{X}_{i,C}(ns)\frac{|C|}{|C|\ell^\varepsilon(a_i,a_i)\frac{1}{n}\bar{X}_{i,C}(ns)}\mathrm{d}s \\
&\qquad = \frac{t}{L_C},
\end{aligned}$$

where we use the fact that for all $0 \leq i \leq N_\varepsilon - 1$, $\ell_\varepsilon(a_i, a_i) = 1$.

We use Prohorov's Theorem (see Theorems 5.1 and 5.2 of [26]) to obtain that the sequence of processes $\left\{\frac{1}{n}\bar{X}_{i,C}(n\cdot)\ \ R^n_{i,C}(\frac{1}{n}\bar{\mathbf{X}}_\varepsilon(n\cdot))\right\}$ is tight. Finally, because $M^n_{i,C}(z) \to 0$ as n goes to infinity for all z (using the strong law of large numbers), we can conclude that:

$$\lim_{n\to\infty} M^n_{i,C}\left(\frac{1}{L_C}\int_0^t \frac{1}{n}\bar{X}_{i,C}(ns) R^n_{i,C}\left(\frac{1}{n}\bar{\mathbf{X}}_\varepsilon(ns)\right)\mathrm{d}s\right) = 0,$$

which leads to the intended result. □

For $v : [0,T) \to \mathbb{R}$ and $0 \leq t_1 \leq t_2 \leq T$, let us define:

$$w(v,[t_1,t_2]) = \sup\left\{|v(u_1) - v(u_2)|, u_1, u_2 \in [t_1,t_2]\right\}.$$

Let us define the modulus of continuity $\omega(v,\delta,T) = \sup\{w(v,[s,t]), 0 \leq s,t \leq T, |s-t| < \delta\}$. We introduce the concept of *C-tightness* and a useful characterization (see Definition VI.3.25 and Proposition VI.3.26 from [51]):

Definition 3.1 (C-tightness)**.** *A sequence* $\{V^n, n \geq 1\}$ *of functions is* C-tight *if and only if, for all* $t_0 > 0$, $\eta > 0$, $T > 0$, *there exists* K^0_η, n^0_η *and* δ^0_η *such that, for all* $n \geq n^0_\eta$*:*

i) $\mathbb{P}\left[\sup_{0\leq t\leq T}|V^n(t)| \geq K^0_\eta\right] < \eta.$

ii) $\mathbb{P}\left[\omega(V^n,\delta^0_\eta,t_0) > \eta\right] < \eta.$

Condition *ii)* implies that any limit point of V^n has continuous sample paths, $\mathbb{P}$-almost surely: let V be a limit point of the sequence V^n. By definition, for all $\eta > 0$, we have:

$$\mathbb{P}\left[\omega(V,\delta^0_\eta,t_0) > \eta\right] < \eta. \tag{3.5}$$

This means, that, $\mathbb{P}$-almost surely, $\omega(V, \delta^0, t_0) > \eta$ for each $T > 0$ and $\delta_C > 0$. By continuity of the function $\delta \mapsto \omega(V, \delta, t_0)$ at 0, we can conclude that V is $\mathbb{P}$-almost surely continuous.

We can prove the following lemma:

Lemma 3.2. *If $\bar{\mathbf{x}}_0$ exists and is finite, the sequence of processes $\{\frac{1}{n}\bar{\mathbf{X}}_\varepsilon(n\cdot), n \geq 0\}$ is C-tight.*

Proof. Let $T > 0$ and $\eta > 0$. As n goes to infinity, we know that $\bar{Y}^n_{i,C}(t) \to \bar{X}_{i,C}(0) + \lambda p_C \varepsilon^2 t$ $\mathbb{P}$-almost surely from Lemma 3.1. For each $\eta > 0$, there exists $n_\eta^{T,1}$ such that for $n \geq n_\eta^{T,1}$:

$$\mathbb{P}\left[\sup_{0\leq t\leq T} |\bar{Y}^n_{i,C}(t)| \geq \lambda p_C \varepsilon^2 T + 1\right] \leq \eta. \tag{3.6}$$

We also know that $\frac{1}{n}\bar{X}_{i,C}(nt) R^n_{i,C}(\frac{1}{n}\bar{\mathbf{X}}_\varepsilon(nt)) \leq 1$ at all times t, a fortiori for all $t \leq T$. Using (3.3), we deduce that for all $n \geq n_\eta^{T,1}$:

$$\mathbb{P}\left[\sup_{0\leq t\leq T} \left|\frac{1}{n}\bar{X}_{i,C}(nt)\right| \geq \lambda p_C \varepsilon^2 T + 1 + 1\right] \leq \eta. \tag{3.7}$$

We set $K^0_\eta = \lambda p_C \varepsilon^2 T + 2$ to obtain condition i).

To obtain condition ii), we remark that proving the continuity of the limits is equivalent to showing that there exists a $\delta^0_\eta > 0$ such that for all i, C and at all times $t < T$, we have:

$$\mathbb{P}\left[\omega\left(\frac{1}{n}\bar{X}_{i,C}(nt), \delta^0_\eta, t_0\right) > \eta\right] < \eta.$$

Let $\delta > 0$. (3.3) gives at all times $t \geq 0$:

$$\frac{1}{n}\bar{X}_{i,C}(n(t+\delta)) - \frac{1}{n}\bar{X}_{i,C}(nt) = \bar{Y}^n_{i,C}(t+\delta) - \bar{Y}^n_{i,C}(t) - \frac{1}{L_C}\int_t^{t+\delta} \frac{1}{n}\bar{X}_{i,C}(nu) R^n_{i,C}\left(\frac{1}{n}\bar{\mathbf{X}}_\varepsilon(nu)\right) \mathrm{d}u.$$

Taking the supremum over $t \in [0, T]$, and we remind that:

$$\frac{1}{n}\bar{X}_{i,C}(nt) R^n_{i,C}(\frac{1}{n}\bar{\mathbf{X}}_\varepsilon(nt)) \leq 1. \tag{3.8}$$

We have:

$$\sup_{0\leq t\leq T}\left|\frac{1}{n}\bar{X}_{i,C}(n(t+\delta)) - \frac{1}{n}\bar{X}_{i,C}(t)\right| \leq \sup_{0\leq t\leq T}\left|\bar{Y}^n_{i,C}(t+\delta) - \bar{Y}^n_{i,C}(t)\right| + \frac{\delta}{L_C}.$$

From Lemma 3.1, we know that $\bar{Y}^n_{i,C}(t) \to \bar{X}_{i,C}(0) + \lambda p_C \varepsilon^2 t$ $\mathbb{P}$-almost surely. This implies that there exists $n_\eta^{T,2} > 0$ and $\kappa^0_\eta > 0$ such that, with probability at least $1 - \eta$, $|\bar{Y}^n_{i,C}(t+\delta) - \bar{Y}^n_{i,C}(t)| < \lambda p_C \varepsilon^2 \delta + \delta \kappa^0_\eta$.

This implies that for all i, C, we have, with probability at least $1-\eta$:

$$\omega\left(\frac{1}{n}\bar{X}_{i,C}, \delta, t_0\right) < \delta\left(\lambda p_C \varepsilon^2 + \kappa_\eta^0 + \frac{1}{L_C}\right). \tag{3.9}$$

Let us set $\delta_\eta^0 = \eta\left(\lambda p_C \varepsilon^2 + \kappa_\eta^0 + \frac{1}{L_C}\right)^{-1}$. Thus, we get, for all $n \geq n_\eta^{T,2}$:

$$\mathbb{P}\left[\omega\left(\frac{1}{n}\bar{X}_{i,C}, \delta_\eta^0, t_0\right) < \eta\right] > 1-\eta. \tag{3.10}$$

Setting $n_\eta^0 = \max(n_\eta^{1,0}, n_\eta^{2,0})$ concludes the proof of the C-tightness of the sequence of processes $(\frac{1}{n}\bar{\mathbf{X}}_\varepsilon(t))$.

□

We can now establish the equation ruling the evolution of the fluid scaled model:

Theorem 3.3. *If $\frac{1}{n}\bar{\mathbf{X}}_\varepsilon(0) \to \bar{\mathbf{x}}_0$ as n goes to ∞, then the sequence of processes $\frac{1}{n}\bar{\mathbf{X}}_\varepsilon(n\cdot)$ converges $\mathbb{P}$-almost surely to $\bar{\mathbf{x}}_\varepsilon(s) = (\bar{x}_{i,C}(s))$, which is the unique solution of the following system of differential equations:*

$$\begin{cases} \frac{\mathrm{d}}{\mathrm{d}t}\bar{x}_{i,C}(t) & = \lambda p_C \varepsilon^2 - \frac{1}{L_C}\frac{|C|\bar{x}_{i,C}(t)}{\sum_{k=0}^{N_\varepsilon^{-1}}\sum_{U\in\mathcal{P}(K)}|C\cap U|\ell^\varepsilon(a_k,a_i)\bar{x}_{k,U}} \quad \text{if } \bar{\mathbf{x}} \neq 0 \\ \bar{\mathbf{x}}(0) & = \bar{\mathbf{x}}_0. \end{cases} \tag{3.11}$$

Proof. From Lemma 3.2, the sequences $\{\frac{1}{n}\bar{\mathbf{X}}_\varepsilon(n\cdot), n \geq 1\}$ and $\{\bar{\mathbf{Y}}^n, n \geq 1\}$ are both tight. It follows from Theorem 11.6.8 from [89] that the sequence $\{(\frac{1}{n}\bar{\mathbf{X}}_\varepsilon(n\cdot), \bar{\mathbf{Y}}^n), n \geq 1\}$ is tight in $D([0,\infty], \mathbb{R}^{N_\varepsilon \times 2^K - 1})$, and thus, by using Prohorov's Theorem, relatively compact.

Let n_l be a subsequence along which $\left(\frac{1}{n_l}\bar{\mathbf{X}}_\varepsilon(n_l\cdot), \bar{\mathbf{Y}}^{n_l}\right)$ converges to a limit point $(\bar{\mathbf{x}}_\varepsilon, \bar{\mathbf{Y}})$ as l goes to infinity.

We use the Skorokhod representation theorem (see Theorem 6.7 in [26]) to get a probability space $(\hat{\Omega}, \hat{\mathcal{F}}, \hat{\mathbb{P}})$ with a sequence of processes $\{(\hat{\mathbf{X}}^{n_l}, \hat{\mathbf{Y}}^{n_l}), l \geq 1\}$ and two processes $\hat{\mathbf{x}}_\varepsilon$ and $\hat{\mathbf{Y}}$ such that:

- $\left(\hat{\mathbf{X}}^{n_l}, \hat{\mathbf{Y}}^{n_l}\right) \to (\hat{\mathbf{x}}_\varepsilon, \hat{\mathbf{Y}})$, $\hat{\mathbb{P}}$-almost surely;
- $\left(\hat{\mathbf{X}}^{n_l}, \hat{\mathbf{Y}}^{n_l}\right) \overset{d}{\sim} (\frac{1}{n_l}\bar{\mathbf{X}}_\varepsilon(n_l, \cdot), \bar{\mathbf{Y}}^{n_l})$ for all $l \geq 1$;
- $(\hat{\mathbf{x}}_\varepsilon, \hat{\mathbf{Y}}) \overset{d}{\sim} (\bar{\mathbf{X}}_\varepsilon, \bar{\mathbf{Y}})$.

The second point gives, for all $l \geq 1$:

$$\hat{X}_{i,C}^{n_l}(t) = \hat{Y}_{i,C}^{n_l}(t) - \frac{1}{L_C}\int_0^t \hat{X}_{i,C}^{n_l}(s) R_{i,C}^n(\hat{\mathbf{X}}^{n_l}(s))\mathrm{d}s. \tag{3.12}$$

Using the C-tightness of $\bar{\mathbf{X}}_\varepsilon$, $\hat{\mathbf{X}}$ and $\hat{\mathbf{Y}}$ are continuous. This implies that:

$$\sup_{l\geq 1}\sup_{0\leq t\leq T}\|X_{i,C}^{n_l}(t)\| < \infty.$$

Furthermore, we have, for all $x \in \mathbb{N}^{\varepsilon \times 2^K - 1}$:

$$\lim_{l \to \infty} R_{i,C}^{n_l}(x) = \frac{|C|}{\sum_{k,U} \ell^{\varepsilon}(a_k, a_i)|C \cap U| x_{k,U}} \equiv R_{i,C}(x). \tag{3.13}$$

Combining all these results, we can take the limits as l goes to infinity in (3.12) and use the dominated convergence theorem to get the following equation for $(\hat{\mathbf{x}}_{\varepsilon}, \hat{\mathbf{Y}})$:

$$\hat{x}_{i,C}(t) = \hat{Y}_{i,C}(t) - \frac{1}{L_C} \int_0^t \frac{|C| \hat{x}_{i,C}(s)}{\sum_{k,U} \ell^{\varepsilon}(a_k, a_i)|C \cap U| \hat{x}_{k,U}(s)} \mathrm{d}s. \tag{3.14}$$

Let us remind that, from Lemma 3.1, $\bar{Y}_{i,C}(t) = \bar{X}_{i,C}(0) + \lambda p_C \varepsilon^2 t$, which gives us the following equation for the limit process:

$$\hat{x}_{i,C}(t) = \hat{x}_{i,C}(0) + \lambda p_C \varepsilon^2 t - \int_0^t \frac{1}{L_C} \frac{|C| \hat{x}_{i,C}(s)}{\sum_{k,U} \ell^{\varepsilon}(a_k, a_i)|C \cap U| \hat{x}_{k,U}(s)} \mathrm{d}s. \tag{3.15}$$

To obtain the intended equations, we differentiate (3.15), which concludes the proof.

□

3.2 Proof of Theorem 2.4

In this section, we provide a proof for Theorem 2.4 using Lemma A.13, which is applicable to our model. We have:

Lemma 3.4. *Assume that there exists* $\mathbf{z} \in \mathbb{R}_{+,\star}^{N_{\varepsilon} \times 2^K - 1}$ *such that for all* i, C*:*

$$\lambda p_C \varepsilon^2 \leq \frac{1}{L_C} \frac{|C| z_{i,C}}{\sum_{k,U} \ell^{\varepsilon}(a_k, a_i)|C \cap U| z_{k,U}}$$

Then, the Markov chain $\bar{\mathbf{X}}_{\varepsilon}$ *is positive Harris recurrent.*

Proof. To obtain this result, we use Lemma A.13: the fluid limit $\mathbf{x}(t)$ meets the intended requirements. Let us take such a $\mathbf{z} \in \mathbb{R}_{+,\star}^{N_{\varepsilon} \times 2^K - 1}$. We know that for all $0 < \delta < M < \infty$, there exists $T > 0$ such that whenever $\|\mathbf{x}(0)\| = M$, we have $|\mathbf{x}(T)\| < \delta$.

Theorem 4.2 from [37] with the fluid limit $\bar{\mathbf{x}}$ allows us to obtain positive Harris recurrence for the chain $\mathbf{X}$. □

We use this result in $\mathbb{R}_{+}^{N_{\varepsilon} \times 2^K - 1}$ by setting $\psi_{i,C}(\mathbf{x}) = \frac{1}{L_C} \frac{|C| x_{i,C}}{\sum_{k,U} \ell^{\varepsilon}(a_k, a_i)|C \cap U| x_{k,U}}$, which is 0-homogeneous, and non-increasing in $x_{k,U}$ for $(k, U) \neq (i, C)$.

The goal here is to find an appropriate vector z to get the desired upper bound on λ. Let us set $z_{i,C} = p_C L_C$ for all $C \in \mathcal{P}(K)$. We want that, for each $C \in \mathcal{P}(K)$:

$$\lambda p_C \varepsilon^2 \leq \frac{1}{L_C} \frac{|C| p_C L_C}{\sum_{k,U} \ell^\varepsilon(a_k, a_i)|C \cap U| p_U L_U}. \tag{3.16}$$

Using the torus property in our system, Equation (3.16) becomes:

$$\lambda \leq \frac{1}{\langle \ell^\varepsilon_{\mathcal{D}} \rangle} \frac{|C|}{\sum_U |C \cap U| p_U L_U}. \tag{3.17}$$

We will use the following Lemma to simplify (3.17):

Lemma 3.5. *Let $(y_C)_{C \in \mathcal{P}(K)} \in \mathbb{R}^{2^K - 1}$ be such that $|C| = |D| \Rightarrow y_C = y_D$. We have:*

$$\forall C \in \mathcal{P}(K), \qquad \sum_{U \in \mathcal{P}(K)} |C \cap U| y_U = \frac{|C|}{K} \sum_{U \in \mathcal{P}(K)} |U| y_U. \tag{3.18}$$

Proof. Let $C \in \mathcal{P}(K)$ with $|C| = j$, and $(y_U)_{U \in \mathcal{P}(K)} \in \mathbb{R}^{2^K - 1}$ be such that $y_U = y_V$ whenever $|U| = |V|$. We have:

$$\sum_{U \in \mathcal{P}(K)} |C \cap U| y_U = \sum_{l=1}^{K} \sum_{m=1}^{j \wedge l} \sum_{\substack{U : |U| = l \\ |C \cap U| = m}} m y_U. \tag{3.19}$$

The number of sets $U \in \mathcal{P}(K)$ such that $|U| = l$ and $|C \cap U| = m$ is equal to $\binom{j}{m}\binom{K-j}{l-m}$. Using the symmetry property of y, we know that $y_U = y_{[1,l]}$. Using the fact that we have $y_U = \frac{1}{\binom{K}{l}} \sum_{|V|=l} y_V(t)$. We can rewrite (3.19) as:

$$\begin{aligned} \sum_{U \in \mathcal{P}(K)} |C \cap U| y_U &= \sum_{l=1}^{K} y_{[1,l]} \sum_{m=1}^{j \wedge l} m \binom{j}{m} \binom{K-j}{l-m} \\ &= \sum_{l=1}^{K} \left(\sum_{|U|=l} y_U \right) \sum_{m=1}^{j \wedge l} m \frac{\binom{j}{m}\binom{K-j}{l-m}}{\binom{K}{l}}. \end{aligned} \tag{3.20}$$

We can prove that $\sum_{m=1}^{j \wedge l} m \frac{\binom{j}{m}\binom{K-j}{l-m}}{\binom{K}{l}} = \frac{lj}{K}$ by using the formula for the expectation of a hypergeometric variable with parameters K, j and l. Replacing l by $|U|$ and j by $|C|$ leads to:

$$\sum_{U \in \mathcal{P}(K)} |C \cap U| y_U = \frac{|C|}{K} \sum_{U \in \mathcal{P}(K)} |U| y_U, \tag{3.21}$$

which concludes the proof of Lemma 3.5.

□

The vector $(p_C)_{C\in\mathcal{P}(K)}$ verifies the conditions of Lemma 3.5, which allows us to obtain, after setting $\mathfrak{L} = \sum_U |U| p_U L_U$:

$$\lambda \leq \frac{1}{\langle \ell^{\varepsilon}_{\mathcal{D}} \rangle} \frac{K}{\mathfrak{L}}. \tag{3.22}$$

The result of Lemma 3.4 gives us stability for the fluid model (3.11) in the sense of Definition 4.1 of [37] with $M = 1$. Applying the result from Theorem 4.2 of the same paper gives us positive Harris recurrence for the chain $\bar{\mathbf{X}}_\varepsilon$. $\bar{\mathbf{X}}_\varepsilon$ is an irreducible Markov jump process that is also positive recurrent. Thus, $\bar{\mathbf{X}}_\varepsilon$ is ergodic, which concludes the proof of Theorem 2.4.

3.3 Proof of Theorem 2.5

To prove the instability of the chain $\underline{\mathbf{X}}_\varepsilon$, we start by introducing, for each i, C, the function $r_{i,C}$ defined as:

$$r_{i,C} : \mathbf{x} \in \mathbb{R}_{+,*}^{N_\varepsilon \times 2^K - 1} \mapsto \frac{1}{p_C L_C \varepsilon^2} \frac{|C| x_{i,C}}{\sum_{k,U} \ell_\varepsilon(a_k, a_i) |C \cap U| x_{k,U}}.$$

For all i, C, $r_{i,C}$ is continuous and 0-homogenous, and it is not defined for $\mathbf{x} = 0$: let us take the sequences $\mathbf{x}_n$ and $\mathbf{y}_n$ such that $x_{0,\{1\},n} = y_{0,\{1\},n} = \frac{1}{n}$, $y_{1,\{1\},n} = \frac{1}{n}$ and all the other coordinates set to 0. Immediately, $\lim_{n\to\infty} \mathbf{x}_n = \lim_{n\to\infty} \mathbf{y}_n = 0$. Using the 0-homogeneity of the functions, we have:

$$\forall n, \quad r_{0,\{1\}}(\mathbf{x}_n) = \frac{1}{p_{\{1\}} L_{\{1\}} \varepsilon^2}, \qquad r_{0,\{1\}}(\mathbf{y}_n) = \frac{1}{p_{\{1\}} L_{\{1\}} \varepsilon^2} \frac{1}{1 + \ell_\varepsilon(a_0, a_1)},$$

which have different limits as n goes to infinity.

Let us now consider the function $\mathbf{x} \in \mathbb{R}_{+,*}^{N_\varepsilon \times 2^K - 1} \mapsto \min_{i,C} r_{i,C}(\mathbf{x})$. It is also 0-homogenous is not defined at $\mathbf{x} = 0$, and it is continuous on the set $\mathcal{S} = \{\mathbf{x} \in \mathbb{R}_{+,*}^{N_\varepsilon \times 2^K - 1} : |\mathbf{x}| = 1\}$, which is compact. Thus, it admits a maximum on $\mathcal{S}$, and on $\mathbb{R}_{+,*}^{N_\varepsilon \times 2^K - 1}$ as a consequence. We set

$$\mathcal{B} = \underset{\mathbf{x}\in\mathbb{R}_{+,*}^{N_\varepsilon \times 2^K - 1}}{\arg\max} \left\{ \min_{i,C} \frac{1}{p_C L_C \varepsilon^2} \frac{|C| x_{i,C}}{\sum_{k,U} \ell_\varepsilon(a_k, a_i) |C \cap U| x_{k,U}} \right\}, \tag{3.23}$$

which is non-empty.

Lemma 3.6. *Let $\mathbf{z} \in \mathcal{B}$ and let $i^\star, C^\star$ be the coordinates of a point where the maximum is attained. Let $\lambda > 0$ be such that:*

$$\lambda p_{C^\star} \varepsilon^2 > \frac{1}{L_{C^\star}} \frac{|C^\star| z_{i^\star, C^\star}}{\sum_{k,U} |C \cap U| \ell_\varepsilon(a_k, a_i^\star) z_{k,U}}.$$

Then, $\underline{\mathbf{X}}_\varepsilon$ is transient.

Proof. Let $\mathbf{z} \in \mathcal{B}$. By definition, there exists $i^\star, C^\star$ such that the maximum value of $\min_{i,C} r_{i,C}$ is equal to $r_{i^\star,C^\star}(\mathbf{z})$. Let us take $\lambda > 0$ such that:

$$\lambda p_{C^\star} \varepsilon^2 > \frac{1}{L_{C^\star}} \frac{|C^\star| z_{i^\star,C^\star}}{\sum_{k,U} |C \cap U| \ell_\varepsilon(a_k, a_i^\star) z_{k,U}}.$$

We define the process $\underline{\mathbf{Y}}$ such that:

– Arrivals in queue i, C happen with rate $\lambda p_C \varepsilon^2$, for all i, C;

– Departures in queue i, C happen with rate:

  – $\frac{1}{L_{C^\star}} \frac{|C^\star| z_{i^\star,C^\star}}{\sum_{k,U} |C \cap U| \ell_\varepsilon(a_k, a_i) z_{k,U}}$ if $i, C = i^\star, C^\star$,

  – $\frac{1}{L_C} \frac{|C| \underline{Y}_{i,C}(t)}{\sum_{k,U} |C \cap U| \ell_\varepsilon(a_k, a_i) \underline{Y}_{k,U}(t) + \mathcal{N}_0}$ else.

$\underline{\mathbf{Y}}$ is a Markov jump process, with state space $\mathbb{N}^{N_\varepsilon \times 2^K - 1}$. By definition of $\mathbf{z}$, we have, at all times $t \geq 0$:

$$\frac{1}{L_{C^\star}} \frac{|C^\star| z_{i^\star,C^\star}}{\sum_{k,U} |C \cap U| \ell_\varepsilon(a_k, a_i) z_{k,U}} \geq \frac{1}{L_{C^\star}} \frac{|C^\star| \underline{X}_{i^\star,C^\star}(t)}{\sum_{k,U} |C \cap U| \ell_\varepsilon(a_k, a_i) \underline{X}_{k,U}(t) + \mathcal{N}_0}.$$

Using a coupling argument similar to the one used in the proof of Theorem 1.2, we obtain, for all i, C and at all times t:

$$\underline{Y}_{i,C}(t) \leq \underline{X}_{i,C}(t), \quad \mathbb{P}\text{-a.s.}$$

The queue $\underline{Y}_{i^\star,C^\star}$ is an M/M/1 queue with constant arrival rate $\lambda p_{C^\star} \varepsilon^2$ and a departure rate equal to $\frac{1}{L_{C^\star}} \frac{|C^\star| z_{i^\star,C^\star}}{\sum_{k,U} |C \cap U| \ell_\varepsilon(a_k, a_i) z_{k,U}}$.

It is unstable and $\mathbb{P}\left[\lim_{t \to \infty} \underline{Y}_{i^\star,C^\star}(t) = +\infty\right] = 1$, implying the same for $\underline{X}_{i^\star,C^\star}$, which concludes the proof.

□

We can note that queue $\underline{X}_{i^\star,C^\star}$ is not the only queue whose population diverges to infinity. The departure rates in all queues (except for queue $i^\star, C^\star$) are decreasing functions of $\underline{X}_{i^\star,C^\star}(t)$. Thus, for a given queue $\underline{X}_{j,D}$, there exists a time $T_{j,D}$ after which the departure rate in this queue becomes lower than its arrival rate. We can then bound from below $\underline{X}_{j,D}$ after time $T_{j,D}$ by an adequate M/M/1 queue and obtain that the population in queue j, D goes to infinity, $\mathbb{P}$-almost surely for all j, D.

To complete the proof of Theorem 4.5, we characterize the value of $\mathbf{z}$:

Lemma 3.7. *Let $\mathbf{z} \in \mathcal{B}$. Then, $\mathbf{z}$ is a solution to the following system of equations, for all $0 \leq i, j \leq N_\varepsilon - 1$ and $C, D \in \mathcal{P}(K)$:*

$$\frac{1}{p_C L_C}\frac{|C|z_{i,C}}{\sum_{k,U}\ell_\varepsilon(a_k,a_i)|C\cap U|z_{k,U}} = \frac{1}{p_D L_D}\frac{|D|z_{j,D}}{\sum_{k,U}\ell_\varepsilon(a_k,a_j)|D\cap U|z_{k,U}}. \tag{3.24}$$

Proof. Let $\mathbf{z}$ be such that:

$$\mathbf{z} \in \underset{\mathbf{y}\in\mathbb{R}_+^{N_\varepsilon\times 2^K-1}}{\arg\max}\ \min_{i,C} r_{i,C}(\mathbf{y}).$$

To prove this result, we use the maximality of $\mathbf{z}$. Without loss of generality, let us assume that the minimum over i, C of $r_{i,C}(\mathbf{z})$ is reached for $i = 0$ and $C = \{1\}$. We know that the function $r_{0,\{1\}}$ is a decreasing function of $z_{i,C}$ for all $1 \le i \le N-1$ and $C \neq \{0\}$. Hence, these values have to be minimal in order to maximize $r_{0,\{1\}}$.

By definition, for all $1 \le j \le N_\varepsilon - 1$, $C \neq \{1\}$, we have $r_{0,\{1\}}(\mathbf{z}) \le r_{i,C}(\mathbf{z})$. But, for $i \ge 1$ and $C \neq \{0\}$, $r_{i,C}$ is an increasing function of $z_{i,C}$. Thus, the only possible value for $\mathbf{z}$ is such that:

$$r_{0,\{1\}}(\mathbf{z}) = r_{i,C}(\mathbf{z}),$$

which concludes the proof.

□

Finally, we know that $\mathbf{z}$ such that for all i, C, $z_{i,C} = p_C L_C$ is a solution to (3.24). Using Lemma 3.6, the system is unstable if:

$$\begin{aligned}
\lambda p_{C^\star}\varepsilon^2 \ge& \frac{1}{L_{C^\star}}\frac{|C^\star|p_{C^\star}L_{C^\star}}{\sum_{k,U}\ell_\varepsilon(a_k,a_{i^\star})|C^\star\cap U|p_U L_U}\\
\overset{(a)}{=}& \frac{|C^\star|p_{C^\star}}{\frac{1}{\varepsilon^2}\langle\ell_{\varepsilon,\mathcal{D}}\rangle\frac{|C^\star|}{K}\sum_U|U|p_U L_U}\\
=& \frac{\varepsilon^2 p_{C^\star}K}{\langle\ell_{\varepsilon,\mathcal{D}}\rangle\frac{|C^\star|}{K}\sum_U|U|p_U L_U}\\
=& \frac{K}{\langle\ell_{\varepsilon,\mathcal{D}}\rangle\mathfrak{L}},
\end{aligned}$$

where (a) uses Lemma 3.5 with the vector $(p_C L_C)_{C\in\mathcal{P}(K)}$ and the square torus property of $\mathcal{D}$. Setting $\mathfrak{L} = \sum_U |U|p_U L_U$ gives us the intended condition for λ and concludes the proof.

Chapter 4

Generalization to non-symmetric SBD processes and other dynamics

In this chapter, we will extend the result presented in Theorem 2.2 when relaxing the symmetry condition presented in Definition 2.1. This work was firstly motivated by the study of BWP models where the symmetry assumption was relaxed. In these systems, we allow a differentiated use of communication channels, with different arrival rates and different file sizes. Relaxing the symmetry hypothesis for BWP models allows to capture a more diverse array of association policies. When investigating this problem, we obtained a more general stability condition for an array of dynamics of queuing networks with state-dependent departure rates.

This chapter thus focuses on obtaining a general stability condition for queuing networks where the departure rate in a given server is a decreasing function of other queue sizes. To do so, we will focus on a queuing network consisting in N servers for which the queuing discipline is Markovian. We will consider a constant arrival rate with a given routing policy for jobs to be addressed to each server in the network, and the departure rate for jobs in the system will be depending on the state of the system at a given time. We will then apply the main result of this chapter to obtain a stability condition for the non-symmetric SBD process.

4.1 Queuing systems with state dependent departure rates

Let us consider a queueing network of $N \geq 2$ interacting queues, with $(X_i(t))$ denoting the queue length process. In each queue, users carrying jobs arrive at a constant rate and leave the system at a rate depending on the state of the queuing system at a given time. Our model is motivated by wireless networks, so we assume that the departure rate in queue i is a decreasing function of the lengths of queues X_j, for $j \neq i$. Finally, we assume that users leave the system once their job is completed, and we assume that queue lengths are not bounded. Finally, we assume that the system is Markovian (such an example can be found in [84] for instance)

Arrivals in the system happen at rate $\lambda > 0$, and upon arrival, a user is routed independently with probability p_i to server i. Thus, arrivals in server i happen with rate $\lambda_i = \lambda p_i$. We assume that for all i, $p_i \neq 0$.

Departures in server i happen with a state-dependent rate $\Psi_i(\mathbf{X}(t))$, where, for all $0 \leq N-1$, Ψ_i is decreasing in X_j for all $j \neq i$. Furthermore, we assume that, for all i, Ψ_i is such that the following limit exists for all $\mathbf{x} \in \mathbb{R}_+^{\mathbb{N}}$:

$$\lim_{n\to\infty} \Psi_i(n\mathbf{x}) = \psi_i(\mathbf{x}),$$

where ψ_i is non-constant, continuous and 0-homogeneous, i.e., for all $s > 0$ and $\mathbf{x} \in \mathbb{R}_+^{\mathbb{N}}$, $\psi_i(s\mathbf{x}) = \psi_i(\mathbf{x})$.

Using similar coupling arguments as the ones presented in Theorem 1.2 in Section 1.2 of Chapter 1, we can prove the following Theorem:

Theorem 4.1. *Let us take* $\mathbf{X}$ *and* $\mathbf{Y}$ *to realizations of the dynamics with respective arrival rates* λ_X *and* λ_Y*, initial conditions* $\mathbf{X}(0)$ *and* $\mathbf{Y}(0)$*, and departure rates* $(\Psi_i)_{0\leq i\leq N-1}$ *and* $(\Phi_i)_{0\leq i\leq N-1}$*. The following conditions are sufficient for* $\mathbf{X}$ *to dominate* $\mathbf{Y}$ *(when the two other parameters are taken equal):*

A) $\mathbf{Y}(0) \leq \mathbf{X}(0)$ *coordinate-wise,*

B) $\lambda_Y \leq \lambda_X$

C) for all $\mathbf{x}, \mathbf{y} \in \mathbb{R}^N$ *with* $\mathbf{x} \leq \mathbf{y}$ *coordinate-wise,* $\Psi_i(\mathbf{x}) \leq \Phi_i(\mathbf{y})$.

Fluid model

Using a similar proof as the one from Theorem 2.3, we can obtain that the sequence of fluid-scaled processes $\left(\frac{1}{n}X_i(nt)\right)_{n\geq 0}$ admits a limit $(\bar{x}_i(t))$ as n goes to infinity, solution to the following equation:

$$\bar{x}_i(t) = \bar{x}_i(0) + \lambda_i t - \int_0^t \psi_i(\bar{\mathbf{x}(s)})\mathrm{d}s. \tag{4.1}$$

Assumptions made about the functions (Ψ_i) and (ψ_i) give three properties of the fluid system:

i) for all i, ψ_i is non-increasing in x_j for all $j \neq i$ and increasing in x_i,

ii) for all i, ψ_i is 0-homogenous, i.e., for all $\mathbf{t} \in \mathbb{R}_+^N$ and $s \geq 0$, $\psi_i(s\mathbf{t}) = \psi_i(\mathbf{t})$,

iii) the (ψ_i) are such that if $\sum_i \bar{x}_i(\tau) > 0$ for a given τ, there exists $\delta > 0$ such that $\bar{x}_i(t) > 0$ for all i and $t \in [\tau, \tau + \delta]$.

Let us define:

$$\mathcal{B} = \left\{ \lambda \in \mathbb{R}_+ : \lambda \leq \frac{1}{p_i}\psi_i(\mathbf{p}) \text{ for some } \mathbf{p} \in \mathbb{R}_+^N \text{ and all } i \right\}.$$

The main result about the stability of such dynamics is given by Lemma A.13, which allows to conclude about stability for the Markov chain $\mathbf{X}$.The main goal of this chapter is to obtain a converse for this result, and to find a characterization of the maximal value of $\mathcal{B}$ in a particular case.

4.2 An instability condition

The main Theorem of this section is a reciprocal to Lemma 3.4, which will give a condition for stability for the non-symmetric BWP model:

Theorem 4.2. *If $\lambda > \lambda^\star$, where $\lambda^\star = \sup \mathcal{B}$, then the chain $\mathbf{X}$ is transient.*

Proof. The first thing to note is that, because the functions ψ_i are 0-homogeneous, finding a maximum for $\frac{1}{p_i}\psi_i$ over $\mathbb{R}_+^N$ can be resumed to looking its maximum over $(0,1]^N$. Because the ψ_i are continuous, $\mathbf{x} \mapsto \min_i \frac{1}{p_i}\psi_i(\mathbf{x})$ is also continuous, and admits a maximum in $(0,1]^N$. Finally, the value for this function at $\mathbf{x} = 0$ is not defined: because ψ_i is not constant, let us take $\mathbf{x}_1, \mathbf{x}_2$ such that $\psi_i(\mathbf{x}_1) \neq \psi_i(\mathbf{x}_2)$.

We define two sequences $\mathbf{x}_n = \frac{1}{n}\mathbf{x}_1$ and $\mathbf{y}_n = \frac{1}{n}\mathbf{x}_2$. We have $\lim_{n\to\infty} \mathbf{x}_n = \lim_{n\to\infty} \mathbf{y}_n = 0$, but $\lim_{n\to\infty} \psi_i(\mathbf{x}_n) = \psi_i(\mathbf{x}_1)$ and $\lim_{n\to\infty} \psi_i(\mathbf{y}_n) = \psi_i(\mathbf{x}_2)$, which are not equal.

Thus, we can take $\mathbf{z} \in \mathbb{R}_+^N$ such that:

$$\mathbf{z} \in \arg\max_{\mathbf{x}\in\mathbb{R}_+^N} \min_i \frac{1}{p_i}\psi_i(\mathbf{z}).$$

Let $\lambda > \lambda_\star$. By definition, there exists $i^\star$ such that:

$$\lambda p_{i^\star} > \psi_{i^\star}(\mathbf{z}).$$

Let us define the chain $\mathbf{Y}$ as follows:

– For all $0 \leq i \leq N-1$, $Y_i(0) = X_i(0)$

– The arrival rate in Y_i is equal to λp_i

– The departure rate in Y_i is equal to:

  – $\psi_i(\mathbf{Y}(t))$ if $i \neq i^\star$
  – $\psi_{i^\star}(\mathbf{z})$ if $i = i^\star$

By definition of $\mathbf{z}$, we know that for all $t \geq 0$, $\psi_{i^\star}(\mathbf{z}) \geq \Psi_{i^\star}(\mathbf{X}(t))$. Hence, we can apply Lemma 4.1 to obtain, for all $0 \leq i \leq N-1$:

$$Y_i(t) \leq X_i(t) \quad \mathbb{P}-\text{a.s.}$$

To conclude, we can remark that server $i^\star$ is a M/M/1 queue with an arrival rate $\lambda p_{i^\star}$ and a departure rate $\psi_{i^\star}(\mathbf{z})$. We thus have, $\mathbb{P}$-almost surely $\lim_{t\to\infty} Y_{i^\star}(t) = \infty$ if $\lambda \geq \lambda^\star$, which allows us to conclude that $\mathbf{X}$ is transient. □

We can remark that the $i^\star$-th queue length is not the only one to diverge to almost surely diverge to infinity if $\lambda > \lambda^\star$. We know that $X_{i^\star}(t)$ goes to infinity. Because all the functions Ψ_j are decreasing functions of $X_{i^\star}$, for all j, there exists a time T_j after which $\Psi_j(\mathbf{X}(T_j)) < \lambda p_j$. We can then bound from below the j-th queue by a M/M/1 queue whose arrival rate is strictly larger than its departure rate. Hence, we get:

$$\forall j, \qquad \mathbb{P}\left[\lim_{t\to\infty} X_j(t) = \infty\right] = 1.$$

Combining the results of Lemma 3.4 and Theorem 4.2 give us the following result:

Theorem 4.3. *Let $\lambda^\star = \sup \mathcal{B}$. If $\lambda < \lambda^\star$, the Markov chain $\mathbf{X}$ is positive recurrent. If $\lambda > \lambda^\star$, it is transient.*

The behavior of the Markov chain for $\lambda = \lambda^\star$ is not studied in this thesis. We know that in the general case, the study of dynamic systems in the case $\lambda = \lambda^\star$, although results can be obtained using fluid limits in some cases (see [35]).

An interesting remark for this Theorem comes from the consequences of Theorem 4.1. If the system meets a *separability* condition, one can use the saturation rule (see [20]). This rules states that the Markov chain representing our dynamics is either positive recurrent, or transient, and that the stability region is uniquely defined by the value of $\lim_{n\to\infty} \frac{T_n}{n}$, where $(T_n)_{n\geq 0}$ is the sequence of *maximal daters* in the system. Unfortunately, for our dynamics, defining maximal daters and computing the value of the limit seems to be a hard problem, which leads us to obtain stability through different channels.

The second main result of this Chapter is a better characterization of the value of $\lambda^\star$, under a stronger assumption. Let us replace assumption i) for the functions $(\psi_i)_{0\leq i\leq N-1}$ by assumption $i^\star$):

$i^\star$) for all i, ψ_i is non-increasing in x_j for all $j \neq i$ and increasing in x_i.

This stronger assumption is motivated by communication networks, where the departure rates of one user is inversely proportional to a shot-noise of the queue length process and proportional to the queue length of the observed server. To obtain the departure rate of all users in a given server, we have to multiply this departure rate by the queue length of said server, which gives a departure rate in a server increasing with its queue length (see [81], [84] for instance).

Theorem 4.4. *Under assumptions $i^\star), ii), iii)$, $\lambda^\star$, the maximal value of $\mathcal{B}$ is obtained for any $\mathbf{z}$ solution to, for all $0 \leq i, j \leq N-1$:*

$$\frac{1}{p_i}\psi_i(\mathbf{z}) = \frac{1}{p_j}\psi_j(\mathbf{z}). \tag{4.2}$$

We thus have $\lambda^\star = \frac{1}{p_i}\psi_i(\mathbf{z})$, for any $0 \leq i \leq N-1$.

The proof of this result uses the same arguments as the proof of Lemma 3.7, presented in Section 3.3 fo the Appendix. This result gives us a simple condition to characterize the values of $\mathcal{B}$. In the next section, we will use this result to prove stability of non-symmetric BWP models.

4.3 Stability of non-symmetric BWP models

We can now move on to obtaining stability for the non-symmetric multiclass SBD process. In this setup, we allow users transmitting on the same number of bands to have different stochastic properties in the system. This way, we can encompass more complex allocation policies as the symmetric system do. We formulate the following result:

Theorem 4.5. *The non-symmetric multiclass SBD system is stable if $\lambda < \lambda^\star$ and unstable if $\lambda > \lambda^\star$, where:*

$$\lambda^\star = \frac{1}{p_C L_C} \frac{|C| z_C^\star}{\langle \ell_{\mathcal{D}} \rangle \sum_U |C \cap U| z_U^\star},$$

where $\mathbf{z}^\star$ is a solution to the following system of equations:

$$\forall C, D \in \mathcal{P}(K) \quad \frac{1}{p_C L_C} \frac{|C| z_C^\star}{\sum_U |C \cap U| z_U^\star} = \frac{1}{p_D L_D} \frac{|D| z_D^\star}{\sum_U |D \cap U| z_D^\star}. \tag{4.3}$$

Proof. The goal here is to obtain the stability condition for the two chains $\underline{\mathbf{X}}_\varepsilon$ and $\bar{\mathbf{X}}^\varepsilon$, and then to obtain the wanted stability condition for the original system.

Let us start with obtaining the stability condition for the dominating chain $\bar{\mathbf{X}}^\varepsilon$. We take, for all i, C, the function $\Psi_{i,C}(\mathbf{x}) = \frac{1}{L_C} \frac{\mathcal{N}_0 + |C| x_{i,C}}{\sum_{k,U} \ell^\varepsilon(a_k, a_i) |C \cap U| x_{k,U}}$.

Immediately, we can see that, for all $\mathbf{x} \in \mathbb{R}_+^{N \times 2^K - 1}$, we have:

$$\lim_{n\to\infty} \Psi_{i,C}(n\mathbf{x}) = \frac{1}{L_C} \frac{|C|x_{i,C}}{\sum_{k,U} a_{k,i}|C\cap U|x_{k,U}} \triangleq \psi_{i,C}(\mathbf{x}).$$

Moreover, the functions $(\psi_{i,C})$ meet conditions $i^\star) - iii)$, which allow us to use the result from Theorem 4.4 to get that $\mathbf{X}$ is stable whenever $\lambda < \lambda^\star$, where $\lambda^\star$ is such that:

$$\lambda^\star p_C \varepsilon^2 = \psi_{i,C}(\mathbf{z}),$$

where $\mathbf{z}$ is solution to (4.2).

Let us now prove that for all i, j and for all C, $z_{i,C} = z_{j,C}$. Let us take $0 \leq j \leq N$, and define $\mathbf{z}' = (z_{i+j,C})$, where we denote $i + j$ as remainder modulo N of the sum if $i + j \geq N$. We have, for all i, C:

$$\begin{aligned}\psi_{i,C}(\mathbf{z}') &= \frac{1}{L_C} \frac{|C|z_{i+j,C}}{\sum_{k,U} \ell^\varepsilon(a_i, a_k)|C\cap U|z_{k,U}} \\ &\overset{(a)}{=} \frac{1}{L_C} \frac{|C|z_{i+j,C}}{\sum_{k',U} \ell^\varepsilon(a_{i+j}, a_{k'})|C\cap U|z_{k',U}} = \psi_{i+j}(\mathbf{z}).\end{aligned}$$

To explain (a), we use the fact that $\mathcal{D}$ is a square torus, and that the function ℓ^ε is defined on a grid. This way, we know that, for each i, j, k, there exists a unique k' such that $\ell^\varepsilon(a_{i+j}, a_k) = \ell^\varepsilon(a_i, a_{k'})$. We use this reindeixation of the sum to conclude. Finally, we know that $\mathbf{z}$ is solution to (4.2), which gives $\psi_{i+j}(\mathbf{z}) = \psi_i(\mathbf{z})$ and gives:

$$\psi_{i,C}(\mathbf{z}') = \psi_{i,C}(\mathbf{z}).$$

From this result, we know that for any solution $\mathbf{z}$ to (4.3), the value of $\psi_{i,C}(\mathbf{z})$ is invariant by translation on i. From this, we can conclude that for all i, j, $z_{i,C} = z_{j,C} = z_C$. Using this, searching for solutions of the system over $\mathbb{R}^{N_\varepsilon \times 2^K - 1}$ amounts to searching for solutions over $\mathbb{R}^{2^K-1}$. The system becomes:

$$\begin{aligned}\frac{1}{p_C\varepsilon^2}\psi_{i,C}(\mathbf{z}) &= \frac{1}{p_C\varepsilon^2}\frac{1}{L_C}\frac{|C|z_C}{\sum_{k,U}\ell^\varepsilon(a_k,a_i)|C\cap U|z_U} \\ &= \frac{1}{p_C L_C}\frac{|C|z_C}{\langle \ell^\varepsilon_{\mathcal{D}}\rangle \sum_U |C\cap U|z_U}.\end{aligned}$$

After simplification, we get:

$$\frac{1}{p_C L_C}\frac{|C|z_C}{\sum_U |C\cap U|z_U} = \frac{1}{p_D L_D}\frac{|C|z_C}{\sum_U |C\cap U|z_U}. \tag{4.4}$$

We can use the result from Theorem 4.4 and the domination properties from Theorem 1.2 to get the following stability condition for the system:

$$\lambda_c^+ \leq \frac{1}{p_C L_C}\frac{|C|z_C}{\langle \ell^\varepsilon_{\mathcal{D}}\rangle \sum_U |C\cap U|z_U}. \tag{4.5}$$

We can use the same steps with the dominated chain $\underline{\mathbf{X}}_{\varepsilon}$ to obtain the same system as in (4.4), and the reciprocal condition:

$$\lambda_c^- \geq \frac{1}{p_C L_C} \frac{|C| z_C}{\langle \ell_{\varepsilon,\mathcal{D}} \rangle \sum_U |C \cap U| z_U}. \tag{4.6}$$

Finally, let ε tend to 0, which gives the condition:

$$\lambda_c = \frac{1}{p_C L_C} \frac{|C| z_C}{\langle \ell_{\mathcal{D}} \rangle \sum_U |C \cap U| z_U}. \tag{4.7}$$

where $\mathbf{z}$ is solution to (4.4), which concludes the proof. □

We can make two remarks about the result of Theorem 4.4. The first one is that the system of equations we obtain for $\mathbf{z}$ does not depend on the path-loss function ℓ in the system. This lack of dependency comes from the square torus topology we use in our system, which allows for a simplification of the system presented in Theorem 4.3.

The second remark we can make is that this result can be easily generalized to any link length $r > 0$ by taking the same steps as in Subsection 2.3, to get that:

$$\lambda_c = \frac{\ell(r)}{p_C L_C} \frac{|C| z_C}{\langle \ell_{\mathcal{D}} \rangle \sum_U |C \cap U| z_U},$$

To verify this result, we add the symmetry hypothesis to compare it to the result known in [72]: whenever $|C| = |D|$, we have $p_C = p_D$ and $L_C = L_D$, i.e. users with the same number of communication channels have the same stochastic properties in the network. With $K = 2$ bands, we look for a solution to (4.3) in the form $\mathbf{z} = (x, y, z)$. The first equation gives:

$$\frac{1}{p_{\{1\}} L_{\{1\}}} \frac{x}{x+z} = \frac{1}{p_{\{1\}} L_{\{1\}}} \frac{y}{y+z},$$

which yields $x = y$. Injecting this result in the second equation gives:

$$\frac{1}{p_{\{1\}} L_{\{1\}}} \frac{x}{x+z} = \frac{1}{p_{\{1,2\}} L_{\{1,2\}}} \frac{2z}{x+y+2z} = \frac{1}{p_{\{1,2\}} L_{\{1,2\}}} \frac{z}{x+z},$$

which, after solving for z, gives $z = \frac{p_{\{1,2\}} L_{\{1,2\}}}{p_{\{1\}} L_{\{1\}}} x$. The solution to the system are of the form $\mathbf{x} = (x, x, \frac{p_{\{1,2\}} L_{\{1,2\}}}{p_{\{1\}} L_{\{1\}}} x)$, for $x \in (0, \infty)$. We thus get for λ_c:

$$\lambda_c = \frac{2}{\langle \ell_{\mathcal{D}} \rangle \left(p_{\{1\}} L_{\{1\}} + p_{\{2\}} L_{\{2\}} + 2 p_{\{1,2\}} L_{\{1,2\}} \right)},$$

which is the value of the critical arrival rate for this network. If we generalize this result for $K \geq 2$, we can see that $\mathbf{z} = p_C L_C$ is a solution for the system defined in Theorem 4.5. We thus get:

$$\lambda^\star p_C = \frac{1}{L_C} \frac{|C| p_C L_C}{\langle \ell \rangle \sum_U |U| p_U L_U},$$

which, after some combinatorics, give:

$$\lambda^\star = \frac{K}{\langle \ell \rangle \sum_U |U| p_U L_U},$$

which is the critical arrival rate for the symmetric network.

We can also verify this stability region through simulation: Figure 4.1 displays a non-symmetric BWP model ith $K = 2$ bands where bands $\{1\}$ and $\{2\}$ are not considered symmetrically by the system: 80% of users transmitting on one band chose band $\{1\}$, and the remaining 20% chose band $\{2\}$. The rest of network parameters are the same as the ones used in Section 2.3.

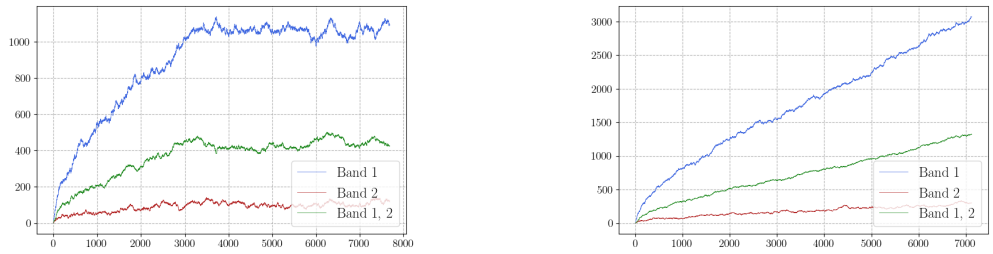

Figure 4.1: Number of active users in the non-symmetric network over time with $K = 2$ bands for two values of λ. In this setup, $p_{\{1\}} = 0.64$, $p_{\{2\}} = 0.16$ and $p_{\{1,2\}} = 0.2$.

Chapter 5

Extension and conclusion

In the first part of this manuscript, we studied the stability of a multiclass SBD model with wireless-type interactions. As mentioned multiple times, these dynamics are leveraged by wireless networks, but in Chapter 4, we were able to obtain a general stability condition for systems that have fluid limits meeting certain requirements. In the chapter, we will discussed the results obtained in this part and interpret them.

5.1 Interpretation of the results

Theorem 2.2 gives the critical arrival rate λ_c below which the dynamics is stable and above which it is not in the symmetric system:

$$\lambda_c = \frac{K\ell(r)}{\mathfrak{L}\langle \ell_{\mathcal{D}} \rangle}. \tag{5.1}$$

We can note that the form of this critical value in question is somewhat unexpected. The quantity $\mathfrak{L} = \sum_U p_U |U| L_U$ appears, while a natural interpretation would have preferred the quantity $\sum_U p_U \frac{L_U}{|U|}$, which denotes the average user load per band in the network. We can give the following interpretation for the value of $\mathfrak{L}$: on average, a user has L_U bits to transmit over $|U|$ bands. Hence, a user of type U brings a time-space load equal to $|U|L_U$ to the network. Taking the average over the distribution of user types, we obtain $\mathfrak{L}$. We can rewrite the stability condition $\lambda < \frac{K\ell(R)}{\langle \ell_{\mathcal{D}} \rangle \mathfrak{L}}$ as:

$$\lambda \frac{\mathfrak{L}}{K} < \frac{\ell(R)}{\langle \ell_{\mathcal{D}} \rangle},$$

Under this form and with the previous remark, we can interpret the left hand side term as the average *load* arriving per unit of time and per channel. The right-hand side is the throughput capacity of one channel in heavy load (the signal power divided by the fluid interference power). This way, the stability condition for the symmetric system can be seen as the classical

condition $\rho < 1$ seen in Jackson networks, for which the density of arriving jobs in the system cannot exceed its throughput.

For the non-symmetric system, we can not reach a closed form condition for the value of λ_c, though we can define it as:

$$\lambda_c = \frac{1}{p_C L_C} \frac{|C|\ell(r) z_C}{\langle \ell_{\mathcal{D}} \rangle \sum_U |C \cap U| z_U}, \tag{5.2}$$

where $\mathbf{z} \in \mathbb{R}^{2^K - 1}$ is the solution of a system of equations given in Theorem 4.5. This results is a corollary of Theorem 4.2, which states that the vector $\mathbf{z}$ is such that:

$$\mathbf{z} \in \arg\max_{\mathbf{x} \in \mathbb{R}^{N_\varepsilon}} \min_i \frac{1}{p_C L_C} \frac{|C|\ell(r) x_{i,C}}{\sum_{k,U} \ell^\varepsilon(a_k, a_i) x_{k,U}}.$$

To interpret this result, we can see $\mathbf{z}$ as the maximal capacity of the channel with the lowest throughput in the network. Due to the nature of the interactions in the system, whenever the population of a queue explodes, it propagates to the other queues, leading to the instability of the system. Once again, we obtain a "load-throughput" condition for the stability of the system in the non-symmetric system.

5.2 Restricting band configurations

In this work, we considered that all band configurations are allowed for users in the system. On top of allowing an exponential number of configurations for users, this setup is not commonly used for wireless networks. For instance, a usual setup for band allocation is to only alow the use of contiguous bands (this way, with $K = 4$, configurations $\{1, 2\}$ and $\{2, 3, 4\}$ are allowed but not $\{1, 3\}$). We will see in this section how to extend the previous results when restricting the band configurations, i.e., when allowing $p_C = 0$ for certain $C \in \mathcal{P}(K)$. Let us now denote $\mathcal{P}(K)^\star = \{C \in \mathcal{P}(K), p_C \neq 0\}$ as the set of used band configurations in the network.

The main result we use to obtain stability in the system is stochastic monotonicity. In simple words, this property states that when we increase the population of one class of users, it slows down transmissions for all the other classes in the system. The second observation about the network we can make is the system of equations obtained in Theorem 4.5: this system needs to have a solution space of dimension 1 (i.e., of the form $\mathbf{x}_0 t$ for a given $\mathbf{x}_0$ and $t > 0$) for the value of λ_c to be uniquely defined.

If there exists a subset of classes "disconnected" from the system in the sense that they do not have an impact on the rate of transmissions, i.e. a subset $H \in \mathcal{P}(K)$ of classes D such that for all $H \notin S$, $C \cap D = \emptyset$, it will act as a single-class SBD process independent from the rest of the dynamics, with its own stability condition.

Assuming the Poisson rain of arriving users stays common to all users, this leads us to obtain a condition on the form of the set $\{C \cap U, C, U \in \mathcal{P}(K)\}$.

This condition can be expressed in terms of the matrix $\mathfrak{I} = (|C \cap U|)_{C,U \in \mathcal{P}(K)}$: if such classes D exists, it implies that the matrix $\mathfrak{I}$ can be rearranged to be a block matrix. Another way to describe it is to consider the graph $\mathcal{G}$ for which the vertices are labelled with the elements of $\mathcal{P}(K)$ and two vertices labelled with U and V are connected if and only if $U \cap V \neq \emptyset$. The conditions then becomes that the graph $\mathcal{G}$ is connected.

Collecting these observations, we can state the following Theorem:

Theorem 5.1. *If the interaction graph $\mathcal{G}$ is connected (or, if the interaction matrix $\mathfrak{I}$ cannot be rearranged in a block matrix), the critical arrival λ_c remains unchanged when allowing the p_C to be equal to 0.*

If the interaction graph $\mathcal{G}$ is not connected (or, if the interaction matrix $\mathfrak{I}$ can be rearranged in a block matrix), let $S_1, \dots, S_n$ be the n sets labelling the connected components of $\mathcal{G}$ (or the blocks of $\mathfrak{I}$), and let $\lambda_{c,1}, \dots, \lambda_{c,n}$ be the critical arrival rates obtained when considering separately each of the configuration sets $S_1, \dots, S_n$. The critical arrival rate for the whole system becomes:

$$\lambda_c = \min_i \lambda_{c,i}. \tag{5.3}$$

An interesting remark is that if we now assume that the Poisson rains for the arrival of users are independent for each of the possible configuration sets $S_1, \dots, S_n$, instead of taking the minimum critical rate for the system, the stability condition becomes:

$$\lambda_c = \sum_i \lambda_{c,i}.$$

Using Theorem 5.1 and the previous remark allows to capture even more resource allocation policies for networks, and this result can be used for load balancing purposes, as one can be interested in maximizing the value of λ_c by tuning the parameters of each of the multiclass SBD processes to desire.

Finally, the results presented in this part have been proved when assuming that the interfering power between channels was equal to the size of their intersection, but they can be extended to any similarity measure $f(C, U) > 0$ between channels C and U by using it instead of the intersection measure in all the previous equations.

5.3 Extension

The work presented in this part is meant to introduce a framework to study multiclass SBD processes. This framework is simple yet it captures some key features leveraged in bandwidth partitioning model. Future work may add more complex features to study a larger variety of networks.

A first direction to look into is the cellular version of the presented network. In the setup we presented in this part, we studied a device-to-device network (D2D). A natural extension would be to study a device-to-network

(D2N) version, where an antenna is located at the origin, and all the transmitter share this antenna as a receiver. In such a setup, if we assume that the antenna has an infinite channel capacity, the rate-of-transmission function becomes:

$$R(x, \Phi_t) = \frac{|C|\ell(\|x\|)}{\mathcal{N}_0 + I(x, \Phi_t)}.$$

The behavior of D2N networks is known to be different than that of D2D networks. For instance, [3] shows a D2N version of the SBD process studied in [80], in which meta-stability appears: the system appears to be stable until a moment where the network population explodes. In this newer setup for example, it not sufficient to have $\ell'(x) \leq \ell(x)$ anymore to obtain domination, but the other conditions from Theorem 1.2 still hold. Thus, a first extension of the problem would be to study the stability of this new system and see how the stability condition from Theorem 2.2 changes.

Among the other possible extensions, one can think of adding fading to the system, to model blocking or atmospheric phenomena that can alter the quality of transmission, and can add line-of-sight models in order to see how the stability condition changes.

This concludes the first part of this work, focusing on describing the stability region of this array of multiclass SBD processes. As positive recurrent Markov processes, these dynamics have a stationary distribution to which they converge. The next part will focus on the study on this stationary distribution as well as the result point processes and some of their properties.

Part II

Stationary interacting point processes

Chapter 6

Study of the steady state dynamics

The main result of Part I, Theorem 2.2, gives the existence of a stationary regime for the multiclass spatial birth-and-death process when $\lambda < \lambda_c$. The existence of a stationary regime of the dynamics raises interesting questions about the nature of this stationary regime and the properties of the resulting point process.

The first question we will tackle in this part is the stationary user densities in the system. We know that the arrival process is a Poisson rain in the system, and we also know the stochastic intensity of the departure process. Given this, we try to estimate the spatial user densities in the stationary regime.

The second question we will answer in this part is revolves around the geometry of the point process in the stationary regime. We know from [80] that the single class system show *clustering*, i.e. attraction in the stationary regime. In a clustered point process, points "attract" each other, which translates in a condition between the regular and the Palm expectation of shot noises of the point process.

Finally, the last question of interest revolves around the stationary distribution of the queuing process. The discretization of the multiclass SBD process introduced in Part I lead us to define two multiclass interference queuing networks (defined similarly as in [81]). We know from [22] that single-class interference queuing networks have exponential moments, which gives as a consequence bounds on the tails of the distribution. This property is interesting for ultra reliable, low latency (URLLC) networks ([62]), as it gives tight bounds for the tails of the distribution of latency in this system.

6.1 First order heuristic and Poisson estimate for λ_c

The goal of this first chapter is to develop two heuristics to estimate the spatial densities of users in the stationary regime. The first heuristic we develop is a mean-field heuristic: in this heuristic, we assume that all the subprocess of users of class $C \in \mathcal{P}(K)$ are homogenous PPP, and we use this assumption to derive an equation giving the first-order heuristic. Such Poisson heuristics have already been studied in different setups, like in replica mean-field models: in [19], the authors prove that as the number of replicas goes to infinity, they behave like independently distributed Poisson processes. In another setup, [5] and [45] provide a quantification of the error of the mean-field approximation. We then define a second heuristic using a *cavity approximation* (see [80]) in order two refine the approximation. We say that this heuristic is of the *second order* because we rely on the cross correlation function $\rho^{(2)}$. We then discuss the relative performance of these two heuristics in a numerical setup.

Let $\mu_C = \frac{1}{|\mathcal{D}|}\mathbb{E}\left[\Phi_{C,0}(\mathcal{D})\right]$ denote the user density of the point process $\Phi_{C,0}$ of users of class $C \in \mathcal{P}(K)$ in the stationary regime.

A first heuristic to estimate μ_C is the Poisson heuristic: we assume that, in the stationary regime, all the point processes $\Phi_{C,0}$ for $C \in \mathcal{P}(K)$ are independent Poisson point processes with intensity μ_C^f. As mentioned earlier, Poisson approximations appear in to replica mean-field methods, where we consider multiple realizations of our stochastic process and interactions between users are picked uniformly at random among replicas of the dynamics. We know that (see [19]) as the number of replicas go to infinity, the processes behave like independent Poisson point processes, which justifies the Poisson approximation. The Poisson heuristic presented here falls in the same line of thought. We define the following heuristic:

Heuristic 1. *We define the* Poisson heuristic μ_C^f *for* μ_C *as the smallest solution of the following equation:*

$$\mu_C^f \int_0^\infty e^{-z\mathcal{N}_0} \exp\left[-\sum_{U\in\mathcal{P}(K)} \mu_U^f \mathcal{I}(z, |C\cap U|)\right] \mathrm{d}z = \frac{\lambda p_C L_C}{|C|\ell(r)}. \tag{6.1}$$

where $\mathcal{I}(z,k) = \int_{\mathcal{D}}(1-e^{-zk\ell(\|x\|)})\mathrm{d}x$.

We numerically observe that the values of the intensities μ_C^f obtained by solving (6.1) do not depend on the value of $\mathcal{N}_0 > 0$. This observation is consistent with the fluid system and the stability condition in the network being independent of the value of $\mathcal{N}_0$.

Proof. Let us apply the RCP to the process $\Phi_{0,C}$ of users of class $C \in \mathcal{P}(K)$ during a time interval dt:

$$\lambda p_C L_C |\mathcal{D}| = \mathbb{E}\left[\sum_{x\in\Phi_{C,0}} R(x,\Phi_0)\right].$$

We use the definition of the Palm probability measure to rewrite this as:

$$\lambda p_C L_C |\mathcal{D}| = \mathbb{E}^0_{\Phi_{C,0}}\left[R(0^C,\Phi_0)\right]\mathbb{E}\left[\Phi_0^C(\mathcal{D})\right]. \tag{6.2}$$

Using this, we get that, in the stationary regime:

$$\lambda p_C L_C = \mu_C \mathbb{E}^0_{\Phi_{C,0}}\left[R(0^C,\Phi_0)\right] = |C|\mu_C \ell(r)\mathbb{E}^0_{\Phi_{C,0}}\left[\frac{1}{N_0+I_C}\right].$$

This is equivalent to:

$$\mu_C = \frac{\lambda p_C L_C}{|C|\ell(r)}\left(\mathbb{E}^0_{\Phi_{C,0}}\left[\frac{1}{N_0+I_C}\right]\right)^{-1}.$$

Let us state use this Lemma (see Lemma 1 from [80]):

Lemma 6.1. *Let Y be a positive random variable with finite expectation and $c>0$ be a real number. Then:*

$$\mathbb{E}\left[\frac{1}{c+Y}\right] = \int_0^\infty e^{-zc}\mathbb{E}[e^{-zY}]\mathrm{d}z.$$

Using Lemma 6.1 with $Y \equiv I(0^C,\Phi_0)$, which has a finite first moment and with $c \equiv \mathcal{N}_0$, we get:

$$\mathbb{E}^0_{\Phi_{C,0}}\left[\frac{1}{\mathcal{N}_0+I_C}\right] = \int_0^\infty e^{-z\mathcal{N}_0}\mathbb{E}^0_{\Phi_{C,0}}\left[e^{-zI_C}\right]\mathrm{d}z.$$

Let us assume that the processes $\Phi_{0,U}$ are independent Poisson point processes denoted by Ψ^U. Using this, combined with Slivnyak's theorem, we get:

$$\mathbb{E}^0_{\Phi_{C,0}}\left[\frac{1}{N_0+I_C}\right] \approx \int_0^\infty e^{-z\mathcal{N}_0}\prod_{U\in\mathcal{P}(K)}\mathbb{E}\left[e^{-z\sum_{x\in\Phi_0^U\setminus\{0^{C_\}}}P|C\cap U|\ell(\|x\|)}\right]\mathrm{d}z.$$

Using the formula for the Laplace transform of a Poisson point process, we get:

$$\mathbb{E}\left[e^{-z\sum_{x\in\Phi_0^U\setminus\{0^{C_\}}}|C\cap U|\ell(\|x\|)}\right] = \exp\left[-\mu_U^f\int_{\mathcal{D}}(1-e^{-z|C\cap U|\ell(\|x\|)})\mathrm{d}x\right].$$

To conclude the proof, we combine these equations:

$$\mu_C^f\int_0^\infty e^{-z\mathcal{N}_0}\exp\left[-\sum_{U\in\mathcal{P}(K)}\mu_U^f\mathcal{J}(z,|C\cap U|)\right]\mathrm{d}z = \frac{\lambda p_C L_C}{|C|\ell(r)},$$

which is the announced result. □

An observation we can make comes from the symmetry hypothesis. We can conjecture that under this assumption, the stationary user densities follow the same property, i.e., are such that whenever $|C| = |D|$, $\mu_C = \mu_D$. The proof for this result is not presented in this work, but numerical simulations we performed suggest that it holds.

We can use this observation to obtain another version of the system of equations in (6.1): if we define $\mu_j = \frac{1}{|\mathcal{D}|}\mathbb{E}\left[\sum_{U:|U|=j} \Phi_{U,0}(\mathcal{D})\right] = \sum_{U:|U|=j} \mu_U$ as the intensity of users communicating on j channels, for $1 \leq j \leq K$, with $L_j = L_C$ and $p_j = \binom{K}{j} p_C$ for all C such that $|C| = j$, we obtain the following system of equations from Heuristic 1:

$$\mu_j^f \int_0^\infty e^{-z\mathcal{N}_0} \exp\left[-\sum_{l=1}^{K} \mu_l^f \sum_{m=1}^{\min(j,l)} \alpha_{m,j,l} \mathcal{J}(z,m)\right] \mathrm{d}z = \frac{\lambda p_j L_j}{j\ell(r)}, \tag{6.3}$$

where $\alpha_{m,j,l} = \frac{\binom{j}{m}\binom{j-l}{l-m}}{\binom{K}{j}}$. This result if a consequence of Lemma 3.5 applied to the vector of user densities.

This result can be interesting computationally, in the case where we want to quickly estimate the density of users transmitting on a given class in the symmetric system: in contrast to the system proposed in Heuristic 1, which needs to solve $2^K - 1$ equations, the symmetric system from (6.3) possesses K equations. As K grows larger, the gain in performance becomes non-negligible.

A heuristic for λ_c

An interesting result arising from Heuristic 1 is an estimate for the value of λ_c: a necessary condition for the fixed point equation (6.1) to admit solutions is that the system is in it stationary regime, i.e., if $\lambda < \lambda_c$. We define the following estimate for λ_C:

Heuristic 2. *Let λ_P be the largest value of λ such that Equation* (6.1) *admits a solution (or Equation* (6.3) *in the symmetric network). Then, λ_P is an estimate for λ_c, which we call the* Poisson heuristic *estimate.*

This estimate is interesting because it comes from a completely different approach and is only relying on the study of the stationary regime of Poisson approximates of the network. We will discuss in Section 6.3 the performance of this heuristic.

The reason why this heuristic captures the stability region of our dynamics is not yet understood. We do not know if the value of λ_{P} is equal to the value of λ_c presented in Theorem 2.2 or if this value is a precise numerical approximation of the critical arrival rate.

6.2 Second order heuristic

In an effort to refine the first order heuristic for user densities from Heuristic 1, we introduce a *second order* heuristic, which uses an approximation for the pair-wise correlation function in the stationary regime.

Heuristic 3. *The* second-order heuristic *for the intensity of* $\Phi_{0,C}$ *is* μ_C^s *defined as:*

$$\mu_C^s = \frac{\lambda p_C L_C}{|C|\ell(R)} \left(\mathcal{N}_0 + I_C\right), \tag{6.4}$$

where $I_C \triangleq \mathbb{E}^0_{\Phi_{C,0}}\left[I(0^C, \Phi_0)\right]$ *is the interference experienced by the typical user of class* C *in the stationary regime. The vector* $\mathbf{I} = (I_C)_{C\in\mathcal{P}(K)}$ *is the solution to the following equation:*

$$I_C = \sum_{U\in\mathcal{P}(K)} \frac{|C\cap U|}{\mu_C^s} \int_{x\in\mathcal{D}} \ell(\|x\|)\rho^{(2)}_{C,U}(x,0)\mathrm{d}x \quad \forall C \in \mathcal{P}(K), \tag{6.5}$$

with the second order moment measure $\rho^{(2)}_{C,U}$ *is defined as a function of* $\mathbf{I}$*:*

$$\rho^{(2)}_{C,U}(x,y) = \frac{\lambda(\mu_U^s p_C + \mu_C^s p_U)}{\frac{1}{L_C}\frac{|C|\ell(R)}{\mathcal{N}_0+|C\cap U|\ell(\|x-y\|)+I_C} + \frac{1}{L_U}\frac{|D|\ell(R)}{\mathcal{N}_0+|C\cap D|\ell(\|x-y\|)+I_U}}. \tag{6.6}$$

Proof. To obtain this heuristic, we make the following cavity approximation in the system: let us consider a pair of points (x, y) in $\mathcal{D}$, where x is of class C and y is of class D.

The arrival rate of the pair is $\lambda p_C \mu_D + \lambda p_D \mu_C$, taking into account the contributions of the two processes. To obtain the departure rate, let us fix the locations of the two points. The interference experienced by a point located at x of class C in the stationary regime conditioned on a user of class D being present at y is equal to:

$$\begin{aligned} I(x) &= |C\cap D|\ell(\|x-y\|) + \sum_{U\in\mathcal{P}(K)}\sum_{z\in\Phi_{0,U}\setminus\{y\}} |C\cap U|\ell(\|z-x\|) \\ &= |C\cap D|\ell(\|x-y\|) + I_C, \end{aligned} \tag{6.7}$$

where I_C is the interference experienced by the typical user of class C in the network, i.e. $I_C = \mathbb{E}^0_{\Phi_0}\left[I(0^C, \Phi_0)\right]$. Using the definition of the second order moment measure relative to processes $\Phi_{C,0}$ and $\Phi_{U,0}$, $\rho^{(2)}_{C,U}$, we have:

$$\begin{aligned} I_C = \mathbb{E}^0_{\Phi_0}\left[I(0^C, \Phi_0)\right] &= \sum_U \mathbb{E}^0_{\Phi_0}\left[I(0^C, \Phi_0^U)\right] \\ &= \frac{1}{\mu_C}\sum_U |C\cap U| \int_{x\in\mathcal{D}} \ell(\|x\|)\rho^{(2)}_{C,U}(x,0)\mathrm{d}x. \end{aligned}$$

We obtain the departure rate for the pair (x, y) with x being of type C and y being of type D:

$$d_{C,D}(x,y) = \frac{1}{L_C}\frac{|C|\ell(R)}{\mathcal{N}_0 + |C \cap D|\ell(\|x-y\|) + I_C} + \frac{1}{L_D}\frac{|D|\ell(R)}{\mathcal{N}_0 + |C \cap D|\ell(\|x-y\|) + I_D}.$$

In the stationary regime, on average, the umber of arrivals compensate the departures, which gives us:

$$\lambda(\mu_U p_C + \mu_C p_U) = \rho^{(2)}_{C,U}(x,y) d_{C,D}(x,y).$$

Finally, to obtain the second-order heuristic for μ_C, we use Miyazawa's Rate Conservation principle for the process $\Phi_{C,0}(\mathcal{D})$, assuming that all the quantities are distributed according to their stationary distribution:

$$\lambda p_C |\mathcal{D}| = \mathbb{E}\left[\Phi_{C,0}(\mathcal{D})\right] \frac{|C|\ell(r)}{\mathcal{N}_0 + I_C},$$

which gives the intended result.

□

6.3 Numerical simulations and performance of the heuristics

We can compare the heuristics from Heuristic 1 and 2 to the value we obtain through simulation. To compute this intensity, we use an ergodic approximation of the form:

$$\mu_C \approx \frac{1.28}{t}\int_u^{u+t} \frac{\Phi_{w,C}(\mathcal{D})}{|\mathcal{D}|}\mathrm{d}w, \tag{6.8}$$

where u is taken sufficiently large to ensure we are in the stationary regime of the system and t is large enough so that the approximation is correct. The 1.28 factor arising in (6.8) comes from a Palm bias: in the simulation, when we compute the average number of users in $\mathcal{D}$, we introduce an observation bias when estimating the stationary user density, which we correct by using this multiplicative factor.

Figure 6.1 displays the results of both the Poisson (in red, dashed) against the numerical estimation of the user density (in blue, plain) for the process $\Phi_{\{1\}}$ using (6.8).

As we expected from previous results (see Section IV from [80]), the Poisson heuristic for spatial wireless networks does not estimate precisely the stationary user densities. This difference in predicted values can be easily explained by the fact that the stationary point process are not Poisson: making a Poisson approximation amounts to removing the spatial interactions between point processes in the stationary regime, which is likely to

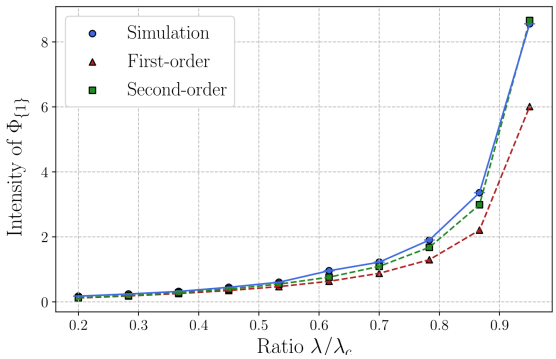

Figure 6.1: Value of $\mu_{\{1\}}$ as a function of λ/λ_c in a symmetric configuration.

not be true in our systems. From [80], we know that the single-class system shows clustering in the stationary regime, which renders the Poisson approximation less accurate when predicting the steady-state user densities. A sensible conjecture to make is that our spatial multiclass wireless network displays the same behavior in the stationary regime, which would provide an explanation for this observation.

On the other hand, we can see that the second-order heuristic is more performant when it comes to predicting the user densities, although the heuristic is more computationally heavy as we have to evaluate double integrals. One can further refine the approximation by developing higher order heuristics. In such a setup, to develop a heuristic of order n, we would have to assume the locations of n points in the system, which we can approximate using the heuristic of order $n-1$. This would lead us to building recursively a sequence of heuristics for the n-th order of which we can study the convergence (see [21]) in order to predict the spatial user densities in the stationary regime.

Poisson heuristic

The Poisson heuristic for λ_c gives us an interesting result: Figure 6.2 shows the respective values of λ_c and λ_{P} both in the symmetric and non-symmetric case for different values of $p_{\{1,2\}}$. In the symmetric case, we use $p_{\{1\}} = p_{\{2\}} = \frac{1-p_{\{1,2\}}}{2}$ and we use the value of λ_c from Theorem 2.2. For the non-symmetric case, we add a dysymmetry factor α, and we set $p_{\{1\}} = \alpha x$, $p_{\{2\}} = (1-\alpha)x$ and $p_{\{1,2\}} = \frac{1-x}{2}$. For the value of λ_c, we solve the system defined in Theorem 4.5.

We can see that the Poisson heuristic for λ_c is very performant in both cases. To explain this result, we can make the following conjecture: the first order heuristic fails to predict correctly the spatial user density, but from Figure 6.1, the difference in the predicted value tends to become smaller as λ/λ_c tends to 1. We can thus conjecture that in the heavy-traffic regime, when λ becomes arbitrarily close to λ_c, the subprocesses $\Phi_{0,C}$ become Poisson as the spatial interactions average out. Thus, the value of μ_C predicted

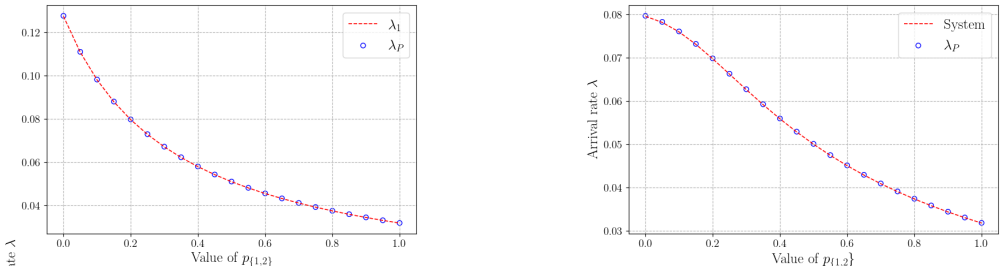

Figure 6.2: Comparison between λ_c and its Poisson heuristic as a function of $p_{\{1,2\}}$ in the network in the symmetric and the non-symmetric case.

through Heuristic 1 becomes exact, and as a consequence, the value of λ_{P} becomes equal to λ_c.

Chapter 7

Clustering

We remind here the definition of clustering, taken from [80]: a point process is said to be *clustered* if the dynamics show attraction in the stationary regime, i.e.:

Definition 7.1. *A PP Φ_0 will be said to be clustered if and only if we have, for all non-negative, non-increasing bounded function f:*

$$\mathbb{E}\left[F(0,\Phi_0)\right] \leq \mathbb{E}^0_{\Phi_0}\left[F(0,\Phi_0)\right]. \tag{7.1}$$

where $F(x,\Phi_0) = \sum_{y\in\Phi_0\setminus\{x\}} f(\|x-y\|)$ for $x \in \Phi_0$.

The goal in this chapter is to study this property in the stationary regime, and we will establish that the dynamics in the steady-state are clustered. This question is of interest to allow for a better description of the stationary regime of the dynamics, and to explain the precision of the Poisson heuristic defined in the previous section.

A useful tool we will use to display clustering in the system is the Ripley-K function, defined as:

$$K_{\Phi_0}(r) = \frac{1}{\lambda}\mathbb{E}^0_{\Phi_0}\left[\phi(B(0,r)-1)\right], \tag{7.2}$$

where λ is the intensity of Φ_0. Using $f(x) = \mathbb{1}\{x \leq r\}$ in (7.1), we obtain a necessary condition for clustered point processes: let Φ be a clustered point process with intensity $\lambda > 0$ and Ψ be a homogenous PPP with intensity λ. Then, we have, for all $r > 0$:

$$K_\Phi(r) \geq K_\Psi(r) = \pi r^2.$$

This results gives the classical interpretation for clustering, where users in the stationary regime attract each other. We know that clustering was proved in the single-class case (see [80]), and we would like to see how this translates in the multiclass setting. First, let us state the following lemma:

Lemma 7.1. *If Φ_t is stable, we have, for all $C \in \mathcal{P}(K)$:*

$$p_C\mathbb{E}[F(0_C,\Phi_0)] + \sum_{U\in\mathcal{P}(K)} p_U\mathbb{E}[F(0_U,\Phi_{0,C})] \\ \leq \mathbb{E}^0_{\Phi_{0,C}}[F(0_C,\Phi_0)] + \sum_{U\in\mathcal{P}(K)} \mathbb{E}^0_{\Phi_{0,U}}[F(0_U,\Phi_{0,C})]. \quad (7.3)$$

Proof. Let $C \in \mathcal{P}(K)$ and let us denote $F_{t,C} = \sum_{x\in\Phi_{t,C}} F(x,\Phi_t)$, where F is a shot-noise following the conditions stated in Definition 7.1.

Let us assume that a user arrives at $a \in \mathcal{D}$ between times t and $t+dt$ so that $\Phi_{t+dt} = \Phi_t \cup \{a\}$. By making a simple case study, if a is of class C, we have:

$$\begin{aligned} F_{t+dt,C} &= \sum_{x\in\Phi_{t+dt,C}} F(x,\Phi_{t+dt}) = \sum_{x\in\Phi_{t,C}} F(x,\Phi_{t+dt}) + F(a,\Phi_{t+dt}) \\ &= \sum_{x\in\Phi_{t+dt,C}} \left(\sum_{y\in\Phi_{t+dt}\setminus\{x\}} f(\|x-y\|)\right) + \sum_{y\in\Phi_{t+dt}\setminus\{a\}} f(\|a-y\|) \\ &= \sum_{x\in\Phi_{t,C}} \left(\sum_{y\in\Phi_t\setminus\{x\}} f(\|x-y\|)\right) + \sum_{y\in\Phi_{t,C}\setminus\{a\}} f(\|a-y\|) + F(a,\Phi_t) \\ &= F_{t,C} + F(a,\Phi_{t,C}) + F(a,\Phi_t). \end{aligned}$$

If a is of class $U \neq C$, we make a similar calculation to get:

$$F_{t+dt,C} = F_{t,C} + F(a,\Phi_{t,C}).$$

Let $F_{0,C}$ denote the stationary regime of the stochastic process $F_{t,C}$, and let $\mathbf{AF}_C = F_{0^+,C} - F_{0,C}$ be the increase in $F_{t,C}$ in the stationary regime after one arrival.

An arriving user in the network choses class C with probability p_C. Let $\mathbb{E}^\uparrow$ be the Palm probability associated with the PP of arrival instants in $\mathbb{R}$. We use the PASTA property i.e., we can assume that an arriving user is the typical user using this class. This means that the increase in $F_{0,C}$ induced by an arrival of a user of class $C \in \mathcal{P}(K)$ is equal to $\mathbb{E}\left[F(0_C,\Phi_{0,C}+F(0_C,\Phi_0))\right]$, and to $\mathbb{E}\left[F(0_D,\Phi_{0,C})\right]$ if the arriving user is of class $D \neq C$. We have:

$$\begin{aligned} \mathbb{E}^\uparrow[\mathbf{AF}_C] &= p_C\mathbb{E}[F(0_C,\Phi_{0,C}) + F(0_C,\Phi_0)] + \sum_{U\neq C} p_U\mathbb{E}[F(0_U,\Phi_{0,C})] \\ &= p_C\mathbb{E}[F(0_C,\Phi_0)] + \sum_{U\in\mathcal{P}(K)} p_U\mathbb{E}[F(0_U,\Phi_{0,C})]. \end{aligned} \quad (7.4)$$

We consider the point process corresponding to deaths instants of users of class C. It admits as stochastic intensity $\mathbf{R}_{t,C} = \frac{1}{L_C}\sum_{x\in\Phi_{t,C}} R(x,\Phi_t)$ with respect to the filtration $\mathcal{F}_{t,C} = \sigma\{\Phi_{C,s}, s<t\}$. Using Papangelou's theorem

(see Theorem 1.9.2 in [14]), the associated Palm probability measure admits a Radon-Nikodym derivative equal to:

$$\frac{\mathrm{d}\mathbb{P}^{\downarrow}}{\mathrm{d}\mathbb{P}_C} = \frac{\mathbf{R}_{0,C}}{\mathbb{E}[\mathbf{R}_{0,C}]}. \tag{7.5}$$

A user located at $b \in \Phi_0$ with class $D \in \mathcal{P}(K)$ leaves the system with probability $\frac{R(x,\Phi_0)}{L_D \mathbb{E}[\mathbf{R}_{0,D}]}$. Let $\mathbf{DF}_C = F_{0,C} - F_{0^-,C}$ denote the decrement process of $F_{0,C}$. We can write the expected decrease in $F_{t,C}$ caused by a departure from the system:

$$\mathbb{E}^{\downarrow}[\mathbf{DF}_C] = \mathbb{E}\left[\frac{\mathbf{R}_{0,C}}{\mathbb{E}[\mathbf{R}_{0,C}]} \sum_{x\in\Phi_{0,C}} \frac{R(x,\Phi_0)}{L_C \mathbf{R}_{0,C}} (F(x,\Phi_0) + F(x,\Phi_{0,C}))\right] + \mathbb{E}\left[\sum_{D\neq C} \frac{\mathbf{R}_{0,D}}{\mathbb{E}[\mathbf{R}_{0,D}]} \sum_{x\in\Phi_{0,D}} \frac{R(x,\Phi_{0,D})}{L_D \mathbf{R}_{0,D}} F(x,\Phi_{0,C})\right].$$

We can rearrange the previous equation by using the definition of the Palm expectation to get:

$$\mathbb{E}^{\downarrow}[\mathbf{DF}_C] = \frac{\mathbb{E}[\Phi_{0,C}(\mathcal{D})]}{L_C \mathbb{E}[\mathbf{R}_{0,C}]} \mathbb{E}^0_{\Phi_{0,C}}[R(0_C,\Phi_0)F(0_C,\Phi_0)] + \sum_{U\in\mathcal{P}(K)} \frac{\mathbb{E}[\Phi_{0,U}(\mathcal{D})]}{L_U \mathbb{E}[\mathbf{R}_{0,U}]} \mathbb{E}^0_{\Phi_{0,U}}\left[R(0_U,\Phi_{0,C})F(0_U,\Phi_{0,C})\right]. \tag{7.6}$$

Let us apply the RCP to the quantity of information present in the network. We get:

$$\begin{aligned} &\mathbb{E}[\mathbf{R}_{0,C}] = \lambda p_C |\mathcal{D}| \\ &\mathbb{E}^0_{\Phi_{0,C}}[R(0_C,\Phi_0)]E[\Phi_{0,C}(\mathcal{D})] = \lambda p_C L_C |\mathcal{D}|. \end{aligned} \tag{7.7}$$

Let $U, C \in \mathcal{P}(K)$. Then, $R(0_U,\Phi_{0,C})$ and $F(0_U,\Phi_{0,C})$ are negatively correlated: if $C \cap U \neq \emptyset$, an arrival of a user of class U increases the shot-noise on users of class C, and slow down the rate-of-transfer for these users. If $C \cap U = \emptyset$, there exists D such that $C \cap D \neq \emptyset$ and $C \cap U \neq \emptyset$ (for example, $D = C \cup U$). An arrival of a user of class U increases the shot-noise for users of class D and decrease the rate-of-transfer for these users. Consequently, the rate-of-transfer for users of class U slows down as well.

Moreover, $R(0_C,\Phi_0)$ and $F(0_C,\Phi_0)$ are also negatively correlated. Using the FKG inequality in (7.6) and the two relations from (7.7) yields:

$$\mathbb{E}^{\downarrow}[\mathbf{DF}_C] \leq \mathbb{E}^0_{\Phi_{0,C}}[F(0_C,\Phi_0)] + \sum_{U\in\mathcal{P}(K)} \mathbb{E}^0_{\Phi_{0,U}}[F(0_U,\Phi_{0,C})]. \tag{7.8}$$

A last application of the RCP to the number of users of class C in the system in the stationary regime gives:

$$\mathbb{E}^{\uparrow}[\mathbf{AF}_C] = \mathbb{E}^{\downarrow}[\mathbf{DF}_C], \tag{7.9}$$

which gives the following inequality, for all $C \in \mathcal{P}(K)$:

$$p_C \mathbb{E}[F(0_C, \Phi_0)] + \sum_{U \in \mathcal{P}(K)} p_U \mathbb{E}[F(0_U, \Phi_{0,C})] \\ \leq \mathbb{E}^0_{\Phi_{0,C}}[F(0_C, \Phi_0)] + \sum_{U \in \mathcal{P}(K)} \mathbb{E}^0_{\Phi_{0,U}}[F(0_U, \Phi_{0,C})], \tag{7.10}$$

which is the intended result. □

We can see that Lemma 7.1 is a consequence of the clustering of the subprocesses $\Phi_{0,C}$: if each of these processes was clustered, then we would have:

$$\mathbb{E}[F(0_C, \Phi_0)] \leq \mathbb{E}^0_{\Phi_{0,C}}[F(0_C, \Phi_0)],$$

which immediately yields the same result.

Let us sum (7.3) over $C \in \mathcal{P}(K)$. Using the law of total expectations, and reminding that the typical user is of type C with probability p_C and that Φ_0 is the superposition of the processes $\Phi_{0,C}$, we have:

$$\begin{aligned} \sum_C \left[p_C \mathbb{E}[F(0_C, \Phi_0)] + \sum_{U \in \mathcal{P}(K)} p_U \mathbb{E}[F(0_U, \Phi_{0,C})] \right] \\ &= \sum_C p_C \mathbb{E}[F(0, \Phi_{0,C} | 0^C)] + \sum_C \sum_{U \in \mathcal{P}(K)} p_U \mathbb{E}[F(0_U, \Phi_{0,C})] \\ &\underset{(a)}{=} \mathbb{E}[F(0, \Phi_0)] + \sum_U \sum_C \mathbb{E}[F(0, \Phi_{0,C} | 0^U)] \\ &= 2\mathbb{E}[F(0, \Phi_0)], \end{aligned}$$

where (a) uses the fact that $\sum_C \mathbb{E}[F(0, \Phi_{0,C}|0^U)] = \mathbb{E}[F(0, \Phi_0|0^U)]$. This yields:

$$2\mathbb{E}[F(0, \Phi_0)] \leq 2 \sum_{C \in \mathcal{P}(K)} \mathbb{E}^0_{\Phi_{0,C}}[F(0_C, \Phi_0)]. \tag{7.11}$$

We thus obtain the following result:

Theorem 7.2. *In the stationary regime, we have:*

$$\mathbb{E}[F(0, \Phi_0)] \leq \sum_{C \in \mathcal{P}(K)} \mathbb{E}^0_{\Phi_{0,C}}[F(0_C, \Phi_0)]. \tag{7.12}$$

The condition established in (7.2) is weaker than the clustering condition established in Definition 7.1. To see why, we can iterate the result from Lemma A.4 over all $C \in \mathcal{P}(K)$ to obtain:

$$\sum_{C\in\mathcal{P}(K)} \frac{\mu_C}{\mu_0}\mathbb{E}^0_{\Phi_{0,C}}[F(0_C,\Phi_0)] = \mathbb{E}^0_{\Phi_0}[F(0,\Phi_0)].$$

In the general case, we have no way to directly compare $\sum_C \frac{\mu_C}{\mu_0}\mathbb{E}^0_{\Phi_{0,C}}[F(0_C,\Phi_0)]$ and $\sum_C \mathbb{E}^0_{\Phi_{0,C}}[F(0_C,\Phi_0)]$, so we cannot establish clustering in the network as it is defined in [80].

Though, the result from Theorem 7.2 can be interpreted. Firstly, we can remark that in case $K = 1$, we obtain the statistical clustering observed in [80], which gives attraction between the points in the single-tier case. In the case $K \geq 2$, we use $f(x) = \mathbb{1}\{x \geq r\}$ and Slyvniak's theorem to obtain the following condition:

$$\pi r^2 \leq \sum_{C\in\mathcal{P}(K)} \frac{\mu_C}{\mu_0} K_{\Phi_{0,C}}(r). \tag{7.13}$$

Equation (7.13) states that the average number of points we see around around a given user is larger than its Poisson equivalent, i.e. that the system shows some kind of attraction in the stationary regime. The reason why we cannot reach per-class attraction in the stationary regime comes from the multiclass setup of the network: due to the difference in relative interference power in the users, some users attract other users more than others. With this observation, users of class C will be attracted by other users of class C, but also by users of class D such that $D \cap C \neq \emptyset$. The condition from Theorem 7.2 averages the observation over all classes to remove this effect.

Chapter 8

Higher order moment measures

In the stationary regime, the definition of stability implies that the first order moment measure is finite. Higher order moment measures are an interesting object of study. In [22], Banerjee and Sankararaman study interference queuing networks on the lattice $\mathbb{Z}^d$ and obtain the existence and finiteness of exponential moment measures. The architecture of this section is based on these results.

From Theorem 2.1, we know that the SBD process $\Phi_0(\mathcal{D})$ can be bounded from above and below by two interference queuing networks (as defined in [81]). The goal of this chapter is to study how the results obtained on this category of queuing network translates to our dynamics, and if we can obtain the existence of exponential moments for the jump process $\Phi_0(\mathcal{D})$. This question is of interest as it allows to obtain information about the stationary distribution of the queuing process $\Phi_0(\mathcal{D})$, which represent the population of users in the network, and allows to bound the tails of the distribution using the probability generating function.

The following Theorem is the main result in this section:

Theorem 8.1. *In the symmetric case, for all $\lambda \leq \lambda_c$, there exists $c_0 > 0$ such that for all $c \in [0, c_0)$, we have:*

$$\mathbb{E}\left[e^{c\Phi_0(\mathcal{D})}\right] < \infty.$$

Proof. We will start by proving that the queuing system $\bar{\mathbb{X}}_\varepsilon$ has exponential moments. We will then conclude with the existence of exponential moments for $\Phi_0(\mathcal{D})$ using the stochastic domination from Theorem 1.2.

Let us start the following Lemma:

Lemma 8.2. *Let $\mathbf{y} \in \mathbb{R}^{N_\varepsilon \times 2^K}$. Then, we have:*

$$\bar{\lambda}_c \sum_{i,C} y_{i,C}^m \leq \sum_{i,C} y_{i,C}^m \frac{1}{L_C p_C \varepsilon^2} R_{i,C}(\mathbf{y}), \tag{8.1}$$

Proof. Using the Cauchy-Schwartz inequality, we have:

$$\left(\sum_{i,C} y_{i,C}^m\right)^2 \leq \left(\sum_{i,C} y_{i,C}^m \frac{1}{L_C p_C \varepsilon^2} R_{i,C}(\mathbf{y})\right) \left(\sum_{i,C} \frac{y_{i,C}^m}{\frac{1}{L_C p_C \varepsilon^2} R_{i,C}(\mathbf{y})}\right). \tag{8.2}$$

Let us focus on the second term of the right-hand side of the inequality. We know, from the definition of $\bar{\lambda}_c$, that it is the largest $\nu > 0$ such that there exists $\mathbf{z} \in \mathbb{R}_+^{N_\varepsilon \times 2^K - 1}$ such that for all i, C, $\nu p_C \varepsilon^2 \leq \frac{1}{L_C} \frac{|C| z_{i,C}}{\sum_{k,U} \ell^\varepsilon(a_k, a_i) |C \cap U| z_{k,U}}$. As a consequence, for all $\mathbf{y} \in \mathbb{R}_+^{N_\varepsilon \times 2^K - 1}$, we have:

$$\frac{1}{L_C} R_{i,C}(\mathbf{y}) \geq \bar{\lambda}_c p_C \varepsilon^2.$$

This yields:

$$\sum_{i,C} \frac{y_{i,C}^m}{\frac{1}{L_C p_C \varepsilon^2} R_{i,C}(\mathbf{y})} \leq \sum_{i,C} \frac{1}{\lambda_c} y_{i,C}^m.$$

Injecting this result into (8.2) gives:

$$\bar{\lambda}_c \sum_{i,C} y_{i,C}^m \leq \sum_{i,C} y_{i,C}^m \frac{1}{L_C p_C \varepsilon^2} R_{i,C}(\mathbf{y}), \tag{8.3}$$

which concludes the proof.

□

We can now prove this next lemma:

Lemma 8.3. *Let $\lambda < \bar{\lambda}_c$ and $D_\varepsilon = \frac{\bar{\lambda}_c - \lambda}{\lambda + 1/\bar{L}\bar{p}\varepsilon^2}$, where $\bar{L}\bar{p} = \min_C L_C p_C$. Then, we have:*

$$D \sum_{i,C} \mathbb{E}\left[X_{i,C}^m\right] \leq \sum_{i,C} \binom{m+1}{k} E\left[X_{i,C}^k\right].$$

Proof. Let us consider the function $V(\mathbf{y}) = \sum_{i,C} \frac{1}{p_C \varepsilon^2} y_{i,C}^{m+1}$, and let $\mathcal{L}$ be the infinitesimal generator associated with the Markov chain $\bar{\mathbf{X}}$. Since the system is stationary, $\mathbb{E}\left[\mathcal{L}V(\bar{\mathbf{X}})\right] = 0$, which translates as:

$$\sum_{i,C} \lambda \mathbb{E}\left[(\bar{X}_{i,C} + 1)^{m+1} - \bar{X}_{i,C}^{m+1}\right] + \sum_{i,C} \mathbb{E}\left[\frac{1}{L_C p_C \varepsilon^2} R_{i,C}(\bar{\mathbf{X}}) \left((\bar{X}_{i,C} - 1)^{m+1} - \bar{X}_{i,C}^{m+1}\right)\right] = 0,$$

After separating the terms of index m on the left side of the equations, and the others in the right side, we get:

$$\sum_{i,C}\mathbb{E}\left[\left(-\lambda+\frac{1}{L_C p_C \varepsilon^2}R_{i,C}(\bar{\mathbf{X}})\right)\bar{X}_{i,C}^m\right] = \sum_{i,C}\sum_{k=0}^{m-1}\binom{m+1}{k}\mathbb{E}\left[(\lambda+\frac{1}{L_C p_C \varepsilon^2}R_{i,C}(\bar{\mathbf{X}})(-1)^{k+1-l})\bar{X}_{i,C}^k\right].$$

We then remind that we have, for all i, C, $\frac{1}{L_C p_C \varepsilon^2}R_{i,C}(\bar{\mathbf{X}}) \leq \frac{1}{L_C p_C \varepsilon^2}$. We apply this to the two sides of the equation, and we use Lemma 8.2 to the left-hand side to get:

$$\sum_{i,C}(\bar{\lambda}_c-\lambda)\,\mathbb{E}\left[\bar{X}_{i,C}^m\right] \leq \sum_{i,C}\sum_{k=0}^{m-1}(\lambda+\frac{1}{L_C p_C \varepsilon^2})\binom{m+1}{k}\mathbb{E}\left[\bar{X}_{i,C}^k\right]$$

Let $\bar{L}\bar{p} = \min_C p_C L_C$. We get:

$$(\bar{\lambda}_c-\lambda)\sum_{i,C}\mathbb{E}\left[\bar{X}_{i,C}^m\right] \leq \left(\lambda+\frac{1}{\bar{L}\bar{p}\varepsilon^2}\right)\sum_{i,C}\sum_{k=0}^{m-1}\binom{m+1}{k}\mathbb{E}\left[\bar{X}_{i,C}^k\right]$$

Let us set $D_\varepsilon = \frac{\bar{\lambda}_c-\lambda}{\lambda+\frac{1}{\bar{L}\bar{p}\varepsilon^2}}$, which concludes the proof.

□

We can move to proving the main result of the theorem. We multiply each side by $\frac{c^m}{m!}$ sum the inequalities for $1 \leq m \leq N$:

$$\begin{aligned}
D_\varepsilon\sum_{m=1}^{N}\mathbb{E}\left[\sum_{i,C}\bar{X}_{i,C}^m\right]\frac{c^m}{m!} &\leq \sum_{m=1}^{N}\sum_{k=0}^{m-1}\frac{c^m}{k!(m+1-k)!}\mathbb{E}\left[\sum_{i,C}\bar{X}_{i,C}^k\right] \\
&\leq \sum_{i,C}\sum_{k=0}^{N-1}\sum_{m=k+1}^{N}\frac{\mathbb{E}\left[\bar{X}_{i,C}^k\right]}{k!}\sum_{m=k+1}^{N}\frac{c^k}{(m+1-k)!} \\
&= \sum_{i,C}\sum_{k=0}^{N-1}\frac{\mathbb{E}\left[\bar{X}_{i,C}^k\right]}{k!}\sum_{u=0}^{N-k-1}\frac{c^{k+u+1}}{(u+2)!} \\
&\leq \sum_{i,C}\sum_{k=0}^{N-1}\mathbb{E}\left[\bar{X}_{i,C}^k\right]\frac{c^{k+1}}{k!}\sum_{u=0}^{\infty}\frac{c^u}{(u+2)!} \\
&\leq ce^c\sum_{i,C}\sum_{k=0}^{N}\mathbb{E}\left[\bar{X}_{i,C}^k\right]\frac{c^k}{k!}.
\end{aligned}$$

Let $S_N = \sum_{i,C}\sum_{m=0}^{N}\mathbb{E}\left[\bar{X}_{i,C}^m\right]\frac{c^m}{m!}$. The last inequality can be rearranged as:

$$D_\varepsilon(S_N - 1) \leq ce^c S_N \Leftrightarrow S_N \leq \frac{D_\varepsilon}{D_\varepsilon - ce^c}. \tag{8.4}$$

We thus obtain that for each i, C, $\mathbb{E}\left[\bar{X}_{i,C}^m\right] \leq S_N \leq \frac{D_\varepsilon}{D_\varepsilon - ce^c}$. Since the sequence is increasing, and bounded from above, it converges, and we can conclude that $\mathbb{E}\left[e^{c\bar{X}_{i,C}}\right]$ is finite as long as $ce^c \leq D_\varepsilon$. We set $\bar{c}_0 = W(D_\varepsilon)$, where W is the Lambert W function, i.e. for all x, $W(x)$ is the unique value such that $x = W(x)e^{W(x)}$.

We have proven that any queue taken at random in $\bar{\mathbf{X}}$ has finite exponential moments, whenever $\lambda < \bar{\lambda}_c$. We can easily observe that $\lim_{\varepsilon \to 0^+} D_\varepsilon = 0$, which gives as a consequence, that $\mathbb{E}\left[e^{c\Phi_0(\mathcal{D})}\right]$ is finite if and only if $c = 0$ (due to the fact that $W(0) = 0$).

We remind that $\Phi_0(\mathcal{D}) \leq \sum_{i,C} \bar{X}_{i,C}$, for all $\varepsilon > 0$. Instead of letting ε go to 0, we can take its largest possible value, i.e. $\varepsilon^2 = |\mathcal{D}|$, which corresponds to the setup where there is only one queue in the region. Let $\bar{\lambda}_0$ be the critical arrival rate for this system, and we define:

$$D_0 = \frac{\bar{\lambda}_0 - \lambda}{\lambda + \frac{1}{\bar{L}\bar{p}|\mathcal{D}|}}.$$

We can use stochastic domination to conclude that for all $c < c_0$, $\mathbb{E}\left[e^{c\Phi_0(\mathcal{D})}\right] < \infty$, with $c_0 = W(D_0)$, whenever $\lambda < \lambda_c$. □

Among the notable consequences of Theorem 8.1, we can obtain interesting bounds for the number of users in the stationary regime:

Theorem 8.4. *There exists $c_1 > 0$ and x_0 such that for all $x > x_0$, we have:*

$$\mathbb{P}\left[\Phi_0(\mathcal{D}) > x\right] \leq e^{-c_1 x}.$$

Proof. We apply Markov's inequality to the variable $e^{c\Phi_0(\mathcal{D})}$, with $0 < c < c_0$:

$$\mathbb{P}\left[e^{c\Phi_0(\mathcal{D})} > e^{cx}\right] \leq \frac{\mathbb{E}\left[e^{c\Phi_0(\mathcal{D})}\right]}{e^{cx}}. \tag{8.5}$$

Let $K > 0$ that $\mathbb{E}\left[e^{c\Phi_0(\mathcal{D})}\right] < K < \infty$. Because the function $x \mapsto e^{cx}$ is positive and increasing, we obtain:

$$\mathbb{P}\left[\Phi_0(\mathcal{D}) > x\right] \leq Ke^{-cx}. \tag{8.6}$$

Through calculation, we can obtain that there exists $x_0 > 0$ and $c_1 > 0$ such that for $x \geq x_0$, $Ke^{-cx} \leq e^{-c_1 x}$, which concludes the proof. □

The result from Theorem 8.4 can provide for bounds for the staying time for users in the system, using Little's law (see [64]), which provides an interesting result about transmitting time in the network.

Figure 8.1 displays the population in the system for two values of λ, one in the stable regime, the other in the unstable regime. The form of the histograms tend to show that in the stable regime, the population in

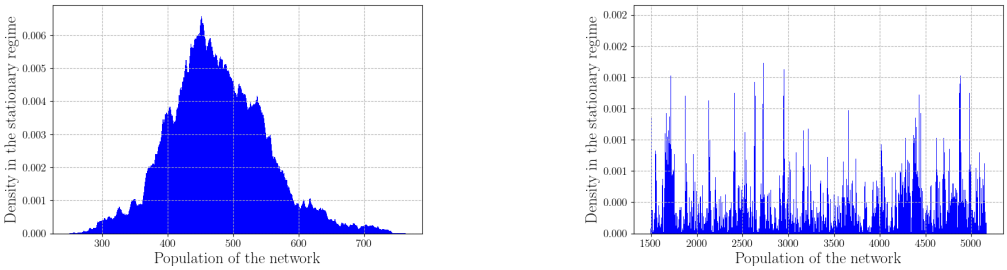

Figure 8.1: Population distribution for two realizations of the network, in the stable regime (left, $\lambda = 0.9\lambda_C$) and unstable regime (right, $\lambda = 1.1\lambda_c$). In the stable regime, we see that the stationary distribution has bounded tails whereas in the unstable regime, the stationary distribution is unbounded.

the network has bounded tails, whereas the unstable system has unbounded tails. This result is displayed in Figure 8.2 shows the distribution tails in the system in the two regimes, and outline the result of Theorem 8.4.

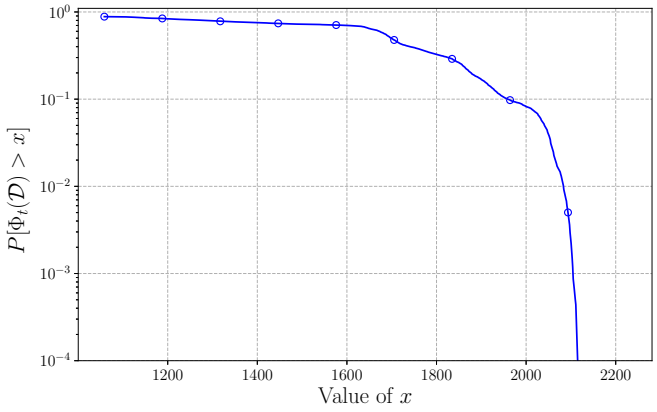

Figure 8.2: Population tails in the symmetric system, with $\lambda = 0.95\lambda_C$

The result of Theorem 8.4 allows to obtain an interesting bound for the population of users in the stationary regime. Using this result with Little's law (see [64]), we can also obtain that the distribution of service times in the system has exponential tails, which is a very interesting property to have in communication networks.

Part III

Velocity-based association policies in multitier wireless networks

Chapter 9

Two-tier 5G wireless network

9.1 Network setup

The classical setup for multi-tier networks relies on maximum power association policies [39], where MUs always connect to the tier and the BS that offers the best received power. These policies only rely on the geometry of the network and do not take into account MU mobility. In [73], the authors studied a class of association policies purely based on user velocity, consisting in setting a velocity threshold deciding which tier an MU should be associated with. The main result of [73] lies in finding an optimal threshold, that maximizes the expected mean effective Shannon rate the typical user in the network receives. These *threshold* association policies are able to outperform the classical max power association policies for densely populated networks with high mobility MUs, but offer poor performance in other mobility or user-density patterns.

The goal of this part and the following ones is to define a class of association policies incorporating both the ideas of max power and velocity-aware association policies, that rely on MU velocity, using only the network parameters and easily obtainable data, such as velocity and received power. This line of thought leads us to introduce *velocity-biased max power* (VBMP) association policies, where users are associated with the network tier that offers the best received power, up to a *bias factor* dictated by the velocity of the MU.

For our study, we propose a simple two-tier network architecture using two types of base stations (BSs) with the same frequency bands and differences in spatial intensity and transmit power: smaller *micro* cells overlay larger *macro* cells. We assume that base stations (BSs) are located according to two independent homogeneous Poisson point processes (PPP): the macro BSs form a PPP $\Phi_M \subset \mathbb{R}^2$ of intensity λ_M and the micro BSs a PPP Φ_μ of

intensity λ_μ, with $\lambda_\mu > \lambda_M$.

We assume that mobile users (MUs) are located according to a third stationary PPP Φ_u of intensity λ_u. Each MU moves on a straight line with an orientation chosen at random and independent of other MUs. Each MU travels at a constant velocity v, sampled from a given distribution f, independently for each user. Without loss of generality, using the homogeneity and isotropy of the PPP, we can assume that the typical MU is located at the origin and that its motion is along the x-axis.

We assume that all BSs are always active. Some of the results presented here can be extended to the case where BSs with no users are shut off, but this does not fall in the scope of this work.

Base stations use directional beamforming with a sector approximation to communicate with the typical MU (see Section B.3). Under this assumption, the probability that the typical MU lies in the main (resp. side) lobe of its serving BS in the macro tier is thus equal to $p_{M,m} = \frac{1}{n_M}$ (resp. $1 - p_{M,m}$). The antenna gain of the typical MU is thus equal to:

$$g_{M,x} = \begin{cases} G_m^M & \text{w.p.} \quad p_{M,m} \\ G_s^M & \text{w.p.} \quad 1 - p_{M,m}. \end{cases} \tag{9.1}$$

The micro and macro tiers share the same spectrum, so they interfere with one another. We call the tier with which the typical MU is associated the *association tier*, and the other tier, the *interferer tier*. An MU in the network always connects to the closest BS in its association tier. This BS association results in cells of BSs forming a Poisson-Voronoi (PV) tessellation (see Section A.3).

Let $\ell(x) \triangleq Kx^{-\alpha}$, with $\alpha > 2$ and $K = \left(\frac{c}{4\pi f_c}\right)^2$, be the path-loss function for the system, where f_c is the carrier frequency and c is the speed of light. We assume Rayleigh fading with mean 1 between the BS located at x and the typical MU at the origin, denoted by h_x. Let P_M and P_μ denote the transmit powers for each tier, with $P_\mu < P_M$, and G_x^M and G_y^μ the antenna gains for macro and micro BSs located at x and y, respectively. We define the interference experienced by the typical MU from macro tier BSs as:

$$I_M(\Phi_M) = \sum_{x \in \Phi_M} h_x g_{M,x} P_M \ell(\|x\|).$$

Let $X_{M,0}$ be the closest macro BS to the typical MU, and $X_{\mu,0}$ be its micro counterpart. Conditioned on that the closest macro BS to which the typical MU connects is at distance $r > 0$, the SINR at the typical MU, denoted as SINR_M is expressed as

$$\text{SINR}_M = \frac{h_0 P_M g_{M,0} K r^{-\alpha}}{\sigma^2 + I_M(\Phi_M \backslash \{X_{M,0}\}) + I_\mu(\Phi_\mu)}, \tag{9.2}$$

where $g_{M,0}$ (given by (B.8)) is the gain of the serving BS of the typical MU and σ^2 is the thermal noise density.

Parameters

We consider that both tiers use a carrier frequency f_c in the 3.5 GHz range with a bandwidth $W = 100$ MHz. The transmit powers of macro and micro BSs are assumed to be 20 W and 4 W, respectively. The antenna gain profile we consider for numerical results is that the main lobe gain is $G_m^M = n_M$ and the side lobe gain is $G_s^M = 1/n_M$, but other gain profiles can be used. The thermal noise σ^2 is -174 dBm.Hz^{-1}. Finally, MU velocities are sampled from an exponential distribution with scale parameter v_u. Table 9.1 gives the parameters used in the numerical results.

Table 9.1: Values of network parameters in Part III

Parameter	Micro tier	Macro tier
Carrier frequency (f_c)	3.5 GHz	
Bandwidth (W)	100 MHz	
Thermal noise density (σ^2)	-174 dBm.Hz^{-1}	
Transmit powers (P_μ, P_M)	36 dBm	43 dBm
Beam reselection time ($T_{\mu,b}$, $T_{M,b}$)	23 ms	
BS handover time ($T_{\mu,c}$, $T_{M,c}$)	43 ms	
SSB burst periodicity (τ)	20 ms	
Path-loss exponent (α)	4	
Number of beams (n_μ, n_M)	8	
MU intensity (λ_u)	1 m^{-2}	
BS intensities (λ_μ, λ_M)	0.1 m^{-2}	0.02 m^{-2}
Velocity scale parameter (v_u)	[1, 10, 35] m.s^{-1}	
Maximum SINR ($Q_{\max}$)	30 dB	

9.2 Shannon rate

We denote the Shannon rate per Hertz in each tier by $\mathcal{R}_M = \mathbb{E}\left[\log(1+\mathrm{SINR}_M)\right]$ and $\mathcal{R}_\mu = \mathbb{E}\left[\log(1+\mathrm{SINR}_\mu)\right]$. Due to RF imperfections and modulation schemes, we set $Q_{\max}$ to be the maximum achievable SINR. Thus, we have

$$\mathcal{R}_M = \int_0^{Q_{\max}} \frac{p_M(T)}{1+T} \mathrm{d}T \tag{9.3}$$

in the macro tier. The same applies in the micro tier by using the appropriate values. Using Theorem 10.1, the Shannon rate achieved by the typical MU can be expressed as

$$\mathcal{R}_M(v) = (1 - p_{\mathrm{bm}}^M(v))\mathcal{R}_{M,m} + p_{\mathrm{bm}}^M(v)\mathcal{R}_{M,s}, \tag{9.4}$$

where $\mathcal{R}_{M,m}$ is the Shannon rate achieved with no beam misalignment, while $\mathcal{R}_{M,s}$ is its equivalent with beam misalignment (as discussed in Section B.3).

Equation (9.3) gives the Shannon rate for the typical MU without considering the overheads associated with beam reselections during intra-cell mobility and BS handovers during inter-cell mobility. To take these overheads into account, we now define the effective Shannon rate.

9.3 Mean Effective Shannon rate under an association policy

The metric we use to compare association policies is the ESR received by the typical MU as given by (B.6). In this chapter and the following, we define an association policy $\mathcal{P}$ as a property for MUs $\mathcal{P}$ such that if for a MU located at x, if $\mathcal{P}(x)$ holds, the MU is associated with the micro tier of the network, and if $\mathcal{P}$ does not hold, it is associated with the macro tier.

In the case of velocity-based association policies, the property $\mathcal{P}$ depends only on the velocity v of the MU, and we denote as $\mathcal{P}(v)$ the truth value of the property. $\bar{\mathcal{P}}$ represents the negation of the proposition $\mathcal{P}$. We have:

Lemma 9.1. *For a given velocity-based association policy $\mathcal{P}$, the average ESR received by the typical MU is given by:*

$$\mathcal{R}(\mathcal{P}) = \int_0^\infty \left(\mathcal{R}_{\mu,\mathit{eff}}(v)\mathbb{1}_{\mathcal{P}(v)} + \mathcal{R}_{M,\mathit{eff}}(v)\mathbb{1}_{\bar{\mathcal{P}}(v)}\right) f(v)\mathrm{d}v, \tag{9.5}$$

where $\mathbb{1}_{(\cdot)}$ is the indicator function and $\bar{\mathcal{P}}$ the negation of $\mathcal{P}$.

This result uses and ergodic interpretation: to obtain the average MESR the typical user experiences over its trajectory, we compute the spatial average of the ESR over a large ball of radius $R > 0$ centered at the origin, with MUs having velocities sampled i.i.d. from the distribution f. Under a velocity-based association policy, the spatial average of the MESR of MUs in this ball becomes an average over the velocities of the MUs. Using Birkhoff's ergodic theorem [27], we can prove that this spatial average converges to a constant, $\mathcal{R}(\mathcal{P})$, which is also equal to the ESR experienced by the typical MU.

This metric will be used throughout this part to compare the performance of the different policies we use. Due to the isotropy and stationarity of the MU and BS processes, finding bounds and computing results for the the average MESR ensures the performance of the network, which are then verified experimentally by simulating the dynamics described here. In the next chapter, we will use the result of Lemma 9.1 to a first array of association policies to obtain a maximal MESR for the network.

Chapter 10

Velocity-based association policies

Among the variety of velocity-based association policies for multi-tier networks, a simple family to study is the family of *threshold* policies.

Definition 10.1. *Let $v_T > 0$. The* threshold policy *associated with v_T is the association policy such that, for a MU moving at velocity v:*

- *if $v \leq v_T$, the MU is associated with the micro tier,*
- *if $v > v_T$, the MU is associated with the macro tier.*

This family of velocity-based association policies have the advantage of being simple to implement, as they act as a binary decision problem, depending only on one parameter which we can estimate with a certain precision for mobile phones (using for instance GPS location data). In the chapter, we propose an in-depth study of threshold policies and how they affect network performance.

10.1 Coverage probability

The first quantity we need to evaluate is the coverage probability under a given threshold association policy

Theorem 10.1 (Coverage probability)**.** *The coverage probability with the macro tier association is*

$$p_M(v,T) = (1 - p_{bm}^M(v))q_M(G_m^M, T) + p_{bm}^M(v)q_M(G_s^M, T), \tag{10.1}$$

where

$$q_M(G,T) = \pi\lambda_M \int_{r\geq 0} e^{-\pi\lambda_M r} \exp\left(-\frac{T\sigma^2}{P_M K G} r^{1/\delta}\right) \exp\left(-\pi r \left(\frac{T}{P_M G}\right)^{\delta} \left(\lambda_M P_M^{\delta} \rho_M(G,T) + \lambda_\mu P_\mu^{\delta} \kappa_\mu\right)\right) \mathrm{d}r.$$

Here $\delta \triangleq 2/\alpha$, *and* ρ_M *and* κ_μ *are given by*

$$\rho_M(G,T) = p_{M,m}(G_m^M)^{\delta} \int_{\left(\frac{TG_m^M}{G}\right)^{-\delta}}^{\infty} \frac{\mathrm{d}u}{1+u^{1/\delta}} + (1-p_{M,m})(G_s^M)^{\delta} \int_{\left(\frac{TG_s^M}{G}\right)^{-\delta}}^{\infty} \frac{\mathrm{d}u}{1+u^{1/\delta}},$$

$$\kappa_\mu = \left(p_{\mu,m}\left(G_m^\mu\right)^{\delta} + \left(1-p_{\mu,m}\right)\left(G_s^\mu\right)^{\delta}\right) \int_0^{\infty} \frac{\mathrm{d}u}{1+u^{1/\delta}}.$$

The coverage probability in the micro tier is obtained by swapping the role of both tiers.

Proof. The proof for this result is given in Section 12.1 of Chapter 12. □

We can verify the result given by Theorem 10.1 numerically. We start by sampling two homogenous PPP for the base stations. We then sample a large number of velocities for the typical MU, and we compute the coverage probability. Figure 10.1 displays the coverage probability, $p_c(\beta) = \mathbb{P}[\mathrm{SINR}_0 > \beta]$ for the macro and micro tier for values of β ranging from 0.01 to 100 dB.

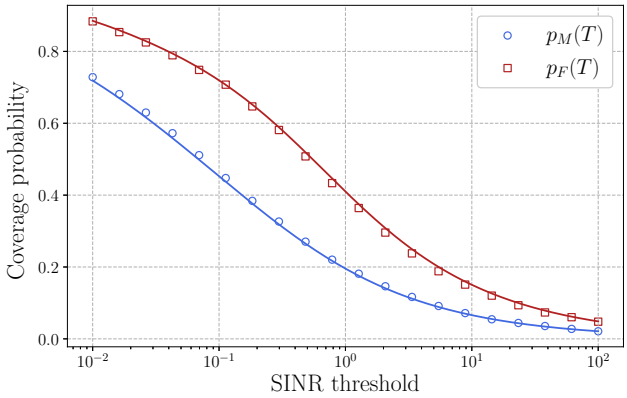

Figure 10.1: Coverage probability in each tier (blue: in the macro tier, red: in the micro tier). Here, the typical MU moves at a constant velocity $v = 10\mathrm{m.s}^{-1}$.

An interesting case to look at is the interference-limited setup, where σ^2 can be considered to be equal to 0. In this case, the functions q_M and q_μ simplify to:

$$q_M(G,T) = \frac{1}{1+\left(\frac{T}{G}\right)^{\delta}\left(\rho_M(G,T) + \Omega\kappa_\mu\right)} \tag{10.2}$$

$$q_\mu(G,T) = \frac{1}{1+\left(\frac{T}{G}\right)^{\delta}\left(\rho_\mu(G,T) + \frac{1}{\Omega}\kappa_M\right)}, \tag{10.3}$$

where we set $\Omega = \frac{\lambda_\mu P_\mu^\delta}{\lambda_M P_M^\delta}$. When setting $\Omega = 0$, which corresponds to setting either $\lambda_\mu = 0$ or $P_\mu = 0$, i.e., removing the micro tier, we obtain the same formula as the one from [7].

10.2 Optimal threshold association policy

A question arising when studying association policies is that of the *optimal* policy, i.e., the policy that maximizes a certain network metric. In the case we are studying, the metric of interest we consider is the average MESR. Our question then becomes: what is the threshold policy that maximizes the average MESR in the system?

Under a threshold policy, the average ESR is given by:

$$\mathcal{R}(v_T) = \int_0^{v_T} \mathcal{R}_{\mu,\text{eff}}(v) f(v) \mathrm{d}v + \int_{v_T}^{\infty} \mathcal{R}_{M,\text{eff}}(v) f(v) \mathrm{d}v. \tag{10.4}$$

We have the following Theorem when considering one MU per antenna:

Theorem 10.2 (Optimal threshold policy)**.** *Under the foregoing assumptions, there exists a unique threshold maximizing the average ESR per user. This optimal threshold $v_T^\star$ does not depend on the velocity distribution f of MUs, and is the unique solution to the following equation:*

$$\mathcal{R}_{\mu,eff}(v_T^\star) = \mathcal{R}_{M,eff}(v_T^\star). \tag{10.5}$$

Proof. The proof for this Theorem is available in Section 12.2 in Chapter 12. □

Figure 10.2 shows the normalized ESR, i.e. the average MESR as a percentage of its maximum value for three exponential distributions for MUs. We can see that the maximum value of the MESR is attained for the same velocity threshold in all cases.

This network setup mimics an ideal situation, in which the antenna have infinite radio resources. In such a setup, we can consider that the system behaves as if only one MU is connected to each antenna, as allocating radio resources to one MU does not affect transmission for the other transmitting MUs. Moreover, the rate received by an MU in the setup corresponds to the peak rate that it receives in the network. A more realistic setup with multiple MUs is studied in the next section.

10.3 Load-dependent threshold policies

If we consider that radio resources for each antenna are not infinite anymore, we have to consider the number of MUs connected to a given antenna. The radio resources are now equally shared among these users. This sharing can either be done temporally, where transmission are scheduled sequentially

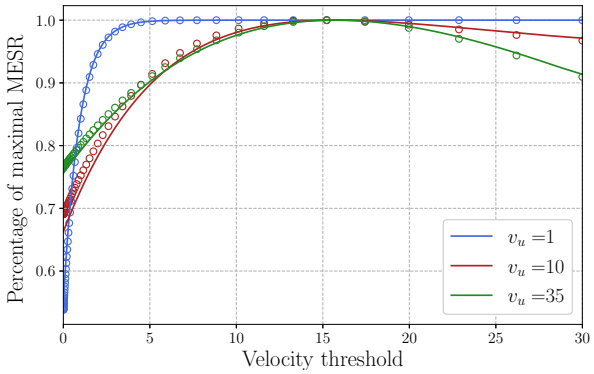

Figure 10.2: Normalized ESR in the network as a function of the velocity threshold v_T. The optimal threshold does not depend on the scale parameter v_u.

(corresponding to a TDMA setup) or spatially, where transmission are encoded in the same signal (corresponding to a CSMA setup). In our study, both cases translate with the same modification in the network metrics, which we detail here.

Let $\mathcal{P}$ be a given velocity-based association policy. Under the association policy $\mathcal{P}$, let $Z_\mu^0(\mathcal{P})$ denote the number of users associated with the micro BS corresponding to the 0-cell, i.e., the Voronoi cell containing the typical MU located at the origin 0, and $Z_M^0(\bar{\mathcal{P}})$ be its macro counterpart. Note that $Z_\mu^0(\mathcal{P})$ and $Z_M^0(\bar{\mathcal{P}})$ are random variables due to the random network geometry and velocity. For this setup, we can modify (9.5) to rewrite the average ESR $\mathcal{R}_{\text{load}}$ as follows:

$$\mathcal{R}_{\text{load}}(\mathcal{P}) = \mathbb{E}\left[\frac{\mathcal{R}_{\mu,\text{eff}}(v)}{Z_\mu^0(\mathcal{P})}\mathbb{1}_{\mathcal{P}(v)} + \frac{\mathcal{R}_{M,\text{eff}}(v)}{Z_M^0(\bar{\mathcal{P}})}\mathbb{1}_{\bar{\mathcal{P}}(v)}\right]. \tag{10.6}$$

In (10.6), the number of MUs associated to the 0-cell and the ESR both depend on the geometry of each PV tessellation. We make the following assumption: let us assume that the number of users in the 0-cell of the PV tessellation in each tier is independent from the SINR. Under this assumption, we can define the following heuristic to approximate $\mathcal{R}_{\text{load}}$:

$$\hat{\mathcal{R}}_{\text{load}}(\mathcal{P}) = \mathbb{E}\left[\frac{1}{Z_\mu^0(\mathcal{P})}\right]\mathbb{E}\left[\mathcal{R}_{\mu,\text{eff}}(v)\mathbb{1}_{\mathcal{P}(v)}\right] + \mathbb{E}\left[\frac{1}{Z_M^0(\bar{\mathcal{P}})}\right]\mathbb{E}\left[\mathcal{R}_{M,\text{eff}}(v)\mathbb{1}_{\bar{\mathcal{P}}(v)}\right], \tag{10.7}$$

where $\mathbb{E}\left[\frac{1}{Z_\mu^0(\mathcal{P})}\right]$ and $\mathbb{E}\left[\frac{1}{Z_M^0(\bar{\mathcal{P}})}\right]$ are the average inverse load in the 0-cell of micro and macro tiers, respectively.

Like in Section 10.2, threshold policies remain good candidates to maximize the average ESR experienced by the typical MU. Let v_T be a velocity

threshold. Under the threshold policy with threshold v_T, the intensity of the PPP of users associated with the micro tier is equal to $\lambda_u F(v_T)$, with F being the CDF of the velocity distribution, and the intensity of the PPP of users associated with the macro tier is equal to $\lambda_u(1 - F(v_T))$. Although we do not have an analytical formula for the average inverse load in the network, we can use the heuristic developed in Lemma A.8.

We set the following notation:

$$\mathbb{E}\left[\frac{1}{Z_\mu^0(v_T)}\right] = L\left(\frac{\lambda_\mu}{\lambda_u F(v_T)}\right) \equiv L_\mu(v_T)$$
$$\mathbb{E}\left[\frac{1}{Z_M^0(v_T)}\right] = L\left(\frac{\lambda_M}{\lambda_u(1 - F(v_T))}\right) \equiv L_M(v_T).$$

Under a velocity-based threshold policy, the average ESR in the TDMA setup becomes

$$\hat{\mathcal{R}}_{\text{load}}(v_T) = L_\mu(v_T)\int_0^{v_T} \mathcal{R}_{\mu,\text{eff}}(v)f(v)\mathrm{d}v + L_M(v_T)\int_{v_T}^{\infty} \mathcal{R}_{M,\text{eff}}(v)f(v)\mathrm{d}v. \tag{10.8}$$

We define the *load-threshold heuristic* for the optimal threshold policy in the TDMA setup as follows:

Definition 10.2 (Load-threshold heuristic)**.** *The load-threshold heuristic is the threshold v_{LT} that maximizes $\hat{\mathcal{R}}_{load}$, i.e., such that:*

$$v_{LT} \triangleq \arg\max\ \hat{\mathcal{R}}_{load}(v_T). \tag{10.9}$$

The optimal load-threshold *policy is the threshold policy associated with v_{LT}.*

As shown in Fig. 10.3, we numerically observe that v_{LT} is uniquely defined although we cannot prove it in the general case that the function $\hat{\mathcal{R}}_{\text{load}}(v_T)$ goes through a unique maximum. Specifically, Fig. 10.3 compares the simulations under TDMA and the heuristic from (10.9). The difference between the simulation and the predicted value of the heuristic comes from the fact that the inverse of the load and the ESR are not independent.

Further simulation can give us an order of magnitude for the difference between the optimal value of the MESR computed and the MESR obtained when selecting the threshold obtained in the load-threshold heuristic from Definition 10.2. Table 10.3 displays the difference in value between these two values.

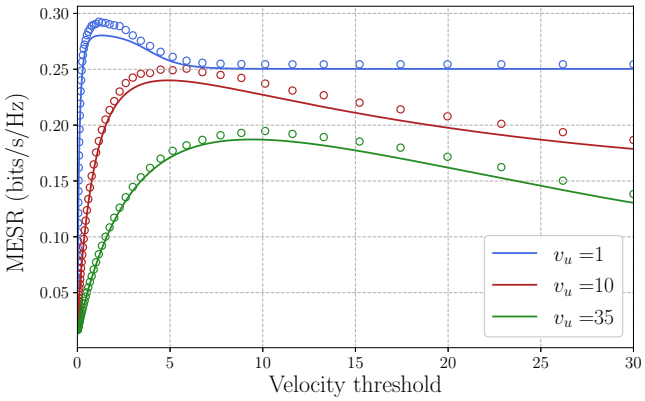

Figure 10.3: Comparison of the heuristic in (10.8) (in plain line) and simulations (circles)

Table 10.1: Numerical illustration of the load-threshold heuristic

v_u (m.s^{-1})	1	10	35
v_{LT} (m.s^{-1})	1.30	4.90	9.41
$\mathcal{R}_{\mathrm{load}}(v_{\mathrm{LT}})$	0.294	0.242	0.201
Optimal MESR	0.289	0.252	0.195

10.4 Discussion and comparison with a classical association policies

When interpreting these results, we can observe that the load-threshold heuristic is rather performant to estimate the maximal MESR in the network with a low computational cost, as the method is based on solving an only fixed point equation. One can try to refine this heuristic by using more performant methods, but this search will come at the cost of an increase in computational costs.

Another interesting question is to investigate the dependence of v_{LT} on the MU parameters. The density λ_u of MUs allows us to understand how well the network performs under different load conditions. Specifically, as $\lambda_u \to 0$, the ESR in the network becomes equal to the Shannon rate without TDMA, which is its peak rate. This translates into v_{LT} becoming equal to $v_T^\star$ from Theorem 10.2. Conversely, as $\lambda_u \to \infty$, the number of MUs associated with the micro tier becomes arbitrarily large. Because its contribution towards the ESR is larger than that from the macro tier, to maximize the average ESR, the optimal velocity threshold approaches zero.

The behavior of the optimal threshold for intermediate values of λ_u depends on the velocity distribution. Figure 10.4 gives the optimal velocity threshold for the heuristic given in (10.9). The MU velocity is a limiting factor in the network: if the velocity of MUs is higher, the average overhead per unit of time in the macro tier increases, leading to a decrease in the contribution of the macro tier to the average ESR. To balance this effect,

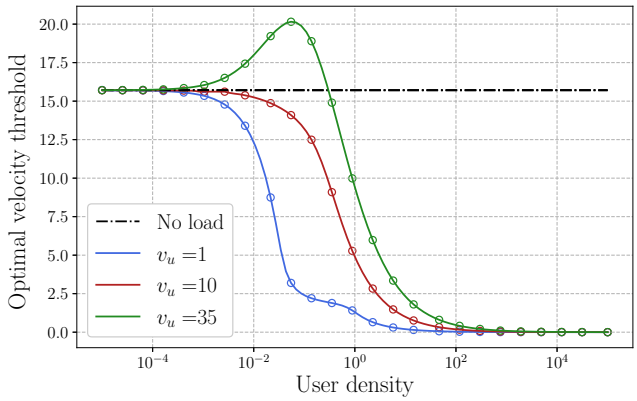

Figure 10.4: Optimal velocity threshold obtained for the heuristic from (10.9) (in plain line) for three velocity distributions against the density of users. In black, dashed, the equivalent network without load.

more MUs are associated with the micro tier, resulting in an increase in the optimal velocity threshold.

We now compare the optimal average ESR using the optimal load-threshold heuristic based on 10.2 to a classical association policy based on the *maximum received power* (MRP), where MUs connect to the BS with the highest average received power. Because MUs move fast in the network, we do not take into account fading in the signal: the typical MU located at the origin connects to the macro tier BS located at $X_{0,M}$ if the received power in the macro tier $RP_M = P_M G_{0,M} \ell(|X_{0,M}|)$ is higher than the received power from the micro BS located at $X_{0,\mu}$, $RP_\mu = P_\mu G_{0,\mu} \ell(|X_{0,\mu}|)$. It is to note that the MARP policy is primarily based on the received *power*, and thus, the network geometry, and the threshold policy on *velocity*. Hence, this comparison allows us a fine-grained view at the ESR, which has two main components as seen from (10.8): $\mathcal{R}_M$, the Shannon rate as a function of the SINR and hence the received power, and $T_o^M(v)$, the overhead as a function of the velocity v of an MU.

As shown in Fig. 10.5, for a given value of MU density, the average ESR decreases faster with velocity under the MRP policy than under the load-threshold heuristic: while for low values of v_u, the MRP policy outperforms the load-threshold heuristic, the threshold policy provides MUs with a better average ESR for velocities v_u higher than 11 m.s^{-1}, up to a gain of 45%. The fact that these results are obtained for parameters representing accurately the sub-6 GHz setting of 5G new radio (NR) supports the importance of the study of velocity-based threshold policies.

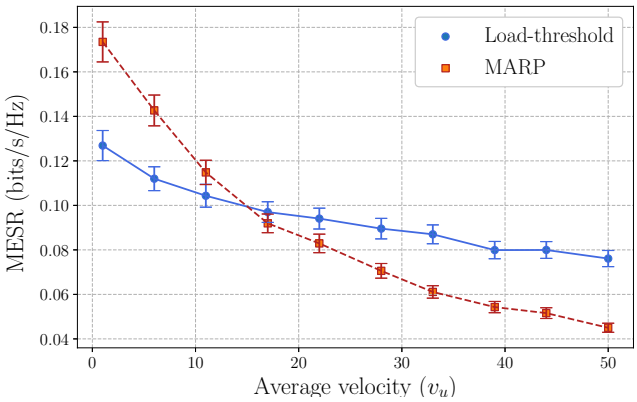

Figure 10.5: Comparison between the MARP policy (square markers, dashed line) and the threshold policy under v_{LT} (circles, plain line) with 95% confidence intervals for three different velocity distributions.

Chapter 11

VBMP association policies

In the last section of the previous chapter, we compared the optimal load-threshold heuristic with a max-power association policy, and observed through simulation that the former policy works better for densely populated network with fast-moving MUs. On the other hand, this policy is not interesting when it comes to sparsely populated networks or with slowly-moving MUs, as it performs worse than the *maximum received power* (MRP) policy, i.e. the policy such that a user associates to the tier that provides the maximal received power at its location.

The goal of this chapter is to look for policies that outperforms both threshold and MRP policies. To do so, we define a class of association policies incorporating both the ideas of max power and velocity-aware association policies. This line of thought leads us to introduce *velocity-biased max power* (VBMP) association policies, where users are associated with the network tier that offers the best received power, up to a *bias factor* dictated by the velocity of the MU.

11.1 VBMP policies

We keep the same network setup as we did in the previous chapter, but for simplicity purposes, we decide to omit beam misalignement. This feature can easily be applied to all the results presented in this section by taking similar steps as the ones we used for threshold policies and adding the adequate terms when considering the main or the side lobes of the antenna.

We define the velocity-biased max power policies as follows:

Definition 11.1. *Let K be a positive real function. The* velocity-biased max power *(VBMP) policy associated with K is the association policy such that:*

– *If* $\mathrm{R}_M \geq K(v)\mathrm{R}_\mu$*, we associate the MU with the macro tier*

– *If* $\mathrm{R}_M < K(v)\mathrm{R}_\mu$, *we associate the MU with the micro tier*

The function K acts as a bias term in the classical MRP policy, in order to take into account MU velocity in the association between the two tiers. It is to note that threshold policies and MRP policies are both types of VBMP policies. The MRP policy is the VBMP policy with the function $K = 1$, and the threshold policy with threshold v_T is associated with the function K such that $K(v) = 0$ if $v < v_T$, and $K(v) = +\infty$ if $v > v_T$.

In this chapter, we will look for the function K that maximizes the MESR in the network. In order to do so, we will use variational calculus, so we will focus only on differentiable functions.

Coverage probability

Let us take a VBMP policy with an associated function K. A first metric of interest is the coverage probability. We have the following theorem:

Theorem 11.1 (Coverage Probability)**.** *Let $\theta > 0$. Under a VBMP policy, the coverage probability in the macro tier is equal to:*

$$\mathbb{P}\left[\mathrm{SINR}_{0,M} > \theta\right] = \delta C \int_{z=0}^{1/K(v)} \frac{z^{-\delta-1} e^{-\theta z}}{\left(1 + Cz^{-\delta} + \theta^\delta F(\theta,\delta) + C\theta^\delta F(zT,\delta)\right)^2} \mathrm{d}z.$$

where $\delta = 2/\alpha$, $\Omega = \frac{\lambda_\mu}{\lambda_M}\left(\frac{P_\mu}{P_M}\right)^\delta$ and $F(\theta,\delta) = \int_{\theta^{-\delta}}^{\infty} \frac{\mathrm{d}u}{1+u^{1/\delta}}$. The coverage probability in the micro tier, defined as the probability that $\mathrm{SINR}_{0,\mu} > \theta$ *and the typical MU is associated with the micro tier - denoted as* Micro *- is obtained by swapping the roles of the two tiers:*

$$\mathbb{P}\left[\mathrm{SINR}_{0,\mu} > \theta\right] = \delta\Omega \int_{z=0}^{1/K(v)} \frac{z^{-\delta-1} e^{-\theta/z}}{\left(1 + \Omega z^{-\delta} + \theta^\delta F\left(\frac{\theta}{z},\delta\right) + \Omega\theta^\delta F\left(\frac{T}{z},\delta\right)\right)^2} \mathrm{d}z.$$

The proof for this result is presented in Appendix 12.3

MESR under a VBMP policy

We can compute the MESR under a VBMP policy using the coverage probability from Theorem 11.1 and using an integration by parts (see (9.3)):

$$\mathcal{R}_{M,\mathrm{eff}}(v) = (1 - T_{o,M}(v))^+ \int_0^{Q_\mathrm{m}} \mathbb{P}\left[\mathrm{SINR}_{0,M} > \theta, \mathrm{Macro}\right] \frac{\mathrm{d}\theta}{\theta+1}.$$

We can define the average MESR for the typical user located at the origin in a similar way as in Lemma 9.1:

$$\mathcal{R}(K) = \int_0^{v_{\max}} \big((1 - T_{o,M}(v))^+ \mathbb{E}\left[\log(1 + \mathrm{SINR}_{0,M}(v, K))\right] \tag{11.1}$$
$$+(1 - T_{o,\mu}(v))^+ \mathbb{E}\left[\log(1 + \mathrm{SINR}_{0,\mu}(v, K))\right]\big) f(v)\mathrm{d}v$$
$$= \int_0^{v_{\max}} \left(\mathcal{R}_{M,\mathrm{eff}}(K, v) + \mathcal{R}_{\mu,\mathrm{eff}}(K, v)\right) f(v)\mathrm{d}v. \tag{11.2}$$

This quantity can be expressed in terms of network parameters by using Theorem 11.1. In the general case, there is no closed-form formula for $\mathcal{R}(K)$ depending on K and v, but we will see in the next section that this result is sufficient to obtain an equation to define the function K that maximizes the average MESR in the network.

11.2 Optimal VBMP policy

We want to find the VBMP policy that maximizes the average MESR in the system. This amounts to finding the function K that maximizes $\mathcal{R}(K)$. We define an optimal VBMP policy:

Definition 11.2. *The* optimal VBMP policy *is the VBMP policy with a function $K^\star$ that maximizes the average MESR in the system.*

From (11.2), the function $\mathcal{R}$ has the following form:

$$\mathcal{R}(K) = \int_{v=0}^{v_{\max}} J(v, K) f(v)\mathrm{d}v, \tag{11.3}$$

with $J(v, K) = \mathcal{R}_{M,\mathrm{eff}}(K, v) + \mathcal{R}_{\mu,\mathrm{eff}}(K, v)$. We use the Euler-Lagrange criterion to obtain:

$$\frac{\partial}{\partial K}\left(\mathcal{R}_{M,\mathrm{eff}}(K^\star, v) + \mathcal{R}_{\mu,\mathrm{eff}}(K^\star, v)\right) = 0. \tag{11.4}$$

Using the definition for the MESR and the result from Theorem 11.1, we can rewrite equation (11.4) in terms of network parameters as follows:

$$\frac{\partial}{\partial K}\mathcal{R}_{M,\mathrm{eff}}(K^\star, v) = -(1 - T_{o,M}(v))^+ \int_0^{Q_{\mathrm{m}}} \frac{\delta\Omega K^\star(v)^{\delta-1}}{\theta + 1} \frac{e^{-\frac{\theta}{K^\star(v)}}}{\left(1 + \Omega K^\star(v)^\delta + \theta^\delta F(\theta, \delta) + \Omega\theta^\delta F\left(\frac{\theta}{K^\star(v)}, \delta\right)\right)^2}\mathrm{d}\theta$$

$$\frac{\partial}{\partial K}\mathcal{R}_{\mu,\mathrm{eff}}(K, v) = (1 - T_{o,\mu}(v))^+ \int_0^{Q_{\mathrm{m}}} \frac{\delta\Omega K^\star(v)^{\delta-1}}{\theta + 1} \frac{e^{-\theta K^\star(v)}}{\left(1 + \Omega K^\star(v)^\delta + \Omega(\theta K^\star(v))^\delta F(\theta, \delta) + (\theta K^\star(v))^\delta F(\theta K^\star(v), \delta)\right)^2}\mathrm{d}\theta.$$

We can state the following theorem:

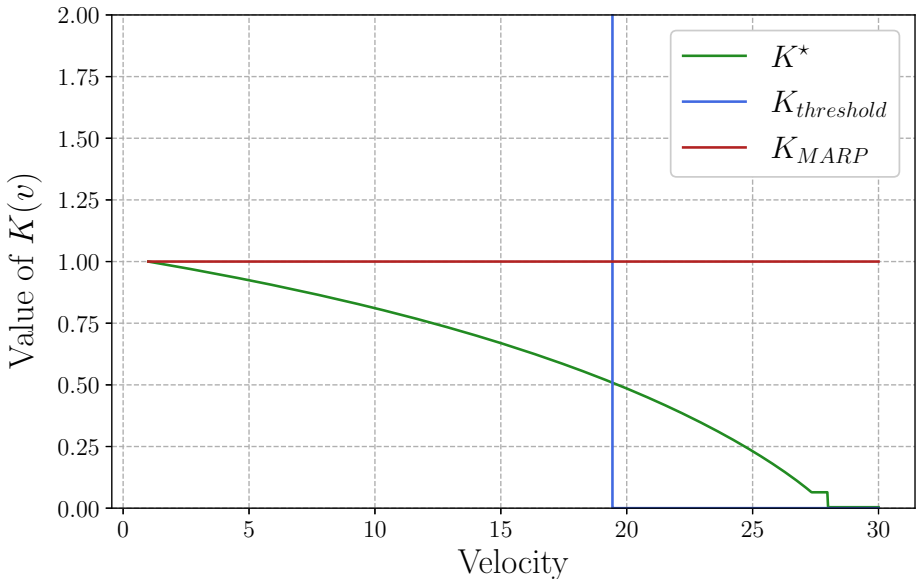

Figure 11.1: Plot of the function $K^\star$ as a function of v against the MRP and the velocity-threshold functions.

Theorem 11.2. *For each $v > 0$, we define $K^\star(v)$ as the smallest positive solution to* (11.4)*. The optimal VBMP policy is the policy associated with $K^\star$.*

We observe numerically, in the network setups we investigated, that (11.4) admits a unique solution, but we did not manage to prove it in the general case.

An important observation to make is that the optimal VBMP policy does not depend on the distribution of velocities in the network: when applying the Euler-Lagrange's criterion to our dynamics, all the terms depending on $f(v)$ disappear in the equation. Thus, this VBMP policy is optimal for any velocity distribution profile.

Numerically, in our network setup, we can observe that (11.4) has a unique solution. Although this result is not proved, we can conjecture that this solution is actually unique. Figure 11.1 shows the solution of (11.4) as a function of v (in green). We can see that for immobile users, the optimal VBMP policy has the same criterion as for the MRP policy, i.e., gives a max-power association. As the MUs move faster, the bias term for the micro tier becomes lower, i.e., we associate more users with the macro tier. This can be explained by the fact that the micro tier gives the best performance, and we prefer to prevent as much as possible fast moving users to connect to it.

Figure 11.2 shows a comparison between the optimal VBP policy with the MRP and the load-threshold policies. As expected, it performs better than the load-threshold in the one MU per cell case, as it showed poor performance, and the gain in performance compared to the MRP policy is negligible. This result could be predicted from the fact that, without tak-

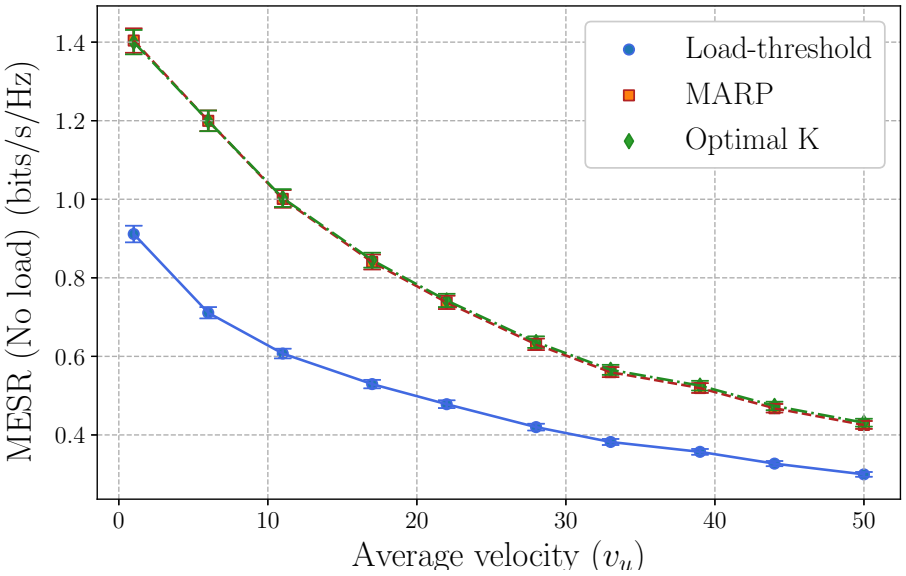

Figure 11.2: Comparison between the MRP policy (red), the load-threshold policy (blue) and the optimal VBMP policy (green) in the one MU per cell case.

ing into account the load in the network, max-power association performs extremely well.

11.3 Load-dependent VBMP policy

As the VBMP policies do not seem to provide a significative improvement to the MESR in the network, we can look into the load-dependent case. We saw in the previous chapter that this network setup changes drastically compared to the one MU per cell. We use the same expression for the MESR as in (10.6).

$$\mathcal{R}_{\text{load}}(K) = \int_0^{v_{\max}} \mathbb{E}\left[\frac{\log(1+\text{SINR}(v,K))}{Z_0(K)}(1-T_o(v))^+\right] f(v)\mathrm{d}v,$$

Let $Z_{0,M}(K)$ and $Z_{0,\mu}(K)$ respectively denote the random variables associated with the number of users in the 0-cell in the macro and the micro tier under the VBMP policy associated with K. We user the following heuristic:

$$\widehat{\mathcal{R}}(K) = \int_0^{v_{\max}} \mathbb{E}\left[\frac{1}{Z_{0,M}(K)}\right] \mathcal{R}_{M,\text{eff}}(v,K) f(v)\mathrm{d}v + \int_0^{v_{\max}} \mathbb{E}\left[\frac{1}{Z_{0,\mu}(K)}\right] \mathcal{R}_{\mu,\text{eff}}(v,K) f(v)\mathrm{d}v.$$

We can use Lemma A.8 to obtain the values of the average inverse load in the network. To do so, we remind that the point processes of MUs associated with each network tier are independent thinnings of the PPP of transmitting MUs Φ_u. We thus need to find the probability that a MU is associated with one tier or the other given a VBMP policy K.

Lemma 11.3. *The probability for an MU moving at velocity v under a given VBMP policy to be associated with the macro tier is equal to:*

$$G_M(K) = \mathbb{P}\left[\text{Macro}\right] = \int_{v=0}^{v_{max}} \frac{f(v)}{1+\Omega K(v)^{\delta}} \mathrm{d}v. \tag{11.5}$$

The probability of being associated with the micro tier is $\mathbb{P}\left[\text{Micro}\right] = 1 - G_M(K)$.

The detail for this result is given in Appendix 12.4. We thus obtain the following average inverse load in the network:

$$\begin{aligned} \mathbb{E}\left[\frac{1}{Z_{0,M}(K)}\right] &= L\left(\frac{\lambda_M}{\lambda_u G_M(K)}\right) \triangleq L_M(K) \\ \mathbb{E}\left[\frac{1}{Z_{0,\mu}(K)}\right] &= L\left(\frac{\lambda_\mu}{\lambda_u (1-G_M(K))}\right) \triangleq L_\mu(K), \end{aligned} \tag{11.6}$$

where $L(x) = x\left(1 - \left(\frac{1}{1+\frac{2}{7x}}\right)^{7/2}\right)$. We get this formula for $\hat{\mathcal{R}}(K)$:

$$\hat{\mathcal{R}}(K) = \int_0^{v_{\max}} \left(L_M(K)\mathcal{R}_{M,\text{eff}}(v,K) + L_\mu(K)\mathcal{R}_{\mu,\text{eff}}(v,K)\right) f(v)\mathrm{d}v.$$

We can thus define the optimal load-dependent VBMP policy as:

Definition 11.3. *The* optimal load-aware VBMP policy *is the function $K^\dagger$ that corresponds to a maximum of $\mathcal{R}_{\text{load}}$. The* load-K heuristic *is the function $K^\star_{load}$ that maximizes $\hat{\mathcal{R}}$.*

Unlike the one MU per BS case, we cannot use the Euler-Lagrange equation to find the function $K^\dagger$. Here, the terms under the integral are not depending on K and its derivatives at the same point, which are local conditions and allow us to obtain the Euler-Lagrange equation. Instead, we have a global condition, in the form of $G_M(K)$, which prevents us from using the classical results in calculus of variations. To obtain an equation defining the optimal load-dependent VBMP policy, let us define the function F as:

$$F(v, K, G(K)) = \left(\mathcal{R}_{M,\text{eff}}(K,v)L_M(G(K)) + \mathcal{R}_{\mu,\text{eff}}(K,v)L_\mu(G(K))\right),$$

so that $\hat{\mathcal{R}}(K) = \int_0^\infty F(v,K,G(K))\mathrm{d}v$. Let us take $\varepsilon > 0$ and h an integrable function such that $h(0) = 0$ and $\lim_{x\to\infty} h(x) = 0$. We define $K_\varepsilon = K + \varepsilon h$

and $F_\varepsilon = F(v, K_\varepsilon, G(K_\varepsilon))$. Using Euler's condition, we know that $\hat{\mathcal{R}}(K)$ is maximal whenever:

$$\frac{\mathrm{d}}{\mathrm{d}\varepsilon}\hat{\mathcal{R}}(K_\varepsilon) = \int_0^{v_{\max}} \frac{\mathrm{d}}{\mathrm{d}\varepsilon} F_\varepsilon \mathrm{d}v = 0.$$

We take the total derivative of F_ε with respect to ε:

$$\frac{\mathrm{d}}{\mathrm{d}\varepsilon}F_\varepsilon = \frac{\mathrm{d}K_\varepsilon}{\mathrm{d}\varepsilon}\frac{\partial F_\varepsilon}{\partial K_\varepsilon} + \frac{\mathrm{d}G(K_\epsilon)}{\mathrm{d}\varepsilon}\frac{\partial F_\varepsilon}{\partial G(K_\epsilon)}$$

We know that:

$$\begin{aligned}
&\frac{\mathrm{d}K_\varepsilon}{\mathrm{d}\varepsilon} = h(v)\\
&\frac{\partial F_\varepsilon}{\partial K_\varepsilon} = L_M(G(K_\varepsilon))\frac{\partial}{\partial K}\mathcal{R}_{M,\mathrm{eff}}(K_\varepsilon, v) + L_\mu(G(K_\varepsilon))\frac{\partial}{\partial K}\mathcal{R}_{\mu,\mathrm{eff}}(K_\varepsilon, v).
\end{aligned}$$

After some calculation, we can also obtain:

$$\frac{\mathrm{d}G(K_\epsilon)}{\mathrm{d}\varepsilon} = C\delta\int_0^\infty \frac{h(u)K(u)^{\delta-1}}{(1+CK(u)^\delta)} f(u)\mathrm{d}u,$$

and:

$$\begin{aligned}
\frac{\partial F_\varepsilon}{\partial G(K_\epsilon)} = \Bigg(&-\frac{\lambda_M}{\lambda_u G(K_\varepsilon)^2}L'\left(\frac{\lambda_M}{\lambda_u G(K_\varepsilon)}\right)\mathcal{R}_{M,\mathrm{eff}}(v,K) + \\
&\frac{\lambda_\mu}{\lambda_u(1-G(K_\varepsilon))^2}L'\left(\frac{\lambda_\mu}{\lambda_u(1-G(K_\varepsilon))}\right)\mathcal{R}_{\mu,\mathrm{eff}}(v,K)\Bigg) f(v).
\end{aligned}$$

Unfortunately, due to the nature of the dependency of $\frac{\mathrm{d}G(K_\epsilon)}{\mathrm{d}\varepsilon}$ on h, we cannot use the fundamental lemma of calculus of variations (see Lemma 1.1.1 in [52]) to obtain an equation defining $K^\dagger$. A way to obtain a numerical approximation of the function $K^\dagger$ is to introduce a discretization for the problem.

Let us assume that velocities can only take a finite number of values $(v_i)_{0\leq N-1}$, ranging from 0 to a velocity v_M, separated by a step $\epsilon = \frac{v_M}{N-1}$, so that $v_i = v_0 + i\epsilon$. Let us denote $p_i = \mathbb{P}\left[v_i \leq v < v_{i+1}\right]$, $K_i = K(v_i)$ and $\mathbf{K} = (K_i)_{0\leq i\leq N-1}$.

This discretization allows us to rewrite the quantities defined earlier as sums:

$$\begin{aligned}
G(\mathbf{K}) &= \sum_{i=0}^{N-1}\frac{p_i}{1+CK_i^\delta},\\
L_M(\mathbf{K}) &= L\left(\frac{\lambda_M}{\lambda_u G(\mathbf{K})}\right),\\
L_\mu(\mathbf{K}) &= L\left(\frac{\lambda_\mu}{\lambda_u G(\mathbf{K})}\right).
\end{aligned}$$

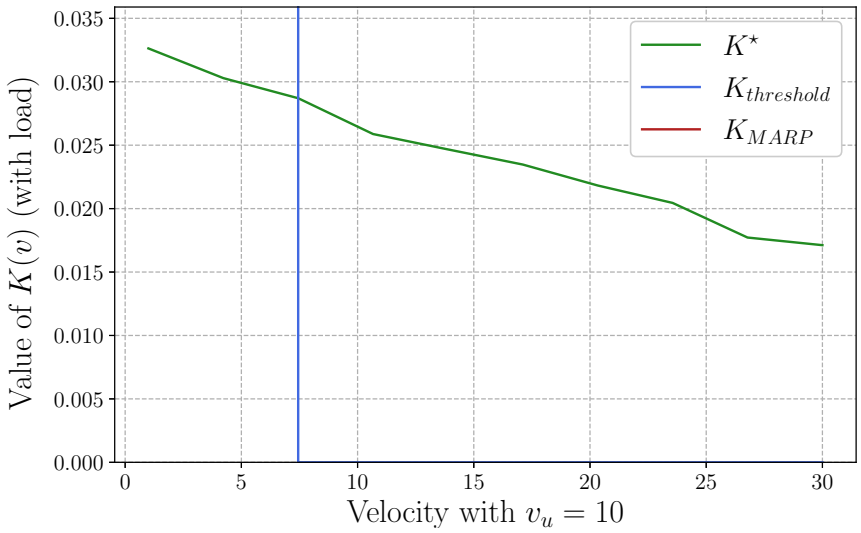

Figure 11.3: Plot of the estimate $\mathbf{K}^\dagger$ (green) of the optimal VBMP policy for an exponential distribution with parameter $v_u = 10$ against the MARP policy (red) and the optimal threshold policy (blue).

We can define a newer version of the target $\hat{\mathcal{R}}$:

$$\mathfrak{R}(\mathbf{K}) = \sum_{i=0}^{N-1} \left(\mathcal{R}_{M,\text{eff}}(K_i) L_M(\mathbf{K}) + \mathcal{R}_{\mu,\text{eff}}(K_i) L_\mu(\mathbf{K}) \right) p_i.$$

Let $\mathbf{K}^\dagger \in \mathbb{R}_+^N$ that maximizes the function $\mathfrak{R}$. Using the dominated convergence theorem as well as Riemann sums, we know that as ϵ goes to 0, the vector $\mathbf{K}^\dagger$ approaches the function $K^\dagger$.

Numerical resolution

We can now move on to solving the system using know algorithmic method. The results presented here are obtained using Python's `scipy.optimize.minimze` function, which implements multiple gradient descent algorithms to solve for $\mathbf{K}^\dagger$.

Using a gradient descent algorithm leads to numerous evaluations of $\mathcal{R}_{M,\text{eff}}(K_i)$ and $\mathcal{R}_{\mu,\text{eff}}(K_i)$, which can become computationally heavy when looking for a small value of ϵ. The regular integration packages in Python to evaluate double integrals use the library QUADPACK ([71]), which achieves slow convergence in the cases we consider here. Among the other methods existing to evaluate multiple integrals, we decide to use the Genz-Malik scheme (as presented in [46]) to evaluate the integrals, which allows to obtain a value of $\mathbf{K}^\dagger$ in reasonable time.

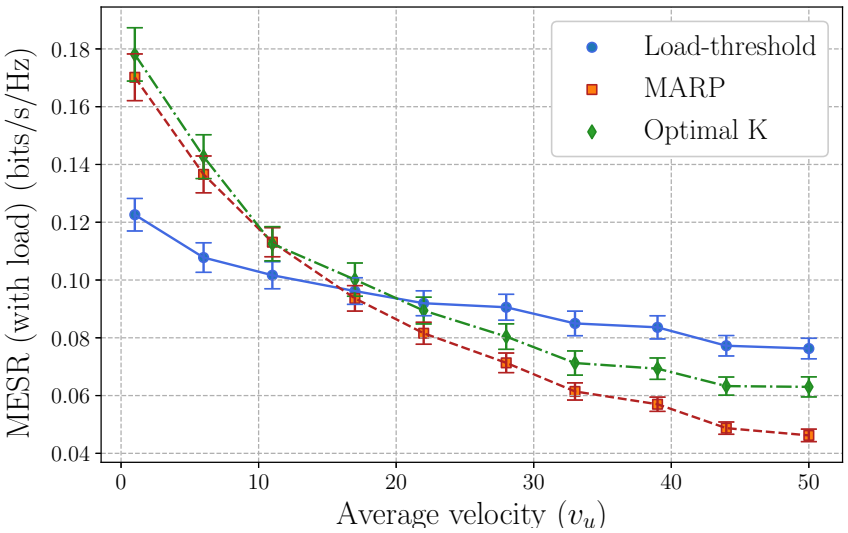

Figure 11.4: Comparison of the three association policies: the optimal VBMP policy (green), the MARP policy (red) and the optimal threshold policy (blue) as a function of v_u.

11.4 Discussion and comparison

We can compare the optimal load-aware VBMP policy defined in Definition 11.3 to the two other association policies defined earlier: the optimal load-threshold policy. Figure 11.4 displays the comparison between the three policies for different values of v_u, where the MU velocity is exponentially distributed with mean v_u.

We can see that the proposed association policy performs better than the classical MARP policy at all velocities, but still is outperformed by the load-threshold policy for high MU velocities, although we originally designed this VBMP policy to outperform it. This observation can be explained by two factors.

The first factor is the precision of the numerical integration methods we use to evaluate $\mathcal{R}_{M,\text{eff}}(K_i)$ and $\mathcal{R}_{\mu,\text{eff}}(K_i)$ at each iteration. In the numerical simulations, we use an adaptive Genz-Malik scheme over the classical numerical integration method to increase the speed of computation. Another candidate to evaluate quickly multiple integrals is Monte-Carlo integration, which is also known to be performant, but can have high variance. We can compare the three methods of integration to compute $\mathcal{R}_M(K_i)$ for values of K_i ranging from 0 to 1 to see the differences in the three methods.

Figure 11.5 shows the three methods of integration, and we can see that the Genz-Malik scheme and the quadpack integration both give similar results for the value of $\mathcal{R}_M(K_i)$, while the Monte-Carlo integration presents high variance, and sometimes can prove to have a very large interval confidence. In the simulation ran here, we can see that it can also present outliers and miss the exact value of the integral. On the other hand, we can see that

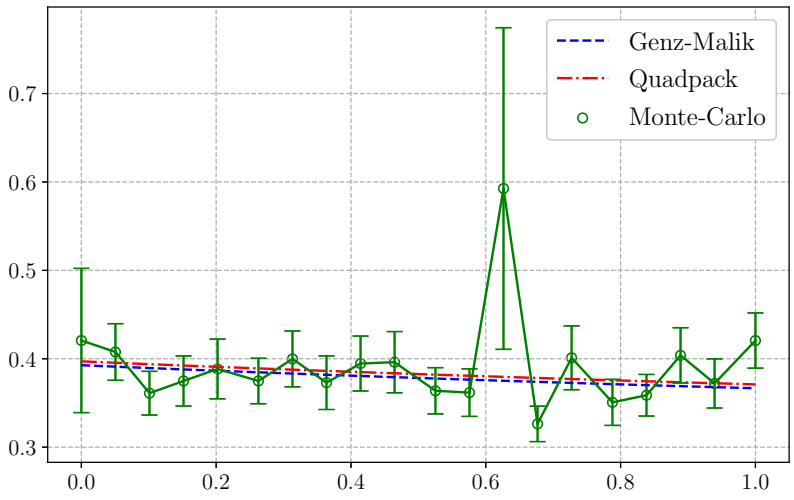

Figure 11.5: Comparison of the three QUADPACK integration (in red), the Genz-Malik scheme (in blue) and the Monte-Carlo integration (in green) with 200 000 samples.

the Genz-Malik integration scheme predicts relatively well that value of the integral, which asserts its utility here.

The second factor that can impact the precision of the load-dependent VBMP policy we obtain is the minimization method we use to obtain the vector $K^{\dagger}$. The library `scipy.optimize` implement by default the L-BFGS-D method ([32]), but other methods can be investigated to see if they yield better results in the cases we are considering, such as Powell's method ([74]), which achieves better results with noisy inputs. Investigating this point to find - or design - a better method to maximize the MESR under a load-dependent VBMP policy needs to be further investigated and may be the focus of a future work.

Although the results in this part did not lead to the original goal we set - obtaining an association policy able to outperform both the load-threshold policy defined in Definition 10.2, we still managed to obtain an association policy that outperforms the classical MARP policy when the load of the antennas is taken into account: Figure 11.4 shows that the proposed load-dependent VBMP policy performs better at all velocities, with the simple addition of a bias term in the original MARP policy.

The work proposed in this part opens a new line of though about incorporating velocity in the design of association policies in multitier wireless networks. We proposed two user-centric, simple associations policies centered around MU velocity, and we showed that they can both outperforme a classical max-power association policy when we consider multiple MU per cell. The work presented here can be seen as a first step into designing more comprehensive association policies incorporating MU velocity, in order to achieve better network performance.

Chapter 12

Proof of Theorems of Chapters 10 and 11

12.1 Proof of Theorem 10.1

Base stations in the macro tier are distributed according a homogenous PPP with intensity λ_M. The probability that the BS X is located at a distance $r > 0$ from the origin and the associated distribution function:

$$F_M(r) = \mathbb{P}[\|X\| \leq r] = 1 - e^{-\lambda_M \pi r^2}$$
$$f_M(r) \equiv \frac{d}{\mathrm{d}r} F_x(r) = 2\pi r e^{-\lambda_M \pi r^2}.$$

We assume that the typical MU is located in the main lobe of its association beam, i.e. $g_0^M = G_m^M$. We get:

$$\begin{aligned}
\mathbb{P}\left[\mathrm{SINR}_{M,0} > T | r, g_0^M = G_m^M\right] &= \mathbb{P}\left[\frac{P_M G_k^M h_0 r^{-\alpha}}{\sigma^2 + I_{M,a} + I_{\mu,i}} > T | r\right] \\
&= \mathbb{P}\left[h_0 > \frac{T r^\alpha}{P_M G_k^M}(\sigma^2 + I_{M,a} + I_{\mu,i}) \, | r\right] \\
&= e^{-\frac{\mu T r^\alpha}{P_M G_k^M}} \mathbb{E}\left[\exp\left(-\frac{\mu T}{P_M G_k^M} I_{M,a} - \frac{\mu T}{P_M G_k^M} I_{\mu,i}\right)\right].
\end{aligned}$$

Focusing on the first term in the expectation, we get:

$$\mathbb{E}\left[\exp\left(-\frac{\mu T}{P_M g_{M,0}} I_{M,a}\right)\right] = \mathbb{E}\left[\prod_{x\in\Phi^M\setminus\{X\}} \mathbb{E}\left[\exp\left(-\frac{\mu T G_x}{g_0^M} r^\alpha h_x \ell(|x|)\right)\right]\right]$$
$$= \mathbb{E}\left[\prod_{x\in\Phi^M\setminus\{X\}} \mathbb{E}\left[\frac{1}{1+\frac{TG_x}{g_0^M} r^\alpha \ell(|x|)}\right]\right]$$
$$= \mathbb{E}\left[\prod_{x\in\Phi^M\setminus\{X\}} \frac{p_{M,m}}{1+\frac{TG_m^M}{g_0^M} r^\alpha \ell(|x|)} + \frac{1-p_{M,m}}{1+\frac{TG_s^M}{g_0^M} r^\alpha \ell(|x|)}\right],$$

Using the formula for the Laplace transform of a PPP, we have:

$$\mathbb{E}\left[\exp\left(-\frac{\mu T}{P_M g_{M,0}} I_{M,a}\right)\right]$$
$$= \exp\left(-2\pi\lambda_M \int_r^\infty \left(1 - \frac{p_{M,m}}{1+\frac{TG_m^M}{g_{M,0}} r^\alpha \ell(|x|)} - \frac{1-p_{M,m}}{1+\frac{TG_s^M}{g_{M,0}} r^\alpha \ell(|x|)}\right) z\mathrm{d}z\right)$$
$$\overset{(a)}{=} \exp\left(-\pi\lambda_M r^2 T^\delta \left(p_{M,m}\left(\frac{G_m^M}{g_{M,0}}\right)^\delta \int_{\left(\frac{TG_j^M}{g_{M,0}}\right)^{-\delta}}^\infty \frac{\mathrm{d}u}{1+u^{1/\delta}}\right.\right.$$
$$\left.\left. +(1-p_{M,m})\left(\frac{G_s^M}{g_{M,0}}\right)^\delta \int_{\left(\frac{TG_j^M}{g_{M,0}}\right)^{-\delta}}^\infty \frac{\mathrm{d}u}{1+u^{1/\delta}}\right)\right).$$

Where (a) uses the change of variables $u = \left(\frac{G_m^M}{Tg_{M,0}}\right)^\delta \frac{z^2}{r^2}$ for the first integral and $u = \left(\frac{G_s^M}{Tg_{M,0}}\right)^\delta \frac{z^2}{r^2}$ for the second one. Using the same steps and some results developed in Appendix A, the second expectation yields:

$$\mathbb{E}\left[\exp\left(-\frac{\mu T}{P_M g_{M,0}} I_{\mu,i}\right)\right]$$
$$= \exp\left(-\pi\lambda_\mu r^2 T^\delta \left(\frac{P_\mu}{P_M g_{M,0}}\right)^\delta \left(p_{\mu,m}(G_M^\nu)^\delta + (1-p_{\mu,m})(G_M^\nu)^\delta\right) C(\delta)\right).$$

Where $C(\delta) = \int_0^\infty \frac{\mathrm{d}u}{1+u^{1/\delta}} = \frac{\delta\pi}{\sin(\pi\delta)}$. Reminding that the typical MU is aligned, we have $g_{M,0} = G_m^M$, which leads to:

$$\mathbb{E}\left[\mathbb{P}\left[\mathrm{SINR}_{M,0} > T | r, g_0^M = G_m^M\right]\right] =$$
$$\pi\lambda_M \int_{r\geq 0} e^{-\pi\lambda_M r} e^{-\frac{\mu T r^{1/\delta}}{P_M G_m^M}} \exp\left(\left(\frac{T}{P_M G_m^M}\right)^\delta \left(\lambda_M P_M^\delta \rho^M(G_m^M, T) + \lambda_\mu P_\mu^\delta \kappa_\mu(\delta)\right)\right) \mathrm{d}r.$$

Finally, we obtain:

$$q_m^M(T) = \int_{r\geq 0} \mathbb{E}\left[\mathbb{P}\left[\mathrm{SINR}_{M,0} > T | r, g_0^M = G_m^M\right]\right] 2\pi\lambda_M r e^{-\pi\lambda_M r^2} dr. \quad (12.1)$$

Making the change of variables $v = r^2$ gives the intended result for $q_m^M(T)$. To obtain the result for q_s^M, q_M^ν and q_s^μ, we simply swap the roles of the two network tiers and use the adequate values.

12.2 Proof of Theorem 10.2

Differenciating (10.4) w.r.t. the velocity threshold v_T gives:

$$\frac{\mathcal{D}}{\mathcal{D}v_T}\mathcal{R}(v) = \mathcal{R}_{\mu,\mathrm{eff}}(v)f(v) - \mathcal{R}_{M,\mathrm{eff}}(v)f(v). \quad (12.2)$$

Granted that $f > 0$, the points where the derivative is equal to zero are solutions to:

$$\mathcal{R}_{\mu,\mathrm{eff}}(v) = \mathcal{R}_{M,\mathrm{eff}}(v). \quad (12.3)$$

Using definitions from Section 9.3, we know that:

$$\mathcal{R}_{M,\mathrm{eff}}(v) = (1 - T_o^M(v))^+ \mathcal{R}_M$$

and that $T_o^M(v) = \nu_{M,c}(v)T_{M,c} + \nu_{M,e}(v)T_{M,b}$. We also know that $\nu_{M,e}(v)$ is equal to $\nu_{M,b}(v)$ for $v < v_{M,\tau} = \frac{\pi}{n_M \tau\sqrt{\lambda_M}}$, and to $\frac{1}{\tau}$ else. We can solve for $T_o^M(v) = 1$ depending on the value of v. We obtain two solutions:

$$\begin{cases} w_{M,1} = \dfrac{\pi}{\sqrt{\lambda_M}(4T_{c,M} + n_M T_{b,M})} & \text{if } v < v_{M,\tau} \\ w_{M,2} = \dfrac{\pi}{\sqrt{\lambda_M} 4T_{c,M}} \left(\dfrac{T_{M,b}}{\tau} - 1\right) & \text{if } v \geq v_{M,\tau}. \end{cases}$$

Using the numerical parameters from Table 9.1, we obtain $v_{M,\tau} = 138.84$ m.s^{-1}, $w_{M,1} = 62.40$ m.s^{-1} and $w_{M,2} = 19.37$ m.s^{-1}. Because $w_{M,2} < v_{M,\tau}$, we reject this second solution, which gives us the following formula for $\mathcal{R}_{M,\mathrm{eff}}(v)$:

$$\mathcal{R}_{M,\mathrm{eff}}(v) = \begin{cases} \mathcal{R}_M \left(1 - v\frac{\sqrt{\lambda_M}}{\pi}\left(4T_{c,M} + n_M T_{b,M}\right)\right) & \text{for } v \leq w_{M,1} \\ 0 & \text{else} \end{cases}$$

Conducting the same analysis for the micro network, we define $v_{\mu,\tau}$, $w_{\mu,1}$ and $w_{\mu,2}$ similarly. When evaluating the numerical values, we reject the solution $w_{\mu,2}$, because $w_{\mu,2} < v_{\mu,\tau}$, and we obtain the following expression for $\mathcal{R}_{\mu,\mathrm{eff}}$:

$$\mathcal{R}_{\mu,\text{eff}}(v) = \begin{cases} \mathcal{R}_\mu \left(1 - v\frac{\sqrt{\lambda_\mu}}{\pi}\left(4T_{c,\mu} + n_\mu T_{b,\mu}\right)\right) & \text{for } v \leq w_{\mu,1} \\ 0 & \text{else} \end{cases}$$

$\mathcal{R}_{M,\text{eff}}(v)$ and $\mathcal{R}_{\mu,\text{eff}}(v)$ are two linear functions of v, with negative slopes respectively equal to $-\mathcal{R}_M\frac{\sqrt{\lambda_M}}{\pi}\left(4T_{c,M} + n_M T_{b,M}\right)$ and $-\mathcal{R}_\mu\frac{\sqrt{\lambda_\mu}}{\pi}\left(4T_{c,\mu} + n_\mu T_{b,\mu}\right)$. Because $\mathcal{R}_\mu > \mathcal{R}_M$ and $\lambda_\mu > \lambda_M$, the lines intersect at a unique point, and we can conclude that (12.3) admits a unique positive solution, denoted as $v_T^\star$.

Finally, because $\mathcal{R}_{\mu,\text{eff}} \geq \mathcal{R}_{M,\text{eff}}$ for $v < v_T^\star$ and $\mathcal{R}_{\mu,\text{eff}} \leq \mathcal{R}_{M,\text{eff}}$ for $v > v_T^\star$, the threshold $v_T^\star$ corresponds to a maximum of the function $\mathcal{R}$.

12.3 Proof of Theorem 11.1

Let $\theta > 0$. The coverage probability in the macro tier as the probability that $\text{SINR}_{0,M}$ is greater than $\theta > 0$ and the typical MU is associated with the macro tier. To evaluate this probability, we condition the event $\text{SINR}_{0,M} > \theta$ and that the typical MU is associated with the macro tier on the closest BS in the macro tier $X_{0,M}$ being at a distance r of the origin and its micro counterpart, $X_{0,\mu}$, being at a distance s. We have:

$$\begin{aligned}
&\mathbb{P}\left[\text{SINR}_{0,M} > \theta, \text{Macro} \,||X_{0,\mu}| = s, |X_{0,M}| = r\right] \\
&= \mathbb{P}\left[h_0 > \frac{\theta r^\alpha}{P_M\kappa}\left(\sigma^2 + I_M\left(\Phi_M\backslash\{X_{0,M}\}\right) + I_\mu\left(\Phi_\mu\right)\right)\right] \\
&= \mathbb{E}\left[\exp\left(-\frac{\theta r^\alpha}{\kappa P_M} I_\mu\left(\Phi_\mu\right)\right), \text{Macro}\middle| \, |X_{0,\mu}| = s\right] \\
&\mathbb{E}\left[\exp\left(-\frac{\theta r^\alpha}{\kappa P_M} I_M\left(\Phi_M\backslash\{X_{0,M}\}\right)\right), \text{Macro}\middle| \, |X_{0,M}| = r\right]
\end{aligned}$$

The first expectation gives:

$$\begin{aligned}
&\mathbb{E}\left[\exp\left(-\frac{\theta r^\alpha}{\kappa P_M} I_M\left(\Phi_M\backslash\{X_{0,M}\}\right)\right), \text{Macro}\middle| \, |X_{0,M}| = r\right] \\
&= \mathbb{E}\left[\prod_{x\in\Phi_M\backslash\{X_{0,M}\}} \mathbb{E}\left[\exp(-\theta h_x\left(\frac{r}{x}\right)^\alpha\right]\right] \\
&\overset{(a)}{=} \mathbb{E}\left[\prod_{x\in\Phi_M\backslash\{X_{0,M}\}} \frac{1}{1+\theta\left(\frac{r}{x}\right)^\alpha}\right] \\
&\overset{(b)}{=} \exp\left(-2\pi\lambda_M\int_r^\infty \frac{\mathrm{d}x}{1+\theta\left(\frac{r}{x}\right)^\alpha}\right),
\end{aligned}$$

where (a) uses the Laplace transform of an exponential variable with parameter 1, and (b) uses the Laplace transform of a Poisson process. With the change of variables $u = \theta^{-\delta}\left(\frac{x}{z}\right)^2$, we get:

$$\mathbb{E}\left[\exp\left(-\frac{\theta r^{\alpha}}{\kappa P_M} I_M\left(\Phi_M \backslash \{X_{0,M}\}\right)\right), \text{Macro} \middle| |X_{0,M}| = r\right] = \exp\left(-2\pi\lambda_M r^2 \theta^{\delta} \int_{\theta^{-\delta}}^{\infty} \frac{\mathrm{d}u}{1+u^{1/\delta}}\right).$$

For the second expectation, we remind that the closest BS $X_{0,\mu}$ is at a distance s of the origin. We have:

$$\begin{aligned}
&\mathbb{E}\left[\exp\left(-\frac{\theta r^{\alpha}}{\kappa P_M} I_{\mu}\left(\Phi_{\mu}\right)\right), \text{Macro} \middle| |X_{0,\mu}| = s\right] \\
&= \mathbb{E}\left[\exp\left(-\frac{\theta P_{\mu}}{P_M}\left(\frac{r}{s}\right)^{\alpha} - \frac{\theta r^{\alpha}}{\kappa P_M} I_{\mu}\left(\Phi_{\mu} \backslash \{X_{0,\mu}\}\right)\right)\right] \\
&= e^{-\frac{\theta P_{\mu}}{P_M}\left(\frac{r}{s}\right)^{\alpha}} \mathbb{E}\left[\prod_{x \in \Phi_{\mu} \backslash \{X_{0,\mu}\}} \frac{1}{1+\frac{\theta P_{\mu}}{P_M}\left(\frac{r}{x}\right)^{\alpha}}\right] \\
&= e^{-\frac{\theta P_{\mu}}{P_M}\left(\frac{r}{s}\right)^{\alpha}} \exp\left(-2\pi\lambda_{\mu} \int_{s}^{\infty} \frac{\mathrm{d}x}{1+\frac{\theta P_{\mu}}{P_M}\left(\frac{s}{x}\right)^{\alpha}}\right).
\end{aligned}$$

We introduce the change of variables $u = \theta^{\delta}\left(\frac{P_{\mu}}{P_M}\right)^{\delta} \frac{r^2}{y^2}$ in the inside integral to get:

$$\mathbb{E}\left[\exp\left(-\frac{\theta r^{\alpha}}{\kappa P_M} I_{\mu}\left(\Phi_{\mu}\right)\right), \text{Macro} \middle| |X_{0,\mu}| = s\right] = e^{-\frac{\theta P_{\mu}}{P_M}\left(\frac{r}{s}\right)^{\alpha}} \exp\left(-\pi\lambda_{\mu} \int_{u=\left(\frac{P_M}{P_{\mu}}\right)^{\delta} \frac{s^2}{r^2}}^{\infty} \frac{\mathrm{d}x}{1+u^{1/\delta}}\right).$$

The probability that a BS X is located at a distance $r > 0$ from the origin and the associated distribution function in the macro tier are equal to:

$$\begin{aligned}
F_M(r) &= \mathbb{P}\left[|X_{0,M} \leq r\right] = 1 - \exp\left(-\pi\lambda_M r^2\right) \\
f_M(r) &= \frac{\mathrm{d}}{\mathrm{d}r} F_M(r) = 2\pi\lambda_M r e^{-\pi\lambda_M r^2},
\end{aligned}$$

with a similar expression for the micro tier by using the adequate values. To obtain the coverage probability, we integrate over all the realisations of the PPP Φ_M and Φ_{μ}. A user is associated with the macro tier if $s > \left(\frac{P_{\mu} K(v)}{P_M}\right)^{\alpha} r$, and to the micro tier if $0 \leq s \leq \left(\frac{P_{\mu} K(v)}{P_M}\right)^{\alpha} r$. With these bounds of integration, we get:

$$\begin{aligned}
\mathbb{P}\left[\text{SINR}_{0,M} > \theta\right] = \int_{r=0}^{\infty} \int_{s=\left(\frac{P_{\mu} K(v)}{P_M}\right)^{1/\alpha} r}^{\infty} & e^{-\pi(\lambda_M r^2 + \lambda_{\mu} s^2)} \\
&\times \mathbb{P}\left[\text{SINR}_{0,M} > \theta \middle| |X_{0,\mu}| = s, |X_{0,M}| = r\right] 4\pi^2 \lambda_{\mu} r \lambda_M s \mathrm{d}s \mathrm{d}r.
\end{aligned}$$

We introduce the change of variables $y = \pi\lambda_{\mu}s^2$ and $x = \pi\lambda_M r^2$ to obtain:

$$\mathbb{P}\left[\mathrm{SINR}_{0,M} > \theta\right] = \int_{x=0}^{\infty}\int_{y=CK(v)^{\delta}x}^{\infty} e^{-\theta\left(\frac{Cx}{y}\right)^{1/\delta}} e^{-x-y} e^{\left(-x\left(\theta^{\delta}\int_{\theta^{-\delta}}^{\infty}\frac{\mathrm{d}u}{1+u^{1/\delta}} + C\theta^{\delta}\int_{\frac{y}{x}}^{\infty}\frac{1}{C\theta^{\delta}}\frac{\mathrm{d}u}{1+u^{1/\delta}}\right)\right)}\mathrm{d}y\mathrm{d}x.$$

We introduce a second change of variables for the inside integral, $z = \left(\frac{Cx}{y}\right)^{1/\delta}$, with $\mathrm{d}y = -\delta\frac{Cx}{z^{1+\delta}}\mathrm{d}z$. We have

$$\mathbb{P}\left[\mathrm{SINR}_{0,M} > \theta\right] = \int_{x=0}^{\infty}\int_{z=\frac{1}{K(v)}}^{0} e^{-\theta z}\left(-\delta\frac{Cx}{z^{\delta+1}}\right) e^{\left(-x\left(\theta^{\delta}\int_{\theta^{-\delta}}^{\infty}\frac{\mathrm{d}u}{1+u^{1/\delta}} + C\theta^{\delta}\int_{\frac{1}{(zT)^{\delta}}}^{\infty}\frac{\mathrm{d}u}{1+u^{1/\delta}}\right)\right)} e^{-x\left(1+\frac{C}{z^{\delta}}\right)}\mathrm{d}x\mathrm{d}z.$$

After rearranging the terms and using Fubini's Theorem to swap the two integrals and introducing $F(\theta,\delta) = \int_{\theta^{-\delta}}^{\infty}\frac{\mathrm{d}u}{1+u^{1/\delta}}$, we get

$$\mathbb{P}\left[\mathrm{SINR}_{0,M} > \theta\right] = \delta C\int_{z=0}^{1/K(v)} \frac{z^{-\delta-1}e^{-\theta z}}{\left(1 + Cz^{-\delta} + \theta^{\delta}F(\theta,\delta) + C\theta^{\delta}F(zT,\delta)\right)^2}\mathrm{d}z.$$

For the formula in the micro tier, we swap the role of the two network tiers and use the appropriate values to get the intended result, which concludes the proof.

12.4 Proof of Lemma 11.3

Let us consider an MU located at the origin and moving at a given velocity $v > 0$. It is associated with the macro tier if and only if $\mathrm{R}_M > K(v)\mathrm{R}_{\mu}$. Let us assume that the closest macro BS to the origin, $X_{0,M}$ is located at distance $r > 0$ and its micro counterpart, $X_{0,\mu}$, is at distance $s > 0$.

The MU is thus associated with the macro tier if and only if $s > \left(\frac{P_{\mu}K(v)}{P_M}\right)^{1/\alpha} r$. This leads to:

$$\mathbb{P}[\mathrm{Macro}|\, v] = 4\pi^2\int_{r=0}^{\infty}\int_{s=\left(\frac{P_{\mu}K(v)}{P_M}\right)^{1/\alpha}r}^{\infty} e^{-\pi\lambda_M r^2 - \pi\lambda_{\mu}s^2}\lambda_M\lambda_{\mu}\mathrm{d}s\mathrm{d}r.$$

We use the new variables $x = \pi\lambda r^2$ and $y = \pi\lambda_{\mu}s^2$, and introduce $C = \frac{\lambda_{\mu}}{\lambda_M}\left(\frac{P_M}{P_{\mu}}\right)^{\delta}$, which yields:

$$\mathbb{P}[\mathrm{Macro}|\, v] = \int_{x=0}^{\infty}\int_{y=CK(v)^{\delta}x}^{\infty} e^{-x-y}\mathrm{d}x\mathrm{d}y = \frac{1}{1+CK(v)^{\delta}}.$$

To obtain the probability that the typical MU is associated with the macro tier, we integrate with respect to the MU velocity distribution f, which gives the intended result.

Chapter 13

Conclusion

In this thesis, we developed frameworks using stochastic geometry and elements of queuing theory to study some aspects of the dynamics of spatial queuing systems, aimed at modelling wireless networks. In this chapter, we will summarize the results obtained, focus on some questions of interest that arose during our study, and propose some prospects for future work.

Summary

The first system we studied is a multiclass spatial birth-and-death process. Spatial queuing systems and birth-and-death processes have been studied in various setups ([15], [80]), and some results already exist. In our work, we introduced a form of service differentiation to modify the classical wireless network dynamics, under which users are allocated a given number of frequency bands to transmit on, and interfere only with users that have overlapping frequency bands. This differentiation is motivated by the introduction of bandwidth partitioning ([68]) algorithms in the latest generation of wireless networks as a means to increase network performance.

The first step of our study was to develop a broader framework than the one proposed in [80] to capture the multiclass nature of the interactions we consider here, and to establish several useful properties (monotonicity, irreducibility). We then moved on to studying the stability of the dynamics under a symmetry assumption. To study the stability of this system, we first introduced two queuing systems that bound the dynamics of the original system from above and below, and relied on fluid limits ([78]), which give helpful relations linking the behavior of a system of differential equations and the recurrence of these queuing systems. Once stability for these two systems was reached, we could reach the stability condition for the symmetric spatial birth-and-death process. After this, we relaxed the symmetry assumption and showed that we can reach a more general stability condition for non-symmetric networks using similar fluid limit argument, using a reciprocal to

a stability condition obtained in [84].

In a second part, we looked into the stationary regime of the dynamics introduced in Part I. The first quantities of interest we looked into are spatial user densities, which characterize the steady-state dynamics of this network. We derived two heuristics: a first one relying on a Poisson approximation, similar in a way to replica mean-field methods, and a second one leveraging a cavity approximation and using a second-order approximation. A most interesting result in this section is that the Poisson approximation allowed us to obtain a precise heuristic to estimate the critical arrival rate of the system. The second interesting property of the stationary regime is clustering. We know that such a property arises in the single-class system ([80]). In the multiclass system though, we reached a weaker condition, which can be explained by the fact that not all users interact with each other with the same power, weakening the attraction-inducing properties of wireless interactions. Finally, we completed the study of the stationary regime by showing that the queuing process admits exponential tails, which is of great interest for communication networks as it help to bound precisely latency and service times - two of the requirements of URLLC networks.

The third part of the manuscript focused on a different perspective: instead of considering time dynamics, where immobile users appear and disappear in the network, we consider spatial dynamics, where users move on a straight line inside a fixed network consisting in two types of base stations: macro and micro base stations. Macro BSs provide more power but have a larger coverage than micro BSs, which are more directional but less powerful. This model is motivated by multitier networks using beam-based communications ([39], [40]), which can be found in the newly deployed 5G wireless networks ([49]). The goal of this study of such a network is to design user-centric association policies taking into account user mobility, which are easily implementable and have a low computational cost. This lead us to define two families of association policies: one only considering user velocity, and the second one, offering a trade-off between network geometry and user mobility. Using relevant numerical computations and heuristics, we could prove that these family of policies can be tuned to maximize a certain network performance metric, which can be tied to spectral efficiency. Under this framework, we could compare these two association policies to a classical max-power association policies to find out that the two proposed association policies outperform this max-power association in several cases, notably, in densely populated networks with fast-moving users.

Although our study is separated in two parts leveraging two different frameworks and mathematical tools, the study we present here is a first step towards building a comprehensive framework to model time-spatial interactions in a multitier 5G network. In the next two sections, we will focus on some questions of interest that appeared during this work, and some prospects and natural extensions that can be investigated using the tools we developed here.

Discussion and questions of interest

The systems we considered in this thesis are idealized version of real-world systems, yet the framework we used encapsulates the main features of wireless communications (beam-based communication, bandwidth partitioning, user mobility, communication overheads, etc.). The work we presented here can be seen as a first step on building a more comprehensive framework to model future wireless networks.

The results proved in Part I can be extended to other queuing networks. Stability conditions for spatial queuing systems have already been studied ([15], [28], [58]) using various methods. The framework we present here has the advantage of being robust, as it can be applied to other types of dynamics. We can adapt Theorem 1.2 and the discretization to other types of departing processes, and reach the stability condition using the method developed in the proof of Theorem 2.3. This would allow us to reach stability conditions for any spatial queuing systems with monotonicity and where the arrival rate is constant and the departure rates is inversely proportional to a shot-noise of users in the system.

In Part II, we developed heuristics to estimate the spatial user densities in the network, and we derived from the Poisson heuristic an estimate for the value of λ_c, which turns to be an accurate estimate for the critical arrival rate in the system. The main question arising from this is the relevance of the Poisson heuristic and how can such a result be explained. We know that in replica mean-field systems and under some hypothesis, the replicas behave as independent Poisson processes (see [19]). One can wonder if such a result can be extended to our dynamics, by designing a replica mean-field version of our system and studying the behavior of such a system as the number of copies go to infinity.

When comparing association policies in Part III, we saw that numerically, the optimal load-dependent VBMP policy outperformed the classical max-power association policy for all user velocities, but that it failed to do better than the load-threshold policy for high velocities. The question that arises from this is whether it is possible to obtain an association policy that outperforms both. We saw that the optimization problem for which the theoretical best VBMP policy was not solvable using the classical techniques of calculus of variations, and that we had to rely on a estimate by discretizing that velocity space. This method of estimating the optimal VBMP policy faces two obstacles: the computational cost of decreasing the grid size of velocities is high, and the optimization methods used may face convergence issues to find the global maximum of the MESR. Another explanation why the optimal VBMP policy does not outperform the load-threshold policy is that the VBMP policies use bias factors that are differentiable (even, $\mathcal{C}^1$) while the bias factor in the load-threshold policy is a Heaviside function. These questions need to be investigated and my be the subject of future work.

Prospects and future work

Networks with heterogenous interactions An interesting question coming from this line of thought would be spatial dynamical systems where the interactions between users are of different nature. An instance of such a heterogenous network is the following: let us imagine a network mixing users that transmit by peer-to-peer connection (as presented in [15]) and users that transmit using wireless transmissions. Under this setup, we would have a first class of users for which the intensity of the departure process is proportional to a shot-noise of the point process of users of the class, and a second class of users for which the departure process will have a stochastic intensity inversely proportional to a shot-noise of users of both classes.

Another interesting thing to note is that the framework we developed linking stability with fluid limits is an equivalence between Markov chains and Markov jump processes with systems of differential equations and their stability conditions. In the case we studied, stability regions are intervals of $\mathbb{R}_+$ containing 0 due to the monotonicity of the network, but one can wonder whether other network setups could give different behaviors for the fluid limit and how it could transpose for the original Markov chain.

Load balancing and allocation policy In Part I, the user type distribution $(p_C)_{C\in\mathcal{P}(K)}$ is determined by the user needs in the system, and can be empirically obtained by studying wireless traffic. From Theorem 2.2 and Theorem 4.4, we know that the critical arrival rate λ_c is defined as the maximum rate of transmission of the class that is able to transmit the less (see Theorem 4.4). A first question arising is the question of the maximization of the stability region, although an immediate analysis of the result from Theorem 4.4 gives that the maximum value of λ_c is reached when we set $p_{C^\star} = 1$, where $C^\star$ is the class with the lowest L_C. Another problem we can look into is load balancing in the network: how can we select the value of (p_C) to limit the queue size of certain classes? Theorem 8.1 gives bounds for the queue length of each process linked with the value of λ_c, which is linked as well to the service times in the system, through Little's law ([64]).

We can also consider the case of adaptive allocation policies, which are critical in 5G NR ([63]). Among the possible allocation policies, a possibility is to let each p_C be inversely proportional to its queue length. In such a setup, the larger a queue grows, the smaller the arrival rate in such queue is and we obtain a sort of dampening effect that would prevent queue length from becoming too large. Studying such a network would require to change the network setup a reestablish the fluid limits from Theorem 2.3 in order to account for these changes, and study the new stability region.

Poisson heuristic and critical arrival rate One of the most interesting question arisen in this work comes from the Poisson heuristic for λ_c, which proves to be very efficient to determine an approximate value of λ_c. We can wonder whether this result holds in more general cases. We know from [19]

that replica mean-field models have arrival processes that converge to Poisson point processes as the number of replica goes to infinity.

An idea to prove this result would be to consider n parallel instances of our network, and for each user, to sample users among all the replicas uniformly at random, and to study the evolution of such a system as n goes to infinity using a similar methodology. Such a result would be interesting for two reasons. The first is that it would allow for an easy way to reach a stability condition for spatial birth-and-death processes, as stochastic geometry tools and rate conservation arguments allow to easily reach simple results when working with Poisson point processes. The second one would be more theoretical, as it could be seen as a commutative diagram property, where we could obtain an equality between a certain temporal average in the system (the fluid limit) and a spatial average (the Poisson approximation in the stationary regime).

Spatial birth-and-death processes with mobility As we saw in Part III of the thesis, mobility is a key factor when taking into account wireless communication, which can be easily included in our framework: assume that users move on a straight line with an angle θ with the x-axis i.i.d sampled from a distribution g at a velocity v sampled from distribution f, which forms a spatial birth-and-death move process ([60]). Due to the exponential distribution for file sizes in the system, the system is still a Markov jump process, and still possesses the domination property that allows us to bound the dynamics from above and below by two interference queuing networks. To obtain the stability condition, we have to add two terms, one to represent the users leaving the cell, the second for the users arriving in the cell; these two terms will depend on the distributions f and g. Once the queueing equations for the two systems is established, we could obtain fluid limits and investigate the stability condition of such a network.

An situation where such processes would arise can be found from vehicular networks. A first instance comes from wireless sensor networks, which have been studied for some time ([61]). In the framework of 5G URLLC networks, using service differentiation would allow for more flexibility and possibly low latency in vehicular networks. In such a setup, sensors are represented by transmitters and the onboard computer of car is the receiver, which are located at a fixed distance from each other, which would form a SBD move process. Providing a study for such networks could allow for more efficient wireless sensor networks, and provide useful results about latency. A second instance featuring the dynamics we studied in this thesis is the modelling a fleet of autonomous vehicles. In this framework, moving vehicles transmit in a cellular network and transmit to base stations placed at given locations in space. Such systems have already been deployed ([50]), and leverage features from both the systems we studied in this work.

Chapter 14

Résumé du manuscrit en français

Cette thèse s'intéresse à différents aspects de l'application de la théorie des processus ponctuels pour modéliser les nouvelles générations de réseaux de communication sans fil. Ce manuscrit s'articule en trois parties. Dans une première partie, nous nous intéressons à une classe de processus de saut markoviens qui implémentent une forme de différenciation de service, le partitionement de bande passante, similaire aux echnologies introduites dans les réseaux 5G. Dans une seconde partie, nous étudions les propriétés du régime stationnaire des dynamiques introduites dans la partie I, en étudiant les mesures moments et leur estimation, la distribution stationnaire du processus de saut ainsi que la présence d'attraction statistique. Pour finir, en partie III, nous changeons d'objet d'étude : considérons un réseau sans fil de type 5G avec plusieurs niveaux (dans notre exemple, 2 : un niveau *micro* et un niveau *macro*). Une question importante est la politique d'association dans un tel réseau. Dans les réseaux 5G, la mobilité des utilisateurs est une dimension importante à prendre en compte, car elle affecte de manière non-négligeable les performances du réseau. La question que nous traitons dans cette dernière partie est la performance de politiques d'associations dépendant de la vitesse des utilisateurs.

Partie I - Stabilité d'un processus de vie et de mort spatial mutliclasse avec des interactions sans fil

Dans cette première partie, nous nous intéressons à un modèle similaire à celui présenté dans [80]. Considérons une région fermée et bornée $\mathcal{D}$ du plan euclidien. Par simplicité, supposons que $\mathcal{D}$ est un tore carré plat.

Des récepteurs arrivent dans $\mathcal{D}$ selon une pluie de Poisson d'intensité $\lambda > 0$. Lors de leur arrivée dans le système, chaque récepteur arrive avec un transmetteur situé à une distance $r > 0$ dans une direction aléatoire. Pour transmettre, les paires de récepteurs/transmetteurs (ou *utilisateurs*) peuvent utiliser $K > 1$ canaux de communication orthogonaux, dépendant de leurs besoins (par exemple, des utilisateurs devant transmettre plus d'informations pourraient demander plus de canaux de communication). Pour $C \subset [1, ...\, K]$, un utilisateur recevra l'ensemble de configuration (ou *classe*) C sur lesquels transmettre avec une probabilité $p_C > 0$, et reçoit un fichier distribué indépendamment selon une loi exponentielle de moyenne $L_C > 0$. Comme les canaux sont orthogonaux, un utilisateur de classe C recevra une interférence d'un utilisateur de classe D avec une puissance proportionnelle à la taille de l'intersection de leurs classes, $|D \cap C|$.

Le système ainsi définit forme un processus de vie et de mort spatial, et est une extension du système introduit par Sanakararaman et Baccelli ([80]) dans le cas où plusieurs canaux de communications sont disponibles. Notons Φ^T le processus ponctuel des transmetteurs, Φ^R, celui des récepteurs, Φ le processus des paires récepteurs-transmetteurs. Supposons que l'atténuation du signal dans le système est modélisée par une fonction ℓ de *path-loss* positive, non-croissante et bornée, et nous avons la présence d'un bruit extérieur de densité $\mathcal{N}_0$.

Pour définir le taux de départ des utilisateurs, nous pouvons exprimer l'interférence subie par un point situé en x avec un récepteur situé en y comme un bruit de grenaille (*shot-noise*) du processus des utilisateurs:

$$I(x, \Phi_t) = \sum_{z \in \Phi_t^T \setminus \{y\}} |C_x \cap C_z| \ell(\|x - z\|).$$

En considérant l'interférence dans le système comme du bruit et en supposant que le signal est faible devant l'interférence et le bruit, nous pouvons définir un taux de transfert de fichier comme suit:

$$R(x, \Phi_t) = \frac{|C|}{\mathcal{N}_0 + I(x, \Phi_t)}$$

En l'absence d'abandon de communication, le taux de départ des utilisateurs de classe C est égal à $\frac{1}{L_C} \sum_{x \in \Phi_{t,C}} R(x, \Phi_t)$.

Le processus Φ est un processus de saut markovien, que nous appellerons *processus BWP*. Nous disons que ce processus est stable si et seulement s'il est positif récurrent. La question principale de la partie I est la définition de la région de stabilité de tels processus en fonction du paramètre d'arrivée λ.

L'étude de ce genre de système dynamique peut s'avérer complexe sans information supplémentaire sur les propriétés du système. Parmi les propriétés qui s'avèrent utiles, nous pouvons compter la *monotonie stochastique*. Cette propriété utilise un ordre partiel sur les processus stochastiques, la domination stochastique, pour lier la stabilité ou l'instabilité d'un processus de Markov à celle d'un autre en utilisant des majoration ou des minorations adéquates.

Au vu de la définition de la dynamique, nous pouvons identifier quatre quantités qui ont une influence sur le système : le taux d'arrivée λ, la condition initiale Φ_0, le vecteur des tailles moyennes de fichiers $\mathbf{L}$ et la fonction de transfert de fichier R (ou, de manière équivalente, la path-loss ℓ).

En utilisant des arguments de couplages, nous pouvons prouver que les quatre conditions suivantes sont suffisantes pour qu'un processus BWP Ψ' domine un processus Ψ (avec les trois autres paramètres pris égaux - les quantités marquées d'un prime se rapportent à Ψ' et les autres, à Ψ):

- $\lambda < \lambda'$,
- $\Psi_0 \subset \Psi'_0$,
- $\mathbf{L} \leq \mathbf{L}'$ (par coordonnée),
- Pour tout $\Psi_1 \subset \Psi_2$ et $x \in \mathcal{D}$, $R'(x, \Psi_1) \leq R(x, \Psi_2)$, ou, de manière équivalente, pour tout $s \geq 0$, $\ell(s) \leq \ell'(s)$.

En utilisant les propriétés de monotonie stochastique, nous pouvons déduire que si Ψ' domine Ψ, si Ψ' est stable, Ψ est stable et si Ψ est instable, Ψ' est instable.

Pour obtenir la stabilité du processus Φ, nous allons définir deux systèmes en utilisant une discrétisation de la région $\mathcal{D}$ en cellules de taille ε, puis définir deux nouvelles path-loss ℓ^ε et ℓ_ε dans le système, de sorte que tous les utilisateurs dans la même cellule voient la même atténuation du signal des autres cellules, et telles que :

$$\ell_\varepsilon(x, y) \leq \ell(\|x - y\|) \leq \ell^\varepsilon(x, y).$$

En utilisant les deux nouvelles fonction de path-loss, nous pouvons définir deux *interference queueing networks* (voir [81]), qui sont des réseaux de file d'attente avec un espace d'état fini. Un premier, $\bar{\mathbf{X}}_\varepsilon$ qui domine Φ et un second, $\underline{\mathbf{X}}_\varepsilon$, qui est dominé par Φ. Nous pouvons ensuite obtenir la stabilité de $\bar{\mathbf{X}}_\varepsilon$ en utilisant des limites fluides ([84]) et l'instabilité de $\underline{\mathbf{X}}_\varepsilon$ en utilisant de la domination stochastique avec une fille M/M/1 adéquate.

Nous obtenons deux conditions de stabilité:

- $\bar{\mathbf{X}}_\varepsilon$ est stable si $\lambda < \bar{\lambda}_\varepsilon$,
- $\underline{\mathbf{X}}_\varepsilon$ est instable si $\lambda > \underline{\lambda}_\varepsilon$.

En faisant tendre ε vers 0, nous obtenons que $\bar{\lambda}_\varepsilon$ et $\underline{\lambda}_\varepsilon$ ont une limite commune, $\lambda^\star$, ce qui nous permet d'obtenir le résultat principal de la partie I:

Theorem. *Le modèle BWP est stable si $\lambda < \lambda^\star$ est instable si $\lambda > \lambda^\star$, où:*

$$\lambda^\star = \frac{1}{p_C L_C} \frac{|C| z_C^\star}{\langle \ell_{\mathcal{D}} \rangle \sum_U |C \cap U| z_U^\star},$$

et où $\mathbf{z}^\star$ est solution du système:

$$\forall C, D \in \mathcal{P}(K) \quad \frac{1}{p_C L_C} \frac{|C| z_C^\star}{\sum_U |C \cap U| z_U^\star} = \frac{1}{p_D L_D} \frac{|D| z_D^\star}{\sum_U |D \cap U| z_D^\star}.$$

Partie II - étude de processus ponctuels stationnaire en interaction

La partie II de ce manuscrit se concentre sur l'étude du système défini en partie I dans son régime stationnaire. L'étude de ce régime stationnaire permet d'obtenir des informations intéressantes sur la distribution spatiale des utilisateurs soumis à ce genre de dynamiques. Dans cette partie, nous étudions trois propriétés de ce régime stationnaire : l'estimation des mesures moment, l'existence de moments exponentiels et l'attraction statistique.

Les mesures moments, et plus précisément, l'estimation des densités spatiales d'utilisateurs dans le réseau en régime stationnaire. Pour estimer cette quantité, nous ne pouvons pas obtenir de forme close, mais nous définissons deux heuristiques.

La première heuristique s'appuie sur une approximation de champ moyen : nous supposons que dans le régime stationnaire, les processus $\Phi_{0,C}$ des utilisateurs de classe C sont des processus de Poisson d'intensité μ_C. En utilisant des lois de conservation dans le système, nous piuvons obtenir sous cette hypothèse, un système d'équations dont les μ_C sont solutions. Cette heuristique poissonienne fournit une première approximation des densités spatiales. Un résultat intéressant, conséquence de ces calcules, est le suivant: si le système a un régime stationaire,donc la dynamique est stable, nous pouvons calculer les μ_C par cette méthode. Par contraposée, si nous ne pouvons pas les calculer, le système est instable. Si λ_{P} est la plus grande valeur de λ telle que nous pouvons calculer les μ_C par cette méthode, nous obtenons une estimation de la valeurs de $\lambda^\star$, taux critique d'arrivée dans le système. En comparant cette valeur, obtenue numériquement, et la valeur obtenue en partie I, λ_{P} est une estimation assez précise de $\lambda^\star$. La raison de ce résultat n'est pas étudiée dans ce manuscrit.

La seconde heuristique que nous développons est une approximation par cavité, provenant de la physique statistique. En supposant la présence de deux utilisateurs, un en x de classe C et l'autre en y de classe D, nous pouvons estimer la fonction de corrélation croisée $\rho^{(2)}_{C,D}$ et appliquer des lois de conservation dans le système pour obtenir une seconde estimation, meilleure que la première, pour les densités spatiales d'utilisateurs μ_C, au prix d'un calcul plus coûteux.

Pour ce qui est des mesures moments d'ordre supérieur, nous avons obtenu l'existence de moments exponentiels dans le système, i.e. l'existence de $c_0 > 0$ tel que pour tout $0 \leq c < c_0$, $\mathbb{E}\left[e^{c\Phi_{0,C}(\mathcal{D})}\right] < \infty$. L'existence de moments exponentiels dans le système permet de borner les queues de la distribution stationnaire et d'obtenir des garanties de performance dans le réseau.

La dernière propriété intéressante sur laquelle nous nous sommes penchés est l'attraction statistique en régime stationnaire. Nous savons que le cas $K = 1$ crée de l'attraction en régime stationnaire, i.e. que la dynamique fait que les utilisateurs se regroupent en grappes où les communications sont plus lentes. Dans le cas $K \geq 2$, nous avons prouvé une version relaxée de cette attraction, que nous pensons être due aux non-linéarités introduites par la différenciation de service dans notre modèle.

Partie III - Politique d'association basée sur la mobilité dans des réseaux sans fil 5G

Dans la troisième partie de ce manuscrit, nous nous intéressons à un réseau sans fil 5G possédant deux niveaux d'antennes : un premier niveau, appelé *macro*, avec des antennes puissantes à large couverture et un second niveau, *micro*, d'antennes plus faibles avec une plus faible couverture.

Dans les réseaux 5G, les antennes utilisent des faisceaux étroits et directifs pour communiquer avec les appareils connectés. Lorsqu'un appareil sort du faisceau de la station à laquelle il est connecté, il doit resélectionner un nouveau faisceau. Cette opération prend un certain temps pendant lequel l'appareil ne peut pas transmettre avec le réseau. De la même façon, si l'appeil connecté sort de la couverture de la station à laquelle il est connecté, il doit sélectionner une nouvelle station, opération pendant laquelle il ne pourra pas communiquer avec le réseau. Suivant cette obersation, la prise en compte de la mobilité des appareils connectés dans les réseaux 5G sans fil devient une composante importante de la mesure des performances du réseau. Plus particulièrement, dans les réseaux étagés, nous allons nous demander comment la prendre en compte pour concevoir des politiques d'association intéressantes.

Nous considérons un réseau sans fil à deux niveaux, macro et micro. Les stations de base (SBs) de chacun des deux niveaux sont distrivuées selon deux processus ponctuels de Poisson indépendants, Φ_M et Φ_μ, d'intensités respectives λ_M et λ_μ, possédant n_M et n_μ faisceaux et de puissances P_M et P_μ. Les utilisateurs mobiles (UMs) dans le réseau sont distribués selon un troisième PPP indépendant Φ_u d'intensité λ_u. Ces UMs se déplacent en ligne droite à une vitesse distribuée indépendamment selon une distribution f.

On suppose que les communications sont descendantes dans le réseau, et les UMs se connectent à la SB la plus proche d'eux dans leur niveau d'association, ce qui forme deux tessellations de Poisson-Voronoï - une par niveau du réseau.

En utilisant l'isotropie et l'invariance du réseau, nous pouvons résumer l'étude des performances dans le réseau à l'étude de l'utilisateur typique situé à l'origine du repère. Nous pouvons également supposer qu'il se déplace sur une ligne droite selon l'axe des abscisses.

Nous pouvons calculer les intensités temporelles de resélections de fais-

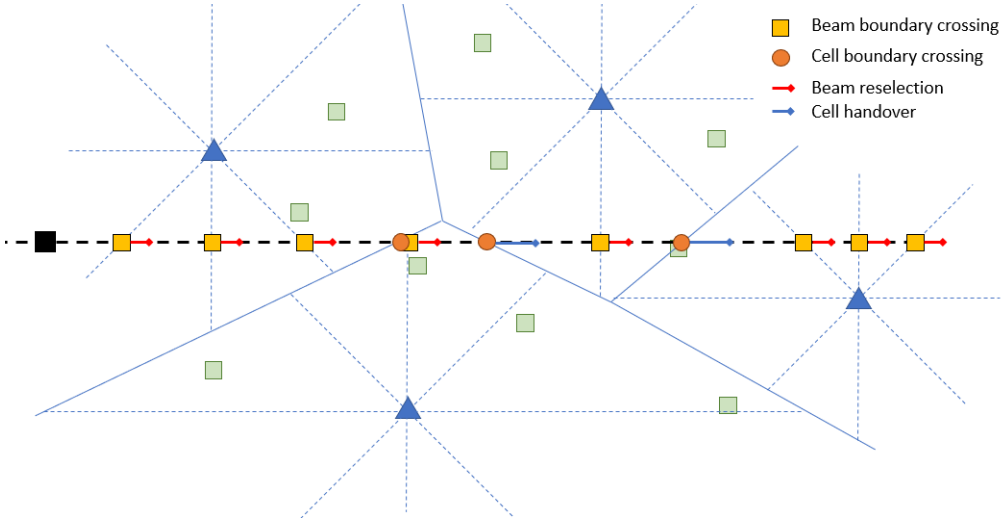

Figure 14.1: Illustration de l'overhead par unité de temps dans un réseau mobile. Les resélections de faisceaux sont en jaune, les changements de SB, en orange

ceaux et de changement de cellule (voir [53]) en fonction des paramètres du réseau et en fonction de la vitesse v d'un UM:

$$\nu_{c,M} = \frac{4\sqrt{\lambda_M}}{\pi} v \qquad \nu_{b,M} = \frac{n_M \sqrt{\lambda_M}}{\pi} v$$

Nous définissons alors l'overhead par unité de temps comme la proportion du temps pendant laquelle l'UM ne transmet pas avec le réseau:

$$T_o^M = \nu_{c,M} T_{c,M} + \nu_{b,M} T_{b,M}.$$

Grâce à une interprétation ergodique, nous pouvons définir un taux de Shannon effectif dans un niveau du réseau comme étant le taux de Shannon global pondéré par la proportion du temps pendant laquelle l'UM transmet, en prenant en compte l'overhead, ce qui mène à la définition suivante:

$$\mathcal{R}_{M,\text{eff}}(v) = \mathcal{R}_M \left(1 - T_o^M(v)\right)^+,$$

Nous allons donc définir des politiques d'association ayant pour but de maximiser le taux moyen effectir de Shannon (MESR) dans le réseau.

La première famille de politiques que nous étudions sont les politiques de seuil: en fixant un seuil $v_T > 0$, tous les UM de vitesse inférieure à v_T sont associés avec le niveau micro, et tous ceux ayant une vitesse supérieure à v_T sont associés avec le niveau macro. Nous pouvons calculer le MESR de l'utilisateur typique dans le réseau sous une politique de seuil donnée:

$$\mathcal{R}(v_T) = \int_0^{v_T} \mathcal{R}_{\mu,\text{eff}}(v) f(v) \mathrm{d}v + \int_{v_T}^{\infty} \mathcal{R}_{M,\text{eff}}(v) f(v) \mathrm{d}v.$$

Dans un premier temps, nous supposons qu'il n'y a qu'un seul UM par SB dans le réseau. Nous obtenons le théorème suivant:

Theorem (Politique de seuil optimale)**.** *Il existe un unique seuil v_T qui maximise le MESR dans le réseau. Ce seuil optimal $v_T^\star$ ne dépend pas de la distribution de vitesse f, et est solution de l'équation suivante:*

$$\mathcal{R}_{\mu,\mathit{eff}}(v_T^\star) = \mathcal{R}_{M,\mathit{eff}}(v_T^\star).$$

Si nous relaxons la supposition selon laquelle nous avons un seul UM par SB, nous introduisons $Z_M^0(v_T)$ la variable aléatoire dénotant le nombre d'UM partageant la SB de l'utilisateur typique sous une politique de seuil dans le niveau macro. Nous pouvons redéfinir le MESR dans le réseau :

$$\hat{\mathcal{R}}_{\text{load}}(v_T) = \mathbb{E}\left[\frac{\mathcal{R}_{\mu,\text{eff}}(v)}{Z_\mu^0(v_T)}\mathbb{1}_{v\le v_T} + \frac{\mathcal{R}_{M,\text{eff}}(v)\mathbb{1}_{v>v_T}}{Z_M^0(\bar{v_T})}\right],$$

Dans le cas général, nous ne pouvons pas calculer facilement le maximum de cette fonction. Nous devons utiliser deux heuristiques pour simplifier cette expression:

- Nous supposons que le SINR et les Z^0 sont indépendantes,
- Nous utilisons une heuristique pour la taille des cellules d'une tessellation de Poisson-Voronoi pour approcher la moyenne de $1/Z_M^0(v_T)$ et $1/Z_\mu^0(v_T)$ par deux fonctions $L_M(v_T)$ et $L_\mu(v_T)$.

Le MESR moyen dans le réseau devient alors, sous ceux deux heuristiques:

$$\hat{\mathcal{R}}_{\text{load}}(v_T) = L_\mu(v_T)\int_0^{v_T}\mathcal{R}_{\mu,\text{eff}}(v)f(v)\mathrm{d}v + L_M(v_T)\int_{v_T}^{\infty}\mathcal{R}_{M,\text{eff}}(v)f(v)\mathrm{d}v.$$

Nous pouvons définir une nouvelle politique de seuil optimale en prenant en compe la charge dans le système:

Theorem. *L'heuristique de charge-seuil est le seuil v_{LT} qui maximise $\hat{\mathcal{R}}_{load}$, i.e., tel que :*

$$v_{LT} \triangleq \arg\max\ \hat{\mathcal{R}}_{load}(v_T).$$

La politique de charge-seuil optimale *est la politique de seuil associée avec v_{LT}.*

Nous pouvons comparer cette politique de charge-seuil optimale à une politique d'association classique : la politique max-power (MARP), où les UMs sont associés au niveau du réseau qui leur fournit le meilleur SINR dans le cas où la vitesse de UM est distribuée selon une distributuion exponentielle.

Nous pouvons voir sur la Figure 14.2 que la politique de charge-seuil optimale offre des performances supérieures à celles de la politique MARP dès que la vitesse moyenne de UM devient grande, ce qui donne un exemple simple de cas de figure où les politiques définies dans ce travail surpassent une politique déjà établie.

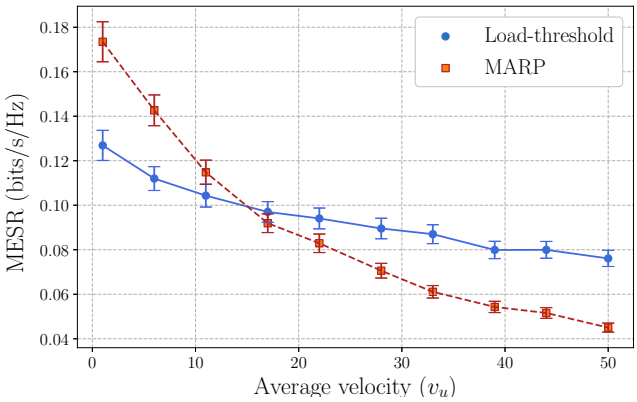

Figure 14.2: Comparaison entre la politque max-power (marquers carrés, en pointillés) et la politique de charge-seuil optimale (cercles, ligne pleine).

La seconde catégorie de politiques d'association que nous explorons sont des politiques de biabs dépendant de la vitesse. Les politique de seuil dépendent uniquement de la vitesse des UMs, et ignorent la géométrie du réseau. Le but de cette étude est de concevoir une famille de politiques d'association combinant les idées de la politique MARP et des politiques de seuil.

Soit K une fonction continue, positive. Nous définission la politique VBMP (max-power biaisée par la vitesse) de la façon suivante : si R_M et R_μ sont les puissances reçues par l'UM typique située à l'origine, alors :

- si $\mathrm{R}_M > K(v)\mathrm{R}_\mu$, on associe l'UM avec le niveau macro,
- sinon, on l'associe avec le niveau micro.

Nous pouvons reformuler les résultats obtenus avec les politiques de seuil pour obtenir un MESR dépendant de la charge sous une politique VBMP:

$$\mathcal{R}_{\text{load}}(K) = \int_0^{v_{\max}} \mathbb{E}\left[\frac{\log(1+\text{SINR}(v,K))}{Z_0(K)}(1-T_o(v))^+\right] f(v)\mathrm{d}v.$$

Nous allons utiliser les mêmes heuristiques que celles utilisées précédemment pour déifnir la politique VBMP qui maximise le MESR sujet à la charge dans le réseau:

$$\hat{\mathcal{R}}(K) = \int_0^{v_{\max}} \left(L_M(K)\mathcal{R}_{M,\text{eff}}(v,K) + L_\mu(K)\mathcal{R}_{\mu,\text{eff}}(v,K)\right) f(v)\mathrm{d}v,$$

où:

- $L_M(K) = L\left(\frac{\lambda_M}{\lambda_u G_M(K)}\right)$,
- $G_M(K) = \int_{v=0}^{v_{\max}} \frac{f(v)}{1+\Omega K(v)^\delta}\mathrm{d}v$ est la probabilité que l'UM typique est associée avec le niveau macro.

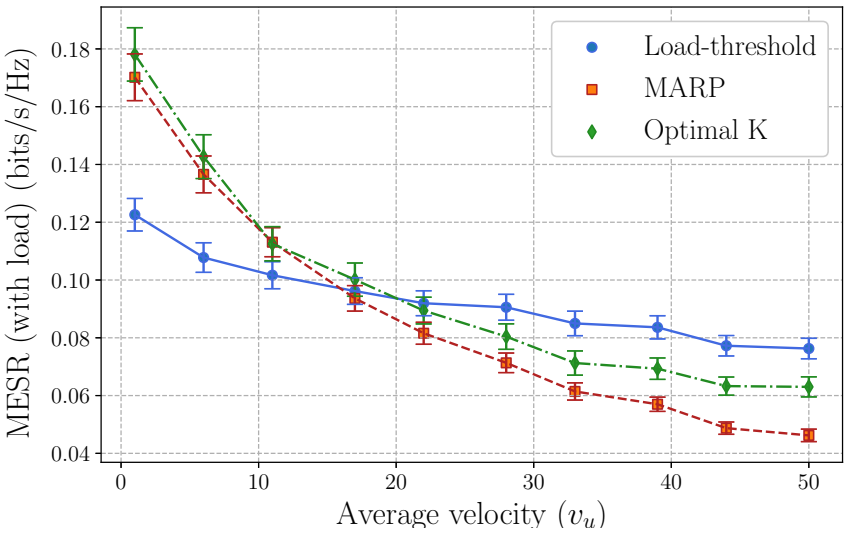

Figure 14.3: Comparaison des trois politiques d'associations : MARP (en rouge), charge-seuil optimale (en bleu) et VBMP optimale (en vert)

La forme du MESR $\hat{\mathcal{R}}(K)$ que nous cherchons à maximiser est particulière, car elle ne nous permet pas d'utiliser des résultats de calculs de variations pour obtenir une condition sur la fonction K qui maximise le MESR.

Pour approcher le maximum, nous utilsons une discrétisation de l'espace des vitesses et de la fonction K, et nous utilisons des méthodes d'optimisation numériques pour chercher le maximum du MESR. Malheureusement, les méthodes utilisées ne nous ont pas permis d'obtenir le résultat escompté : la politique que nous obtenons est meilleure que la politique MARP, mais offre des performances inférieures à la politique de charge-seuil. La raison de ce résultat reste une question ouverte dans ce manuscrit (voir Figure 14.3).

Conclusion

Dans ce manuscrit, nous avons exploré deux modèles mathématiques faisant intervenir des technologies mises en ouevre dans les dernières générations de réseaux de communication sans fil : la différenciation de service, le beamforming directionel et les réseaux étagés.

Dans les deux premières parties, nous avons étudié la différenciation de service et son impact sur un réseaux de files d'attente spatial en proposant un cadre d'étude qui peut être généralisé à un ensemble de dynamiques. Nous avons également obtenu des résultats sur les mesures moments, la distribution stationaire des dynamiques et un résultat sur l'attraction statistique que les dynamiques sans fil engendrent.

La troisième partie se concentre sur l'étude d'un réseau 5G à deux niveaux, où la mobilité joue un rôle important. Nous avons proposé un cadre simple présentant des particularités des réseaux 5G de nouvelle génération, défini une métrique et étudié deux familles de politiques d'associations : une pre-

mière basée uniquement sur la vitesse des utilisateurs dans le réseau et une seconde, mélangeant mobilité et géométrie. Nous les avons ensuite comparées à une politique d'association classique pour estimer leurs performances.

Le travail présenté dans ce manuscrit peut être vu comme une premère étape vers la définition d'un cadre d'étude plus large pour modéliser des réseaux plus complexes. Les résultats présentés dans ce manuscrit peuvent être étendus à des cadres d'étude voisins possédant des propriétés similaires. Les travaux présentés dans cette thèse ouvrent également de nouvelles perspectives, avec plusieurs questions ouvertes sur certains résultats présentés, qui pourraient faire l'objet de futures recherches.

Bibliography

[1] 3GPP, *NR; User Equipment (UE) radio transmission and reception; Part 1: Range 1 Standalone*, 2022. [Online]. Available: https://portal.3gpp.org/desktopmodules/Specifications/SpecificationDetails.aspx?specificationId=3283.

[2] 3GPP, *NR; User Equipment (UE) radio transmission and reception; Part 2: Range 2 Standalone*, 2022. [Online]. Available: https://portal.3gpp.org/desktopmodules/Specifications/SpecificationDetails.aspx?specificationId=3284.

[3] A. AlAmmouri, J. G. Andrews, and F. Baccelli, "A unified asymptotic analysis of area spectral efficiency in ultradense cellular networks," *IEEExplore*, 2018.

[4] A. AlAmmouri, J. G. Andrews, and F. Baccelli, "Stability and metastability of traffic dynamics in uplink random access networks," *CoRR*, 2019. [Online]. Available: http://arxiv.org/abs/1906.04683.

[5] S. Allmeier and N. Gast, "Mean field and refined mean field approximations for heterogeneous systems: It works!" *Proc. ACM Meas. Anal. Comput. Syst.*, volume 6, number 1, 2022. [Online]. Available: https://doi.org/10.1145/3508033.

[6] J. G. Andrews, F. Baccelli, and R. K. Ganti, "A tractable approach to coverage and rate in cellular networks," *IEEE Transactions on Communications*, volume 50, number 11, pages 3122–3134, 2011.

[7] J. G. Andrews, F. Baccelli, and R. K. Ganti, "A tractable approach to coverage and rate in cellular networks," *IEEE Transactions on Communications*, volume 50, number 11, pages 3122–3134, 2011.

[8] J. G. Andrews and S. Weber, *Transmission capacity of wireless networks*, Foundations and T. in Networking, Eds. NoW Publishers, 2012, volume 5.

[9] J. G. Andrews *et al.*, "What will 5G be?" *IEEE Journal on Selected Areas in Communications*, volume 32, number 6, pages 1065–1082, 2014.

[10] R. Arshad, H. ElSawy, S. Sorour, T. Y. Al-Naffouri, and M. Alouini, "Velocity-aware handover management in two-tier cellular networks," *IEEE Transactions on Wireless Communication*, volume 16, number 3, pages 1851–1867, 2017.

[11] O. E. Ayach, S. Rajagopal, S. Abu-Surra, Z. Pi, and R. W. Heath, "Spatially sparse precoding in millimeter wave mimo systems," *IEEE Transactions on Wireless Communications*, volume 13, number 3, pages 1499–1513, 2014.

[12] F. Baccelli and B. Blaczszynczyn, *Stochastic Geometry and Wireless networks*. NoW Publishers, 2009.

[13] F. Baccelli and B. Błaszczyszyn, *Stochastic Geometry and Wireless Networks*, Baccelli, F., Blaszczyszyn, and B., Eds. NoW Publishers, 2009.

[14] F. Baccelli and P. Brémaud, *Elements of Queueing Theory: Palm Martingale Calculus and Stochastic Recurrences*. Springer, 2003.

[15] F. Baccelli, F. Mathieu, and I. Norros, "On spatial point processes with uniform birth and death by random connection," *Queueing Systems*, volume 86, number 1-2, pages 95–140, 2017.

[16] F. Baccelli and S. Foss, "Poisson hail on a hot ground," *Journal of Applied Probability*, volume 48, number A, pages 343–366, 2011.

[17] F. Baccelli, S. Foss, and V. Shneer, *Migration-contagion processes*, 2022. [Online]. Available: https://arxiv.org/abs/2208.03512.

[18] F. Baccelli, B. Blaszczyszyn, and M. Karray, *Random Measures, Point Processes, and Stochastic Geometry*. Inria, Jan. 2020. [Online]. Available: https://hal.inria.fr/hal-02460214.

[19] F. Baccelli, M. Davydov, and T. Taillefumier, "Replica-mean-field limits of fragmentation-interaction-aggregation processes," *Journal of Applied Probability*, pages 1–22, 2022. [Online]. Available: https://hal.archives-ouvertes.fr/hal-03542535.

[20] F. Baccelli and S. Foss, "On the saturation rule for the stability of queues," *Journal of Applied Probability*, volume 32, number 2, pages 494–507, 1995.

[21] R. N. Baccelli F, "A computational framework for evaluating the role of mobility on the propagation of epidemics on point processes.," *J Math Biol.*, volume 84, number 4, 2021.

[22] S. Banerjee and A. Sankararaman, "Ergodicity and steady state analysis for interference queueing networks," *Research report*, 2020.

[23] W. Bao and B. Liang, "Stochastic geometric analysis of user mobility in heterogeneous wireless networks," *IEEE Journal on Selected Areas in Communications*, volume 33, number 10, pages 2212–2225, 2015.

[24] F. Baskett, K. M. Chandy, R. R. Muntz, and F. G. Palacios, "Open, closed, and mixed networks of queues with different classes of customers," *J. ACM*, volume 22, number 2, pages 248–260, Apr. 1975.

[25] D. Bethanabhotla, O. Y. Bursalioglu, H. C. Papadopoulos, and G. Caire, "Optimal user-cell association for massive mimo wireless networks," *IEEE Transactions on Wireless Communications*, volume 15, number 3, pages 1835–1850, 2016. DOI: 10.1109/TWC.2015.2496942.

[26] P. Billingley, *Convergence of Probability Measures*, 2nd. Wiley, 1999.

[27] G. D. Birkhoff, "Proof of the ergodic theorem," *Proceedings of the National Academy of Sciences*, volume 17, number 12, pages 656–660, 1931. DOI: 10.1073/pnas.17.2.656. eprint: https://www.pnas.org/content/17/12/656.full.pdf. [Online]. Available: https://www.pnas.org/content/17/12/656.

[28] C. Bordenave, "Stability of spatial queueing systems," INRIA, Tech. Rep. RR-5305, 2004, page 22. [Online]. Available: https://hal.inria.fr/inria-00070695.

[29] C. Bordenave, S. Foss, and V. Shneer, "A random multiple access protocol with spatial interactions," *Journal of Applied Probability*, volume 46, number 3, pages 844–865, 2009.

[30] M. Bramson, "A stable queueing network with unstable fluid model," *The Annals of Applied Probability*, volume 9, number 3, pages 818–853, 1999.

[31] P. Brémaud and L. Massoulié, "Stability of nonlinear Hawkes processes," *The Annals of Probability*, volume 24, number 3, pages 1563–1588, 1996.

[32] R. H. Byrd, P. Lu, J. Nocedal, and C. Zhu, "L-bfgs-b: Algorithm 778: L-bfgs-b, fortran routines for large scale bound constrained optimization," *ACM Transactions on Mathematical Software.*, volume 23, number 4, pages 550–560, 1997.

[33] N. Campbell, "The study of discontinuous phenomena," in *Proceedings of the Cambridge Philosophical Society*, volume 15, 1909, page 250.

[34] D. Chizhik *et al.*, "Multiple-input-multiple-output measurements and modeling in manhattan," *IEEE Journal on Selected Areas in Communications*, volume 21, number 3, pages 321–331, 2003.

[35] N. Chornova, S. Foss, and B. Kim, "On the stability of a polling system with an adaptive service mechanism," *Annals of Operations Research*, volume 198, pages 125–144, 2012.

[36] T. M. Cover and J. A. Thomas, *Elements of Information Theory*. John Wiley & Sons, Ltd, 2005.

[37] J. G. Dai, "On positive harris recurrence of multiclass queueing networks: A unified approach via fluid limit methods," *The Annals of Applied Probability*, volume 5, number 1, pages 49–77, 1995.

[38] J. G. Dai, "A fluid limit model criterion for instability of multiclass queueing networks," *The Annals of Applied Probability*, volume 6, number 3, pages 751–757, 1996.

[39] H. Dhillon, R. K. Ganti, F. Baccelli, and J. G. Andrews, "Modeling and analysis of K-tier downlink heterogeneous cellular networks," *IEEE Journal on Selected Areas in Communications*, volume 30, number 3, pages 550–560, 2012.

[40] H. Dhillon, R. K. Ganti, F. Baccelli, and J. G. Andrews, "Modeling and analysis of k-tier downlink heterogeneous cellular networks," *IEEE Journal on Selected Areas in Communications*, volume 30, number 3, pages 550–560, 2012.

[41] W. Feller, "Die grundlagen der volterraschen theorie des kampfes ums dasein in wahrscheinlichkeitstheoretischer behandlung," *Acta Biotheoretica*, volume 5, number 1, pages 11–40, 1939.

[42] K. Feng and F. Baccelli, *Spatial network calculus and performance guarantees in wireless networks*, 2023.

[43] J.-S. Ferenc and Z. Néda, "On the size distribution of Poisson voronoi cells," *Physica A: Statistical Mechanics and its Applications*, volume 385, number 2, pages 518–526, 2007.

[44] F. G. Foster, "On the Stochastic Matrices Associated with Certain Queuing Processes," *The Annals of Mathematical Statistics*, volume 24, number 3, pages 355–360, 1953.

[45] N. Gast, L. Bortolussi, and M. Tribastone, "Size expansions of mean field approximation: Transient and steady-state analysis," *Performance Evaluation*, volume 129, pages 60–80, 2019.

[46] A. Genz and A. Malik, "Remarks on algorithm 006: An adaptive algorithm for numerical integration over an n-dimensional rectangular region," *Journal of Computational and Applied Mathematics*, volume 6, number 4, pages 295–302, 1980.

[47] M. Haenggi, "The meta distribution of the SIR in poisson bipolar and cellular networks," *IEEE Transactions on Wireless Communications*, volume 15, number 4, pages 2577–2589, 2016.

[48] M. Haenggi, *Stochastic Geometry for Wireless Networks*. Cambridge University Press, 2012.

[49] H. Holma, A. Toskala, and T. Nakamura, *5G Technology: 3GPP New Radio*, H. Holma, Ed. John Wiley & Sons Ltd., 2020.

[50] Huawei, Inc., *The World's Largest Automated Container Port Operates Using First-of-Its-Kind 5.8 GHz LTE*, 2017. [Online]. Available: https://e.huawei.com/topic/leading-new-ict-ua/yangshan-port-case.html.

[51] J. Jacod and A. N. Shiryaev, *Limit Theorems for Stochastic Processes*. Springer-Verlag, 1987, volume 288, Grundlehren der Mathematischen Wissenschaften [Fundamental Principles of Mathematical Sciences].

[52] J. Jost and X. Li-Jost, *Calculus of Variations*, C. U. Press, Ed. 1998.

[53] S. K. Kalamkar, F. M. Abinader Jr, F. Baccelli, A. S. Marcano Fani, and L. G. Uzeda Garcia, "Stochastic geometry-based modeling and analysis of beam management in 5G," *IEEE Globecom*, 2020.

[54] S. S. Kalamkar, F. Baccelli, F. M. Abinader Jr, A. S. Marcano Fani, and L. G. Uzeda Garcia, "Beam management in 5G: A stochastic geometry analysis," *IEEE Transactions on Wireless Communications*, 2021.

[55] F. Kelly, *Reversibility and Stochastic Networks*. New-York: Wiley, 1979.

[56] F. Kelly, "Charging and rate control for elastic traffic," *European Transactions on Telecommunications*, volume 8, number 1, pages 33–37, 1997.

[57] D. N. Knisely, T. Yoshizawa, and F. Favichia, "Standardization of femtocells in 3gpp," *IEEE Communications Magazine*, volume 47, number 9, pages 68–75, 2009. DOI: 10.1109/MCOM.2009.5277458.

[58] Y. Kondratiev and A. Skorokhod, "On contact processes in continuum," *Infinite Dimensional Analysis, Quantum Probability and Related Topics*, volume 9, number 2, pages 187–198, 2006.

[59] S. Kullback and R. A. Leibler, "On Information and Sufficiency," *The Annals of Mathematical Statistics*, volume 22, number 1, pages 79–86, 1951.

[60] F. Lavancier and R. Le Guével, "Spatial Birth–Death–Move Processes: Basic Properties and Estimation of their Intensity Functions," *Journal of the Royal Statistical Society Series B: Statistical Methodology*, volume 83, number 4, pages 798–825, 2021.

[61] F. L. Lewis, "Wireless sensor networks," in *Smart Environments*. John Wiley & Sons, Ltd, 2004, ch. 2, pages 11–46.

[62] Z. Li, M. A. Uusitalo, H. Shariatmadari, and B. Singh, "5G urllc: Design challenges and system concepts," in *2018 15th International Symposium on Wireless Communication Systems (ISWCS)*, 2018, pages 1–6.

[63] H. Liang and W. Zhang, "A survey and taxonomy of resource allocation methods in wireless networks," *Journal of Communications and Information Networks*, volume 6, number 4, pages 372–384, 2021. DOI: 10.23919/JCIN.2021.9663102.

[64] J. D. C. Little, "A Proof for the Queueing Formula: $L = \lambda W$," *Operations Research*, volume 9, number 3, pages 383–387, 1961.

[65] D. Liu *et al.*, "User association in 5G networks: A survey and an outlook," *IEEE Communications Surveys & Tutorials*, volume 18, number 2, pages 1018–1044, 2016.

[66] M. A. Martinez-Beneito *et al.*, "Source detection in an outbreak of legionnaire's disease," *Case Studies in Spatial Point Process Modeling. Lecture Notes in Statistics*, volume 185, pages 169–182, 2006.

[67] L. Massoulie and J. Roberts, "Bandwidth sharing: Objectives and algorithms," in *IEEE INFOCOM '99. Conference on Computer Communications.*, volume 3, 1999, 1395–1403 vol.3.

[68] L. Massoulié and J. Roberts, "Bandwidth sharing and admission control for elastic traffic," *Telecommunication Systems*, volume 15, pages 185–201, 2000.

[69] J. Mecke, "On the relationship between the 0-cell and the typical cell of a stationary random tessellation," *Pattern Recognition*, volume 32, pages 1645–1648, 1998.

[70] S. P. Meyn and R. L. Tweedie, *Markov Chains and stochastic stability.* Springer Science and Business Media, 2012.

[71] R. Piessens, E. de Doncker-Kapenga, C. W. Überhuber, and D. Kahaner, *QUADPACK: A subroutine package for automatic integration.* Springer-Verlag, 1983.

[72] P. Popineau and F. Baccelli, *On multiclass spatial birth-and-death processes with wireless-type interactions*, 2022.

[73] P. Popineau, S. S. Kalamkar, and F. Baccelli, "On velocity-based association policies for multi-tier 5G wireless networks," in *2021 IEEE Global Communications Conference (GLOBECOM)*, 2021, pages 1–6.

[74] M. J. D. Powell, "An efficient method for finding the minimum of a function of several variables without calculating derivatives," *The Computer Journal*, volume 7, number 2, pages 155–162, 1964.

[75] C. Preston, "Spatial birth-and-death processes," *Advances in Applied Probabilities*, volume 7, number 3, 1975.

[76] J. Reed and B. Zwart, "Limit theorems for markovian bandwidth sharing networks with rate constraints," *Operations Research*, 2014.

[77] M. Remerova, S. Foss, and B. Zwart, "Random fluid limit of an overloaded polling model," *Advances in Applied Probability*, volume 46, number 1, pages 76–101, 2014.

[78] A. N. Rybko and A. Stolyar, "Ergodicity of stochatsic processes describing the operation of open queueing networks," *Problems of Information Transmission*, volume 28, number 3, pages 199–221, 1992.

[79] C. Saha, H. S. Dhillon, N. Miyoshi, and J. G. Andrews, "Unified analysis of hetnets using poisson cluster processes under max-power association," *IEEE Transactions on Wireless Communications*, volume 18, number 8, pages 3797–3812, 2019.

[80] A. Sankararaman and F. Baccelli, "Spatial birth-and-death wireless networks," *IEEE Transactions on Information Theory*, volume 63, number 6, pages 3964–3982, 2017.

[81] A. Sankararaman, F. Baccelli, and S. Foss, "Interference queueing networks on grids," *The Annals of Applied Probabilities*, volume 29, number 5, pages 2928–2987, 2019.

[82] R. Serfozo, "Spatial queueing systems," in *Introduction to Stochastic Networks.* New York, NY: Springer New York, 1999, pages 264–287. [Online]. Available: https://doi.org/10.1007/978-1-4612-1482-3_10.

[83] C. E. Shannon, "A mathematical theory of communication," *The Bell System Technical Journal*, volume 27, 1948.

[84] S. Shneer and A. Stolyar, "Stability conditions for a decentralised medium access algorithm: Single- and multi-hop networks," *Queueing Systems*, volume 94, pages 109–128, 2020.

[85] S. Shneer and A. Stolyar, "Stability of a standard decentralised medium access," *SIGMETRICS Perform. Eval. Rev.*, volume 46, number 2, pages 33–35, Jan. 2019.

[86] D. Stoyan, W. S. Kendall, S. N. Chiu, and J. Mecke, *Stochastic Geometry and its Applications*. John Wiley & Sons, 2013, Third Edition, Wiley Series in Probability and Statistics. DOI: 10.1002/9781118658222.

[87] M. Viswanathan, *5G NR Resource Block*, 2022. [Online]. Available: https://www.gaussianwaves.com/2022/02/5g-nr-resource-block/.

[88] White paper, *Bandwidth part adaptation: 5G NR user experience and power consumption enhancements*, 2015. [Online]. Available: https://newsletter.mediatek.com/hubfs/mwc/download/bandwidth-part-adaptation.pdf.

[89] W. Whitt, *Stochastic-process limits: an introduction to stochastic-process limits and their application to queues*. Springer-Verlag, 2002.

[90] G. U. Yule, "A mathematical theory of evolution, based on the conclusions of Dr. J. C. Willis, F. R. S," *Philosophical Transactions of the Royal Society B*, volume 213, number 402-410, pages 21–87, 1925.

RÉSUMÉ

Grâce aux nouveaux paradigmes introduits dans la dernière génération de réseaux sans fil, les attentes concernant le temps de service, la latence et la performance du réseau ont augmenté. Pour modéliser ces réseaux, la théorie des processus ponctuels et la géométrie stochastique se sont avérées utiles car elles fournissent un cadre polyvalent et robuste pour obtenir des résultats lorsque l'on travaille avec ces réseaux sans fil. L'ajout d'une dynamique markovienne pour modéliser les connexions et les temps de service complète le cadre d'analyse de ces réseaux sans fil.
La première contribution du travail présenté dans cette thèse réside dans l'analyse de la différenciation des services : les réseaux 5G NR ont introduit le partitionnement de la bande passante comme outil pour augmenter la performance du réseau. Dans cette configuration de réseau, tous les utilisateurs n'interfèrent pas les uns avec les autres avec la même puissance : les utilisateurs qui émettent avec un spectre de fréquence d'émission plus large auront une plus grande bande passante, mais ils rencontreront également plus d'interférences de la part des autres utilisateurs dans le réseau. En revanche, les utilisateurs dont le spectre est plus étroit subiront moins d'interférences. Nous définissons un cadre markovien pour étudier un tel processus spatial multiclasse de naissance et de mort, et nous décrivons sa région de stabilité. Pour de tels systèmes, les propriétés du régime stationnaire sont analysées, telles que les mesures moment ou l'attraction, ce qui permet de mieux comprendre cette dynamique.
Le deuxième problème que nous examinons est celui de la mobilité, qui est devenue une caractéristique importante des réseaux sans fil en raison de l'utilisation d'antennes hautement directionnelles. En utilisant une architecture simple pour un réseau cellulaire à deux niveaux, nous étudions deux familles de politiques d'association : une première famille qui s'appuie uniquement sur la mobilité de l'utilisateur, et une seconde qui offre un compromis entre la géométrie du réseau et la mobilité de l'utilisateur afin d'augmenter les performances du réseau. Ces politiques sont ensuite comparées à une politique d'association classique de puissance maximale afin d'évaluer leurs performances.

MOTS CLÉS

Géométrie aléatoire, Chaînes de Markov, Processus ponctuels, Réseaux de communication sans fil, Limites fluides, Calcul de Palm

ABSTRACT

Thanks to the new paradigms introduced in the latest generation of wireless networks, expectations concerning service time, latency and network performance have increased. To model such networks, point process theory and stochastic geometry have proven to be useful as they provide a versatile and robust framework to obtain results when working with such wireless networks. Adding to this Markov dynamics to model connections and service times completes this framework to analyze such wireless networks.
The first contribution of the work presented in this thesis lies in the analysis of service differentiation: 5G NR networks have introduced bandwidth partitioning as a tool to increase network performance. Under this network setup, not all users interfere with each other with the same power: users transmitting with a broader transmitting frequency spectrum will have a larger bandwidth, but they will also encounter more interference from the other users in the network. In contrast, users with a narrower spectrum will experience less interference. We define a Markovian framework to study such a multiclass spatial birth-and-death process, and we describe its stability region. For such systems, properties of the stationary regime are analyzed, such as moment measures or statistical clustering, leading to a better understanding of these dynamics.
The second problem we look into is mobility, which has become an important feature in wireless networks due to the use of highly directional antennas. Using a simple architecture for a two-tier cellular network, we study two families of association policies: a first family which only relies on user mobility, and the second offers a trade-off between network geometry and user mobility to increase network performance. These policies are then compared to a classical max-power association policy to assert their performance.

KEYWORDS

Stochastic geometry, Markov chains, Point processes, Wireless communication networks, Fluid limits, Palm calculus